

New and Emerging Technologies from Skeletal Muscle Tissue Engineering: Insect Muscle Bioactuators for Robotic Applications

A dissertation

submitted by:

Amanda Lee Baryshyan, B.S.

In partial fulfillment of the requirements
for the degree of

Doctor of Philosophy

in

Biomedical Engineering

TUFTS UNIVERSITY

August 2013

© 2013, AMANDA L. BARYSHYAN

ADVISER:

PROFESSOR DAVID L. KAPLAN, PhD.

Abstract

Bioactuation involves using biological components, such as muscle cells, to generate mechanical force. The applications for this technology include microelectromechanical systems (MEMS), actuators in small robots, and moving parts in any meso-scaled device. The advantages of fabricating an actuator from cells, rather than synthetic materials, are their ability to self-assemble, be powered by natural fuel sources such as sugar and fat, operate silently over fast time scales, and biodegrade. Several studies have investigated the feasibility of forming bioactuators from mammalian muscle, but their stringent environmental requirements limit their applicability to real-world devices. Therefore, we have investigated the use of insect cells toward a bioactuation system; insect tissues are known to tolerate a wide range of temperature, pH and starvation conditions.

Manduca sexta cells were isolated from embryos staged for the presence of myoblasts and, using insect hormone 20-hydroxyecdysone, differentiated into functional muscle fibers. The cultures display cross-striations, are multinucleated, and survive for periods of > 3 months without medium replenishment. We investigated the potential cause for this and found that maternally-derived yolk cells were also present in our cultures. In the embryo, these cells are responsible for the storage, breakdown and delivery of carbohydrates, amino acids, and lipids to the developing embryo. We hypothesized that this process could also be taking place in our cultures.

We have further developed these cells into scaffold-free 3-dimensional tissues, grown at high density in PDMS chambers. Over periods of one week, the cells condense into contractile structures; the presence of a mixture of cell types

contributes to the ability of the tissue to maintain its integrity without the need for an extracellular matrix or gel support. The muscle tissues produce forces in the uN range spontaneously, which is comparable to literature results for mammalian engineered tissues stimulated electrically. Additionally, we have shown that these tissues are capable of exerting force onto synthetic supports for robotic displacement. The results of our studies have demonstrated that robotic and microsystem actuation may be achieved using contractile insect muscle tissues generated *in vitro*.

Acknowledgements

I would first like to acknowledge my undergraduate research mentors, Dr. Xiaoqin Wang, and Dr. Michael Lovett. Your guidance and support helped me decide to continue on to graduate school and helped me fully engage in the research experience. Thank you both for your time, patience and advice. I would be remiss if I did not also thank my high school guidance counselor, Dr. Bergin, for introducing me to Tufts, and to Tufts University, for piquing my interest by including a page on tissue engineering in their prospective student brochure.

I would also like to acknowledge my labmates who helped me when I was first becoming acquainted with the lab and graduate school, namely, Dr. Amanda Murphy, Dr. Danielle Rockwood, Dr. Isabella Pallotta, and Dr. Michael Lovett. I also want to thank my fellow graduate students who started in the BME program the same year as me, including Lindsay Wray, Roberto Elia, Dr. Reynald Lescarbou, Christa Margossian, Tom Dabrowski, and Jeremy Fryer-Biggs. I was so fortunate to have shared this experience with such brilliant and wonderful people. I would also like to thank my SciTech office mates for encouragement, support, and productive conversation, including Dr. Isabella Pallotta, Dr. Xiuli Wang, Dr. Keiji Numata, Dr. Qiang Lu, Dr. Keiji Numata, and Dr. Waseem Raja.

Next I would like to acknowledge and express my deep gratitude to my colleagues who contributed to my project. I would like to thank Dr. Qiang Lu for assistance with silk glycerol films, Dr. Biman Mandal for scientific conversation, career advice, and silk scaffolds. I would like to thank Dr. Michael Lovett and Lindsay Wray for help and instruction with bioreactors. Thank you Dr. William

Woods, for helping with early cell extractions, and with force measurements. Thank you Dr. Jelena Rnjak-Kovacina, I wouldn't have gotten as far as I have without your advice, guidance, and finesse with Xacto knives. Thank you also to Jelena for providing silk scaffolds, help with plans, and PDMS construct chambers. Dr. Marie Tupaj and Dr. Corinne Wittmer contributed immensely to my understanding of electrical stimulation and electrospinning, respectively, and were both a pleasure to work with. Thank you to the Smith lab at Northeastern for letting me borrow eggs from you when I was in a pinch and for being so accommodating and helpful.

Thank you to all of my undergraduate students. You have been a joy to work with, and I am so glad to have had the chance to get to know and teach each of you. Jonathan Jo, you were so dedicated, motivated, and wonderful to be around. Thank you so much for your hard work and determination, especially since you worked with me at a time when I didn't have it all figured out yet. Sarah Gardner, I appreciated your diligence, organization, intelligence, and your great sense of humor. You are an awesome person I truly enjoyed working with you. Nikita Saxena and Carter Palmer, you both are so pleasant, observant and intelligent. Thank you for your contributions to the cell separation work. Valerie Luks and Joshua Wilner, you guys were so much fun to work with. You both worked really hard in a short time to devise an electrical stimulation platform with me. I was not only impressed by your work ethic, but by the enjoyable environment you create around yourselves. Wesley Field, thank you so much for all of your help. You worked so hard and were able to accomplish so much, I am very proud of you and appreciate your commitment. Bentley Hunt, you were so great to work with. It was so nice to be able to share an idea with you, and watch

you work out the solution on your own. You're going to do amazing in grad school, congratulations!

I want to thank my friends, who have been with me throughout this experience and have seen me at all stages of joy, frustration, and insanity that go along with the process. Thank you for your support and advice. Thank you so much to my parents, who have supported me infinitely and in so many ways. I know sometimes you didn't know what I was doing or going through, but you were always there for me and I feel your unconditional love every day. To my brother, we are two very different people but we care about the same things. I can't tell you how happy it makes me knowing two days after my thesis defense, I am going to be sitting at your graduation. I am so proud of you and I love you so much. To my boyfriend, Mike, all I can say is thank you for making me the luckiest girl on the planet. You were so understanding and supportive through my journey the past year. Thank you especially for being there for me while I've been writing my thesis, and for taking me to hit a bucket of golf balls when I needed to clear my head. I love you.

Emily Pitcairn and DOCTOR LAURA DOMIGAN, I have been so fortunate to have the two of you come into my life. Emily, thank you for being so enthusiasm, encouragement, and teamwork. You are so much fun to work with, and even more fun to have a glass of wine with. Laura, who knew you could have a soul sister on the other side of the planet? I am so happy David brought you here; you are an amazing colleague and have become a true mentor to me. Thank you for taking so much time to give me advice about my career and my work, and for helping me so much with the writing of my thesis. More importantly, thank you for your friendship. I know we will always be close no matter where our paths end up taking us.

Finally, I would like to acknowledge and thank my thesis committee. You have all been so helpful and supportive and I always look forward to conversations with each one of you. You all have contributed a great deal to the work I have done and I so appreciate your guidance. George, thank you so much for the time you've taken and the interest you've shown in my project. It was so helpful to have a muscle expert to look to for guidance. You're also really enjoyable to be around and I'm looking forward to staying in touch with you. Lauren, thank you for opening up your office and your lab to me, your advice and support have been invaluable. Barry, I truly could not have come this far without you, thank you for always taking the time to sit down with me when I needed help, and for making me a part of your lab. I have really enjoyed the experience. David, first I want to thank you for bringing together such an amazing group. I have had the opportunity to meet and work with so many amazing scientists, and I attribute this to your skills at bringing people together. Thank you also for allowing me to dive into the lab freely and steer things as I went along. Thanks also for exposing me to DARPA and the related ins and outs of funding and grants. But most importantly, thank you for believing in me. I never pictured myself doing a PhD., but your encouragement and advice helped me stay determined and focused and I am so happy with the outcome. You have been the best mentor I could've asked for and working in your lab was a life-changing experience for me. Thank you. J.

Table of Contents

Abstract	ii
Acknowledgements	iv
Table of Contents	viii
Chapter 1. Introduction	2
1.1 Project objective and scope	2
1.2 Bioactuation	4
1.2.1 Current actuators	4
1.2.2 Bioactuation concept and advantages	8
1.2.3 Potential applications.....	8
1.3 Skeletal muscle tissue engineering	9
1.3.1 Vertebrate skeletal muscle physiology and function.....	9
1.3.2 Tissue engineering	12
1.3.3 Current approaches to skeletal muscle tissue engineering	13
1.3.4 Mammalian bioactuators.....	25
1.4 Insect Cells	31
1.4.1 Motivation and potential from organism-level	31
1.4.2 Insect skeletal muscle physiology and function.....	34
1.4.3 Current research in insect cell cultivation <i>in vitro</i>	37
1.4.4 Insect bioactuators.....	38
1.5 References	41
Chapter 2. Cell sourcing and isolation	49
2.1 Introduction	49
2.2 Cell sourcing and staging	52
2.3 Cell isolation approach and culture conditions	55
2.4 Hormonal regulation of differentiation and proliferation	61
2.4.1 Differentiation with 20-hydroxyecdysone (20HE).....	61
2.4.2 Proliferation with juvenile hormone (JH)	64
2.7 Summary	66
2.8 References	68
Chapter 3. Cell population characterization	71
3.1 Introduction	71
3.2 Cell type identification	72
3.2.1 Differentiated muscle	72
3.2.2 Muscle precursor cells (myoblasts)	76
3.2.3 Neurons	78
3.2.4 Yolk cells (vitellophages)	80

3.3 Prolonged survival	81
3.4 Spontaneous contractile activity	83
3.5 Summary	88
3.6 References	89
Chapter 4. Metabolic analyses	91
4.1 Introduction.....	91
4.2 Comparison with mouse.....	93
4.3 Culture responses to subtractive media	97
4.4 Metabolic influence of vitellophages.....	100
4.4.1 Vitellophage metabolism.....	101
4.4.2 Cell separation methods	102
4.4.3 Cell separation metabolism	108
4.5 Summary	110
4.6 References	112
Chapter 5. 3D construct formation	113
5.1 Introduction.....	113
5.2 C2C12 construct development.....	115
5.2.1 Silk-glycerol films	115
5.2.2 Silk sponges	116
5.2.3 Electrospun silk-gel constructs	121
5.3 Insect construct development.....	125
5.3.1 Application of mammalian approaches.....	125
5.3.2 PDMS micropatterned channels	127
5.3.3 ECM extraction and coating.....	130
5.3.4 Scaffold-free constructs constrained by PDMS chambers	135
5.4 Insect construct characterization	138
5.5 Alignment improvement	141
5.6 Multifiber version.....	142
5.7 Performance testing.....	145
5.8 Summary	148
5.9 References	150
Chapter 6. Future directions and conclusions	152
6.1 Further cell system refinement	152
6.1.1 Cell type separation and purification.....	152
6.1.2 Genetic manipulation	155
6.1.3 Immortalization and cryopreservation.....	157
6.1.4 ECM analysis and materials development	161
6.1.5 Cell type “tool box” and medical device applications	163
6.2 Metabolism.....	164
6.2.1 Muscle – yolk cell interactions and metabolic mechanism	164
6.2.2 Muscle – fat interactions	165

6.3 Construct output improvement	165
6.3.1 Reinforced structures.....	165
6.3.2 Mechanical stimulation	166
6.4 Controlling contraction	167
6.4.1 Electrical stimulation	167
6.4.2 Chemical stimulation.....	168
6.5 Device design and modeling to achieve locomotion	168
6.5.1 Moving PDMS structures	168
6.4.2 Modeling bioactuated devices	171
6.6 Silk-based biodegradable robots	172
6.7 Conclusions	174
6.6 References	176
Chapter 7. Experimental	180
7.1 Procedures for cell isolation	180
7.1.1 <i>M. sexta</i> embryo staging.....	180
7.1.2 Isolation and culture of <i>M. sexta</i> myoblasts.....	180
7.1.3 Applying mammalian culture conditions	181
7.1.4 Differentiation with 20-hydroxyecdysone	182
7.1.5 Proliferation with juvenile hormone.....	182
7.1.6 Statistical analysis	183
7.2 Procedures for cell characterization	183
7.2.1 Cell type identification.....	183
7.2.2 Prolonged survival	185
7.2.3 Spontaneous contractile activity	185
7.3 Procedures for metabolic analyses	186
7.3.1 Metabolic comparison with mouse muscle	186
7.3.2 Subtractive media experiments	189
7.3.3 Influence of vitellophages	189
7.4 Procedures for 3D construct formation	191
7.4.1 Silk-glycerol films.....	191
7.4.2 Electrospun silk-gel constructs	192

*NEW AND EMERGING TECHNOLOGIES FROM SKELETAL MUSCLE TISSUE
ENGINEERING: INSECT MUSCLE BIOACTUATORS FOR ROBOTIC APPLICATIONS*

Chapter 1. Introduction

1.1 Project objective and scope

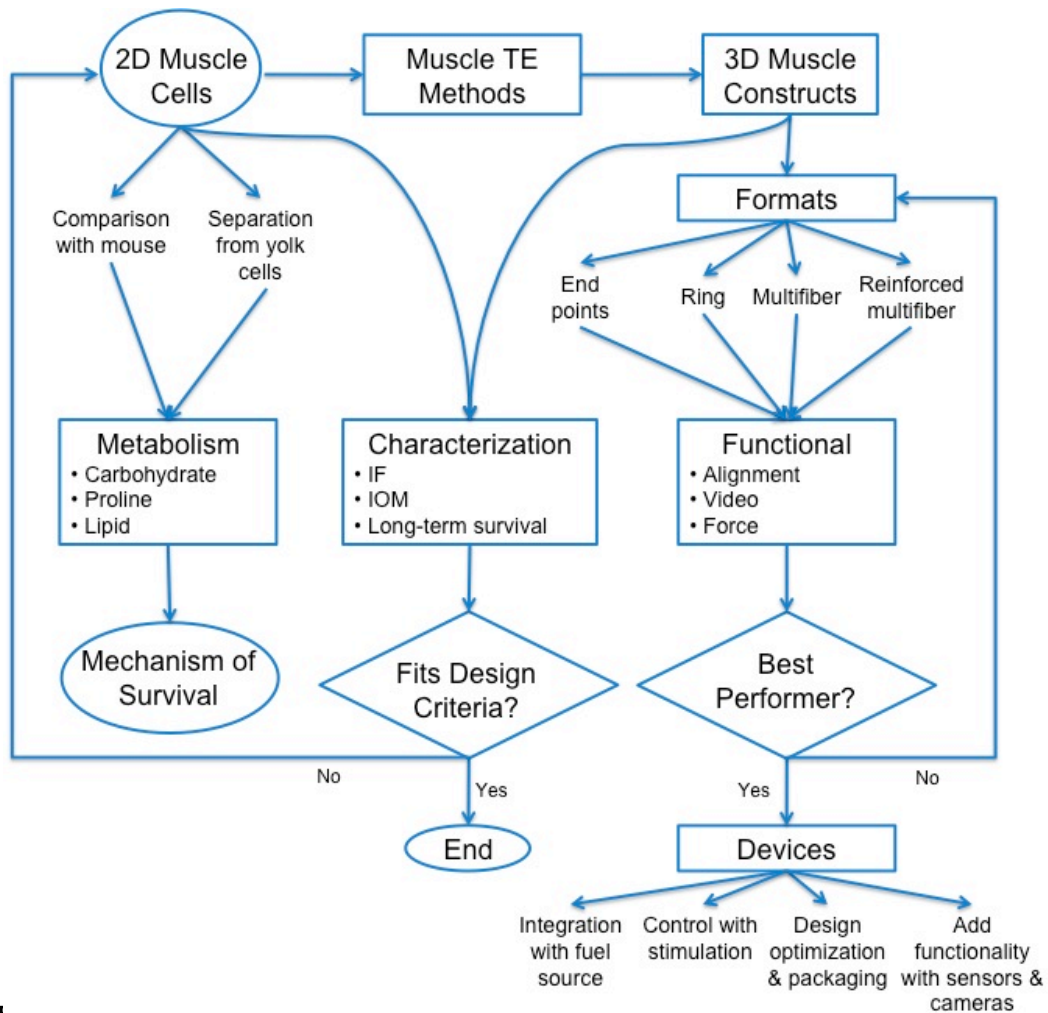
The overall goal of this thesis was to identify, develop, and test a unique cell system for the *in vitro* regeneration of skeletal muscle tissue, appropriate for bioactuation applications. Design criteria for this application include long-term operability, room temperature functionality, and large force production with contractions occurring in the time frame of seconds. Eventually, this work could lead to the development of synthetic or biodegradable devices, driven by biological muscle motors and chemical or cellular fuel, for medical applications, ecological field research, and defense or rescue-related deployment and reconnaissance.

We identified *Manduca sexta* (*M. sexta*), a Lepidopteran insect, as a candidate cell source for this work. In the larval stage, *M. sexta* has large, super-contracting muscles that act as actuators during crawling. Furthermore, insects in general have robust and adaptive tolerances to changes in environmental conditions such as temperature and oxygen levels, as well as internal challenges such as extracellular pH variation and low nutrient availability. We chose to work with embryonic *M. sexta* cells for the development of this *in vitro* culture system, as they lead to the formation of our target tissue, larval muscle. Although insect cells have not been cultured extensively *in vitro*, and have never been tissue engineered into functional 3-dimensional (3D) structures, we used cues from

insect, crustacean, mollusk, and vertebrate literature to derive appropriate techniques and conditions for isolating, propagating, and differentiating skeletal muscle from embryonic *M. sexta* cells. We characterized these cells and examined their metabolism (Figure 1.1). The results of these studies verified our hypothesis that insect cells would be an appropriate cell system due to environmental robustness and longevity *in vitro*.

We then utilized mammalian skeletal muscle tissue engineering methods, along with cues from the *Drosophila melanogaster* (*Drosophila*) muscle developmental program, to generate 3D muscle tissues from our embryonic cell system (Figure 1.1). The versatile techniques we developed allowed for a wide range of muscle geometries and formats to be generated, all of which could be functionally tested to compare their performance to one another and to other bioactuator systems in the literature (Figure 1.1). Simultaneously, functional data helped inform the design of the soft robotic devices, which we would like to integrate with our muscle actuators.

In this thesis, we will demonstrate a unique and fascinating *in vitro* cell system, which may be further developed and refined in future work by the incorporation of genetic manipulation, mechanical stimulation, and electrical stimulation. Furthermore, with the development of a functional chemical or cellular fuel system and appropriate robotic designs, a terrestrial bioactuated robot could be realized (Figure 1.1).



I
 FROM EMBRYONIC *M. SEXTA* CELLS, AS WILL BE DISCUSSED IN THIS THESIS. 2D = 2-DIMENSIONAL, TE = TISSUE ENGINEERING, IF = IMMUNOFLUORESCENCE STAINING, IOM = INDEX OF MOVEMENT ANALYSIS

1.2 Bioactuation

1.2.1 Current actuators

An actuator is a device that converts energy, typically in the form of electricity, magnetism, flow or pressure, into mechanical output. Actuators are

often used to generate motion or action in the systems they are integrated with (Najarian *et. al.*, 2012).

Conventional actuators generally induce locomotion using moving or sliding parts, and include electrostatic, electromagnetic, hydraulic and pneumatic actuator types (Siamak *et. al.*, 2012). Electrostatic actuators utilize electric fields to generate mechanical output. However, magnetic fields tend to have higher energy densities than electric fields; for this reason, electromagnetic actuators are more widely used than electrostatic (Najarian *et. al.*, 2012). Electromagnetic actuator types generate a magnetic field within an air gap, using either a permanent magnet or coil windings. The air gap separates the actuator's stationary and moving parts and, as the magnetic fields interact in the gap, torque is produced. Examples of electromagnetic actuators include electric motors, DC motors, solenoids, and stepper motors. Hydraulic and pneumatic actuators utilize incompressible liquids and compressible gases, respectively, to generate pressure and drive a piston. These actuators are often used in robotic limbs for locomotion. The relative advantages and disadvantages of these actuator types are compared in Table 1.

More novel actuators have been designed and implemented in recent years, especially as the fields of bio-robotics and bio-mimetics have emerged to service the biomedical device industry and for use in next generation robotics. These include piezoelectric materials, shape memory alloys, and electro-reactive gels. Piezoelectric materials respond to electric fields by deforming their shape and dimensions. As described in Table 1.1, there are several advantages to piezoresponsive actuators, such as precise control, fast response time and low power requirements, however these actuators are only suitable for applications where small displacements are required. Shape memory

alloy (SMA) actuators are made with materials having the unique property of recovering a predefined shape after having been deformed (Siamak *et. al.*, 2012). This solid-solid phase transition occurs as a result of a change in the material's crystal structure upon heating above a critical temperature. The most common SMA material is Nitinol, a nickel-titanium alloy (Najarian *et. al.*, 2012). SMAs can be miniaturized, leading to their application in medical equipment and a wide array of robotic devices (Rossi *et. al.*, 2011; Villanueva *et. al.*, 2011; Lin *et. al.*, 2011). However, slow response times and temperature sensitivity impede fast dynamics in these materials. Chemical actuators include polymeric hydrogels that inherently respond to environmental changes such as temperature, pH, and ionic concentration by altering their hydrophilicity. Such actuators have been applied to MEMS (microelectromechanical systems) devices, artificial muscles, and automatic microfluidic systems, where a chemical actuator can simultaneously perform sensor and actuator functions based on the properties of the fluid flowed through the device (Najarian *et. al.*, 2012; Takashima *et. al.*, 2012; Gil *et. al.*, 2010). Even bubbles formed via controlled electrolysis have been used to actuate a lever arm in a MEMS device (Ho *et. al.*, 2005). However, researchers continue to search for strategies to effectively mimic the force-length and force-velocity properties of biological muscle (Klute, *et. al.*, 2002).

TABLE 1.1 COMPARISON OF ADVANTAGES AND DISADVANTAGES FOR VARIOUS ACTUATOR TYPES.
ADAPTED FROM GOMIS-BELLMUNT & CAMPANILE, 2010).

ACTUATOR TYPE	ADVANTAGES	DISADVANTAGES
Electrostatic	<ul style="list-style-type: none"> - Easy to model using Coulomb Law 	<ul style="list-style-type: none"> - Lower energy density than electromagnetic
Electromagnetic	<ul style="list-style-type: none"> - Good energy density - Easily controllable - Power source can be far away 	<ul style="list-style-type: none"> - Lower energy density than hydraulic
Hydraulic	<ul style="list-style-type: none"> - Very good energy density - Strokes as long as needed - Easily controllable - Power source can be far away 	<ul style="list-style-type: none"> - Requires high pressure - Prone to leakage - Flammability due to oil
Pneumatic	<ul style="list-style-type: none"> - Good energy density - Strokes as long as needed - Easily controllable - Power source can be far away - Can work at higher temperatures than hydraulic - Autoclavable - Uses air - Lighter than hydraulic due to lower working pressures 	<ul style="list-style-type: none"> - Lower energy density than hydraulic - Slower than hydraulic - Less efficient than hydraulic - Prone to leakage - Requires lubrication
Piezoelectric	<ul style="list-style-type: none"> - Small, precise position changes - Can be miniaturized - High energy density - Rapid response times - Low power - Magnetic field not required - Compact, no moving parts - Durable 	<ul style="list-style-type: none"> - Small displacement range - High voltage required - Non-linear responses
SMA	<ul style="list-style-type: none"> - High energy density - Can be miniaturized - Multiple configurations 	<ul style="list-style-type: none"> - Slow response time - Temperature-dependent - Low efficiency - Limited lifetime
Chemical	<ul style="list-style-type: none"> - Large size and shape changes - Respond to range of environmental stimuli - Can be used to generate “automatic” microfluidic systems 	<ul style="list-style-type: none"> - Diffusion limits dynamics and practical size - System needs to be designed to change environmental condition, then return to original state

1.2.2 Bioactuation concept and advantages

A bioactuated system would be one that takes advantage of the natural properties and elegant design of muscle tissue in order to achieve locomotion in an abiotic device. With the advent of microtechnology, including MEMS, many traditional means of device design and fabrication have had to be reimagined in order to achieve desired miniaturization. Although components can now be fabricated on the micro- and nanoscale, power supplies and external hardware on the macro scale are often still required.

One proposed solution is to replace actuators requiring external power with living muscle. Such bioactuators could convert the chemical energy in glucose to ATP and, therefore, mechanical work. One of the advantages of fabricating an actuator from cells, rather than materials such as SMA springs or pneumatic pumps, are their ability to self-assemble, which would greatly reduce high fabrication costs associated with manufacturing small actuators. Self-assembly also lends itself to a massively parallel manufacturing process, which would significantly improve time requirements and output over current serial processing (DARPA BAA-10-65, 2010). Additionally, these devices could be powered by natural fuel sources such as sugar and fat, operate silently over fast time scales, and biodegrade after use.

1.2.3 Potential applications

The applications for a bioactuated device include pumps and levers for MEMS devices, actuators in small robots, and moving parts in any meso-scaled device or robot.

MEMS and microfluidic devices are well-suited in size for biomedical applications, and therefore bioactuators could be adapted to such devices and applied as drug dispensing implants or for pressure-mediated nucleic acid transfection, similar to those described in the literature (Sheybani *et. al.*, 2013; Shimizu *et. al.*, 2012). Other microactuated devices that bioactuators could be incorporated with include microtweezers for surgeries and manipulations requiring fine control, and MEMS mirror array deflection (Bhisitkul & Keller, 2005; Xie *et. al.*, 2003).

Although traditionally, people think of robots as being large, heavy, metal machines, potential applications for robots are diversifying greatly, and so are their designs. Small, flexible robots could be used in non-invasive exploratory surgery, search and rescue, and reconnaissance. As such, they should be on a centimeter length-scale, the size of a pill or caterpillar. A bioactuator component based on insect muscle would enhance small robots of this design because such muscles work on a similar soft, hydrostatic system in their native environment when they deform the body wall of a caterpillar larva.

1.3 Skeletal muscle tissue engineering

1.3.1 Vertebrate skeletal muscle physiology and function

Vertebrate skeletal muscle is a highly organized tissue, with alignment and repetition of structure occurring on several scales. At the macroscopic level, muscle is composed of bundles of fibers, known as fascicles, and is enclosed in a layer of connective tissue (Adams, 2004). Each fascicle, which is also wrapped in a connective tissue layer, or perimysium, is composed of bundles of individual muscle fibers. Smaller collections of muscle fiber cells are further ensheathed in

collagenous connective tissue called the endomysium (Lieber, 2002). Both the structural scaffolding and multi-scale organization of the tissue contribute to its ability to coordinate its function.

On the subcellular level, skeletal muscle is further organized into myofibrils and sarcomeres, which are the contractile units of the cell. Sarcomeres are comprised of proteins, the most important of which are myosin and actin. These two proteins lie in a parallel arrangement, overlapping to produce shortening, or contraction, upon calcium binding, and restoring their original separation distance upon relaxation and calcium release.

This process is activated by electrical and chemical signaling occurring around and within the muscle, known as excitation-contraction coupling. Innervating neurons contact the muscle fibers at defined locations, where the muscle expresses a high density of neurotransmitter receptors. In mammals, the molecule that acts as a neurotransmitter between the neuron and muscle is acetylcholine (Ach). The binding of Ach to its receptor on the muscle cell membrane, or sarcolemma, results in an influx of sodium into the cell, causing the internal membrane potential to increase. When this value crosses a threshold, an action potential is generated. The Transverse (T)-tubules are invaginations in the sarcolemma, which allow the action potential impulse to be conducted into the cell. Transmembrane receptors on the T-tubules, called dihydropyridine receptors (DHPRs), interact closely with ryanodine receptors (RyRs) on the sarcomplasmic reticulum (SR) surface. When DHPRs sense voltage change due to an action potential impulse, a conformational change is induced, which activates RyRs, causing calcium release. Calcium binds to troponin, a component of the sarcomere complex. The conformational change in troponin induced by calcium binding causes tropomyosin to be pulled away from

the myosin head, allowing actin to bind to the exposed myosin. The myosin head swivels and pulls the actin; the collective action of many myosin heads swiveling in unison results in muscle shortening. Subsequently, adenosine triphosphate (ATP) binds to myosin, forcing the myosin-actin bond to break. However, if calcium is still available when the ATP dephosphorylates and releases the myosin, it may bind with the next actin molecule on the thin filament and cause further shortening to occur. When the impulse has passed, calcium is pumped back into the SR, and the myosin head once again contacts the overlying tropomyosin, rather than actin. This is known as thin filament-regulated contraction.

The contractile action of one actin-myosin crossbridge is not enough to yield motion in an organism. Rather, the coordinated action of many crossbridges occurring simultaneously in many cells must take place, and these cells are anchored to a lever system in vertebrates, connecting to rigid bones via tendons. In the vertebrate motor unit, one neuron innervates several muscle cells, thereby enacting contraction of several cells at once upon activation. This response can be modulated, to have more or less fibers engaged based on the frequency, duration and number of motor units activated to result in a graded response, with the force output being modulated to match the demand.

Fueling the process of contraction is ATP; therefore, it is crucial that it is accessible to the muscle when contraction is needed. Depending on the substrate available and activity level, this may be derived from several sources. Creatine phosphate is stored in the muscle cells and when it donates a phosphate group to adenosine diphosphate (ADP), ATP is produced. However, this energy source can only maintain contraction for several seconds. Glycogen stored in the cell, or glucose from the bloodstream, can undergo glycolysis,

whereby glucose is anaerobically converted to pyruvic acid and 2 ATP are produced. If oxygen is not available, pyruvic acid will be converted to lactic acid, which eventually accumulates and causes muscle fatigue. If oxygen is available, pyruvic acid from glycolysis, or free fatty acids from the bloodstream, may be transported to the mitochondria. There, they undergo aerobic respiration, breaking down into water and carbon dioxide, while producing thirty-four additional ATP molecules.

Many of the aspects of vertebrate muscle discussed here are in contrast to the physiology and function of insect muscle. These differences will be discussed in Section 1.4.2.

1.3.2 Tissue engineering

Tissue engineering is a field of biomedical research at the intersection of biology and classical engineering disciplines such as mechanical and chemical engineering. The integration of fundamental developmental biology and biochemistry research, along with creative strategies for building complex cell and tissue-scale structures, provide the basis for this area of research.

The field first emerged as both biomaterial implant technologies and cell transfer techniques were being actively explored. Biomaterial implants are meant to strengthen damaged or degenerated tissue, but often host cells do not penetrate the entire material, or they form fibrous tissue instead of the tissue type under repair (Langer *et. al.*, 1990). Similarly, cell transfer techniques are intended to repopulate a damaged tissue area with the appropriate cell type, but when simply injected, they tend to diffuse away from the site of need (Qu *et. al.*, 1998). By combining implantable, biodegradable materials with the cell type of interest first *in vitro*, a neo-tissue may be formed. This resulting cell-biomaterial structure

has a stronger ability both to attract native cells and to hold the transplanted cells in place, resulting in improved tissue outcomes *in vivo* (Langer & Vacanti, 1993; Langer *et. al.*, 1995).

Early successful demonstrations of the tissue engineering paradigm targeted cartilage, bone, and muscle tissue types (Vacanti *et. al.*, 1991; Vacanti *et. al.*, 1995; Saxena *et. al.*, 1999). Since these initial studies, techniques have been refined to provide prevascularization, specialized tissue structural organization, and complex tissue formation (Mikos, *et. al.*, 1993; Grayson *et. al.*, 2009; Mikos *et. al.*, 2006). Furthermore, potential applications for tissue engineering have expanded to include disease models, robotic components, and even food (Subramanian *et. al.*, 2010; this dissertation; Datar & Betti, 2010).

1.3.3 Current approaches to skeletal muscle tissue engineering

A significant effort has been made to generate muscle tissue *in vitro*. Such work mainly seeks to address clinical issues such as degenerative diseases, traumatic injuries and cardiac repair. Thus, mammalian models have been the primary focus (Qu *et. al.*, 1998, Saxena *et. al.* 1999, Scime *et. al.* 2009). Numerous obstacles have been encountered such as the need for vascularization to meet high metabolic demands, the difficulty in recapturing complex cellular and subcellular organization, and the inability to generate contractile forces approaching those of native tissue (Levenberg *et. al.* 2005, Huang *et. al.* 2005). In general, the process of recreating skeletal muscle tissue *in vitro* involves cultivating large numbers of muscle precursor cells, selecting a 3-dimensional biomaterial substrate that will provide appropriate stiffness and guide cellular alignment, and developing appropriate culture conditions for muscle stem cells propagation and differentiation within the scaffold. Growth

factors and cytokines are applied to the cells to induce differentiation. In recent years, additional mechanical and electrical stimuli have been shown to improve differentiation and maturation outcomes. Perfusion bioreactor systems allow for greater viability throughout the structure and can enable larger structures to be generated.

Myogenic Cells

The cell sources most widely used for skeletal muscle tissue engineering are the murine cell line C2C12, and primary satellite cells, which are adult muscle stem cells. The C2C12 line is a myoblast cell line from normal adult C3H mice (Yaffe & Saxel, 1977). These cells are robust, fuse readily, and contract spontaneously. Primary cells may provide a more physiologically-relevant model. Satellite cells are adult muscle stem cells that reside between the muscle fiber and basal lamina in vertebrates. These cells remain quiescent until activated by injury or exercise, at which time they proliferate, commit to myogenic differentiation, and are incorporated into the underlying muscle fibers. Satellite cells are isolated from muscle biopsies and may be released from muscle fibers with enzymatic treatment or from explant cultures. The procedure may be carried out with a variety of species, but mouse and rat cells are the preferred models.

Muscle stem cells such as satellite cells are identified with immunofluorescent labeling, RT-PCR analysis, and histology. Markers used to identify satellite cells include Pax7, desmin, Myf-5, and MyoD (Koning *et al.*, 2011; Choi *et al.*, 2008; Levenberg *et al.*, 2005; Ouellette *et al.*, 2009). Pax7 is a transcription factor required for satellite cell survival and self-renewal in perinatal development (Lepper *et al.*, 2009). It is also involved in the transition to the adult stem cell state. In mature adults, Pax7 is expressed by satellite cells in

quiescence (Zammit *et. al.*, 2006). Desmin is an intermediate filament protein. Its expression differs across species, and can be found in both mitotic and post-mitotic cells (Allen *et. al.*, 1991). Myf-5 is active in both quiescent satellite cells and satellite cell-derived activated myoblasts (Figure 1.2, Zammit *et. al.*, 2006). MyoD expression is necessary for later withdrawal from the cell cycle in preparation for myoblast fusion; its presence is found in activated and committed myoblasts (Kahane *et. al.*, 2001). Figure 1.2 details the events leading from quiescent satellite cells through myofiber formation, and the markers that are frequently used to identify these events.

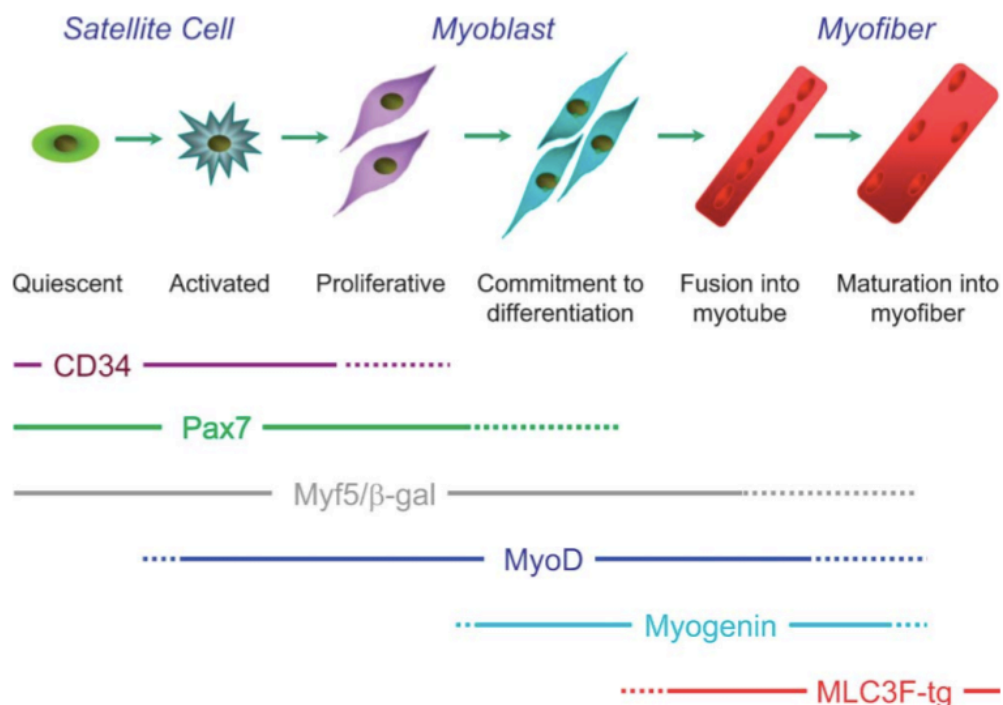


FIGURE 1.2 SCHEMATIC SHOWING SATELLITE CELL PROGRESSION FROM QUIESCENCE TO MYOFIBER FORMATION AND DIFFERENTIATION, WITH ASSOCIATED MARKERS FOR EACH STAGE. TAKEN FROM ZAMMIT *ET. AL.*,2006.

Media

Medium formulations are intended to provide the cells with not only nutrition, but the soluble factors found *in vivo* that signal events to happen such as proliferation and development. Looking to developmental biology is a crucial strategy for successfully directing muscle cells to mature into functional muscle and to monitor their progress.

Skeletal muscle arises from the somites during development. Paracrine signaling instructs the determination of muscle precursor cells, which express MyoD proteins (Gilbert, 2006). Under the influence of growth factors such as hepatocyte growth factor, myoblasts proliferate. Once the cells withdraw from the cell cycle, cell adhesion proteins including fibronectin and laminin, along with integrins, aid in alignment, which leads to cell fusion (Gilbert, 2006). The multinucleated cells thus formed further differentiate, begin expressing muscle-specific proteins, and finally mature into contractile muscle fibers.

Media formulations for cultivating and differentiating skeletal muscle range from very simple to quite complex. In general for proliferation, Dulbecco's Modified Eagle's medium is used as the basal medium, which contains glucose, salts, vitamins and amino acids. Antibiotics are supplied, and a serum concentration of 10% v/v is typical. Differentiation is often achieved simply by lowering the serum concentration, or switching to a sera type less enriched in growth factors, for example, from fetal bovine serum to horse serum (Portier *et al.*, 1999). Through the reduction of available nutrients, cells withdraw from the cell cycle. As is the case for developing muscle, the cessation of proliferation is followed by cell fusion into multinucleated myotubes.

Although this approach successfully leads to differentiation, a growth factor-mediated program may also be followed. Insulin-like growth factor, glial-

derived neurotrophic factor, and brain-derived neurotrophic factor are often incorporated (Greene & Allen, 1991; Das *et. al.*, 2007). Mature muscle cell differentiation is often identified by labeling proteins of the sarcomere, such as myosin heavy chain.

Alignment guidance

Researchers have focused on guiding alignment to enable cell fusion and allow for unidirectional force generation. Electrospun fibers, micropatterned surfaces and selective adhesion have all been successfully employed (Choi *et. al.*, 2008; Bursac *et. al.*, 2002).

Electrospinning is a versatile technique whereby a polymer solution is electrically charged, sheared through a capillary and collected on a grounded substrate. The resulting nanometer-scale fibers closely mimic the structure of extracellular matrices (ECM) found *in vivo*. This strategy may be modified to generate aligned fibers, which can then be employed as a scaffold for tissue engineered skeletal muscle constructs. In one study, a PCL and collagen blend was used to form electrospun fibers, which were aligned by using a grounded rotating mandrel as a collector. The degree of fiber alignment was found to correlate with the mandrel rotation speed. The fibers were cross-linked and the solvent removed under vacuum before human skeletal muscle cells were seeded on them. After seven days of differentiation, cells on aligned meshes had a high degree of alignment and myotubes were significantly longer, though not wider, than cells cultured on randomly-oriented fibers (Choi *et. al.*, 2008). Although this is a good method for aligning cells, it does not result in the three-dimensional cell-cell and myofiber-myofiber bundling that occurs in native muscle.

Micropatterned substrates are often generated using simple techniques, such as microabrasion, or microcontact printing, which is more laborious but enables very precise control of patterns. Microabrasion is a straight-forward method of patterning a 2D surface by rubbing it with sand paper. The resulting surface topography, depending on the grit size used, consists of very fine parallel lines capable of aligning cardiomyocytes (Bursac *et. al.*, 2002). Increasing anisotropy was seen with increasing coarseness, indicating the deeper and wider grooves were, the better the cells responded. In this study, researchers also found a correlation between coarseness of abrading material and longitudinal conduction velocity upon electrical stimulation, further highlighting the importance of cellular alignment for muscle function. Although this method also serves to guide cell alignment, precise control over feature depths and widths is not possible, and since surfaces are abraded by hand, there is likely to be a significant degree of variability between substrate surfaces.

The process of microcontact printing begins with standard lithography, which involves generating a silicon master mold by exposing silicon, spin-coated with photoresist material, to UV light through a photomask designed in engineering drawing software. The regions exposed to UV light are cross-linked, allowing a topographical pattern to be made when the remaining uncross-linked photoresist is removed. Polydimethyl sulfoxone (PDMS), an elastomeric silicone material, is then cast on the master mold and allowed to cure. The PDMS is then demolded and silanized to promote protein adsorption. The patterned PDMS can then be used as a stamp; it is “inked” in a protein solution, allowed to dry, then pressed on to a substrate (Xia & Whitesides, 1998). The protein pattern is thusly transferred to the substrate, on which cells may be cultured. Cells prefer to adhere on the protein pattern; thereby, cell patterns may be generated. In one

study, a polyacrylamide gel was patterned using microcontact printing of laminin lanes (Zatti *et. al.*, 2012). When C2C12 cells were cultured on the patterns, proliferation decreased with increasing lane width, and differentiation increased with increasing lane width. When human myoblasts were used, differentiation also increased with increasing lane width, but there were no differences in proliferation on this basis. This approach allows for rapid and consistent generation of replicate samples, once a master mold is made, and is useful for investigating details of the muscle development process. However, cells will only remain attached to substrates as long as the protein coating remains; with time (days to weeks), cells degrade the protein layer. Once the coating is spent, the cells detach; thus, this approach is not suitable for long-term muscle tissue formation and maintenance.

Scaffolds

Although alignment in monolayer cultures allows cells to fuse and differentiate in a more physiologically-relevant manner than in the absence of alignment, the structure of native vertebrate muscle is much more complex than a single cell layer. Bundles of parallel muscle fibers are ensheathed in extracellular matrix to form 3D bundles of muscle bundles with nerves and blood vessels distributed throughout. Scaffold materials are often chosen or designed to mimic the biomechanical properties of the native extracellular matrix; therefore, for muscle applications, pliable or fibrous biopolymer substrates are often selected. In fact, studies have shown that both proliferation and differentiation of muscle precursor cells are improved on substrates mimicking the stiffness of native muscle ECM (Gilbert *et. al.*, 2010; Engler *et. al.*, 2004). A multitude of strategies have emerged to generate 3D muscle constructs that

mimic the structure and stiffness of skeletal muscle tissue. The following approaches are summarized in Table 1.2.

Self-assembled, contractile “myoids” have been reported by several groups, and typically utilize Matrigel, collagen or fibrin gels to hold the muscle cells together (Vandenburgh *et. al.*, 1996). Decellularized muscle or bladder matrix also provides an appropriate environment for cell growth and differentiation (Borschel *et. al.*, 2004; Merritt *et. al.*, 2010; Machingal *et. al.*, 2011). Similarly, sponge-type scaffolds can mimic the structure and mechanical properties of muscle ECM without the requirement for explanted tissue (Kroehne *et. al.*, 2008). As discussed earlier, alignment guidance enables cell fusion and allows for unidirectional force generation; therefore, micropatterned hydrogel matrices are often incorporated to guide the muscle structures as they form (Yan *et. al.*, 2007).

A widely-used strategy for forming tissue engineered muscle constructs involves seeding cells suspended in a gel on a PDMS surface that has been coated with laminin (Vandenburgh *et. al.*, 1996; Dennis & Kosnik, 2000; Huang *et. al.*, 2005; Lam *et. al.*, 2009). As the cells degrade the laminin, the gel begins to detach and roll up. When braided silk sutures, Velcro or stainless steel mesh pieces are put in place to act as artificial tendons, the result is a free-standing muscle construct (Vandenburgh *et. al.*, 1996). One attractive aspect of this approach is as the gel dehydrates and begins pulling on the attachment points, tension is created, which induces cellular alignment (Vandenburgh *et. al.*, 1996). However, this phenomenon may be dependent on the gel concentration, cell seeding density, and spacing between attachment points. Therefore, alignment outcomes may be difficult to control. Even when cells are successfully organized in aligned arrangements, the “roll-off” method results in a disorganized gross

structure within the cylinder. Since rolling a cell monolayer into a cylindrical shape does not closely mimic the process of muscle formation *in vivo*, an alternative method that enables greater control over the final tissue structure is desired.

The extracellular matrix of muscle itself can be obtained from decellularizing explanted muscle using detergents (Borschel *et. al.*, 2009). When recellularized by injection of cells into the remaining matrix, cells proliferate, differentiate, and partially gain native-like muscle organization and function. In one study, arrays of actin-myosin filaments were observed in regenerated muscles, though not as densely-packed and organized as in native tissue, and force was produced by the constructs. However, the average force production of the recellularized matrices was 17 μN , yielding a specific force of 12 N/m^2 , whereas native muscle excised from the same species produced a specific force of 239.7 kN/m^2 (Borschel *et. al.*, 2009).

Sponges can serve as synthetic versions of decellularized ECM, as they can be designed to mimic the structure and mechanical properties of native ECM. Aligned Type I collagen sponges were formed in one example by directional freezing of a collagen solution (Kroehne *et. al.*, 2008). When seeded with C2C12 cells, myotubes formed throughout the scaffold in an aligned arrangement, expressed myosin heavy chain, and laid down a laminin-rich basal lamina. When implanted in nude GFP-expressing mice with anterior tibia (AT) muscles removed, mice regained gait and function to 5 – 20% of preoperative twitch and tetanic forces, which is comparable to outcomes with an AT transplant. Host cells migrated and differentiated in the periphery of the graft; differentiation of host cells was not observed when an empty scaffold alone was transplanted. Overall, these scaffolds were successful at mimicking the structure

of native muscle, promoting cell development, and recruiting host cells to regenerate.

Since muscle cells grow well in a variety of gel biomaterials, researchers have used several techniques for patterning such gels to improve muscle tissue engineering outcomes. These include patterning the gel cells will be embedded in, or patterning a gel and seeding cells on top of it to guide formation of scaffold-free muscles (Yan *et. al.*, 2007). One approach to guiding tissue formation by patterning gel substrates was to create an aligned collagen structure by using a paintbrush to apply a layer of uncross-linked collagen in a parallel pattern onto a dish, and allowing the collagen to gel. Subsequently, cells are seeded over the gel and, after several days, an additional collagen layer and cell seeding are administered. This procedure resulted in generally aligned tissues packed densely with about 40 layers of cells, to thicknesses of about 150 μm . The tissues produced stresses of 0.95 N/m^2 , which is an order of magnitude less than that produced by muscle tissue grown in decellularized ECM (Yan *et. al.*, 2007; Borschel *et. al.*, 2009). This result highlights the importance of having proper cellular organization in addition to the need for high cell density.

TABLE 1.2 COMPARISON OF CURRENT MUSCLE TISSUE ENGINEERING APPROACHES.

Approach	Description	Advantages	Limitations
Self-assembled "myoids" (Vandenburgh <i>et. al.</i> , 1996)	Cells seeded on gel-coated silicone substrates roll up into free-standing structures	Self-assembly process, endpoints integrated	Small cylindrical constructs, lack proper organization
Decellularized muscle (Borschel <i>et. al.</i> , 2009)	Detergents used to remove cells from muscle biopsy, cells reseeded in matrix	Native-like architecture, appropriate environment for tissue development	Limited supply – biopsy or cadaver needed, low force production
Sponge scaffold (Kroehne <i>et. al.</i> , 2008)	Collagen solution frozen directionally to yield sponge with aligned pores. Seeded with high density cell suspension	Native-like architecture, appropriate environment for tissue development	Pore size limited (20 – 50 μm with this method), no prevascularization, still need cadaveric tissue to produce
Micropatterned Gels (Yan <i>et. al.</i> , 2007)	Collagen gel painted on dish to form aligned collagen fibers for cells to grow on	Simple procedure, high cell density throughout	Inexact method, loss of muscle gene expression over time, low specific force

Electromechanical stimulation

Developing muscle is exposed to a dynamic environment, receiving stimuli from lengthening bones and innervating neurons, in addition to soluble factors and ECM. Consequently, mechanical stimulation studies have been performed on muscle tissues grown *in vitro* to more accurately recapitulate developmental conditions. Such work suggests that tissues formed under strain/relaxation regimens undergo a greater extent of differentiation and yield higher elasticity and myofiber organization (Powell *et. al.* 2002; Vandenburgh *et.*

al., 1991). Mechanical stimulation may prove to be a valuable tool for addressing issues of insufficient organization of tissue engineered muscle constructs.

In addition to cellular organization and alignment, subcellular organization and sarcomere alignment are crucial for improved functional outcomes. The process of sarcomere assembly occurs in developing muscle via spontaneous, transient increases in calcium concentration. Electrical stimulation may be applied to *in vitro* muscle to control and manipulate calcium pulsing, thereby accelerating and improving subcellular organization (Fujita *et. al.* 2007). Stimulation is most often administered as square bipolar pulses of alternating current, at frequencies of 1-10Hz, with pulse widths of 24 ms, and amplitudes of 2-7, 40V/60mm (Park *et. al.*, 2008).

Vascularization and perfusion

Since muscle is such a highly metabolically-active tissue, vascularization must often be addressed in order to avoid tissue necrosis when engineering skeletal muscle *in vitro*. When tissues are cultured statically, cells on the periphery of the scaffold have access to medium nutrients first. If the tissue is dense, medium nutrients are not readily accessible to cells on the interior of the structure. As a result, these interior cells often die, not only due to an inaccess to oxygen and nutrients, but a lack of waste removal as well. Therefore, in dense structures such a muscle tissue, researchers are actively developing methods to deliver medium to all cells of the construct, and allow for waste to be removed.

Scaffold prevascularization may involve the incorporation of physical structures to mimic the vasculature, such as channels or micropatterned channel networks (Maidhof *et. al.*, 2012); by incorporating endothelial cells (Levenberg *et. al.*, 2005); or both (Wray *et. al.*, 2012). Perfusion involves the incorporation of a

pump-driven system, which pushes medium through the scaffold to more actively deliver nutrients to the cells and remove wastes. Existing designs for perfusion bioreactors often include a syringe or peristaltic pump, tubing, and a chamber that holds the scaffolds and media. Systems can be either closed loop, where media circulates continuously, or open loop, where medium flows through the bioreactor and to a collection bottle. In one example, a sterile housing holds custom-made scaffold chambers to allow individual scaffolds to be perfused through a tube incorporated into the scaffold (Lovett *et. al.*, 2010). Such studies demonstrate the improved viability of cells within the interior of engineered tissues when perfusion is employed. Perfusion can also be performed by other dynamic culture methods, such as spinner flasks or rotary bioreactors that simulate continuous falling.

1.3.4 Mammalian Bioactuators

As a result of the work that has already been performed in the field of muscle tissue engineering, new and exciting potential applications for the technology have emerged. For example, in the case of the field of actuation, smaller and less expensive devices are in demand to service the microdevice and MEMS sectors. Current microscale actuators are difficult to manufacture and therefore expensive. As a result, a platform allowing for the self-assembly of microscale actuators would simplify the manufacturing process and lower associated costs. Since muscle stem cells are intrinsically programmed to become muscle tissue, a tissue engineered skeletal muscle system has the ability to self-assemble, and could allow for the production of large numbers of actuators in parallel. Moreover, bioactuators could expand the range of potential

applications for meso-robots, including noninvasive exploratory surgery, as such devices could potentially be biodegradable.

Explants

Several studies have demonstrated the potential for explanted muscles to act as actuators in biotic-abiotic hybrid devices (Herr & Dennis, 2004, Akiyama *et. al.*, 2009). For example, Herr & Dennis created a controllable swimming robot using explanted frog leg muscles (Figure 1.3, 2004). The ends of the muscles were tied to the robot with sutures. One end of the muscle was attached laterally to the body of robot, while the other end of the muscle was attached to the base of an oscillating tail. When electrically stimulated with wire electrodes, muscle shortening caused the tail to swing in one direction, as the opposing muscle was stimulated, the tail swung in the other direction. In this way, the floating robot could swim for around seven hours before muscle failure.

The limited operation time of such a device points out the major limitation of explants; animals have to be sacrificed for each device and the lifetime of explanted tissues is extremely variable and limited in an *ex vivo* application. While this study served as a valuable proof-of-concept, a tissue engineering approach may be more appropriate due to the ability to control dimensions, composition, and force generation of such constructs, in addition to the potential for production scalability.

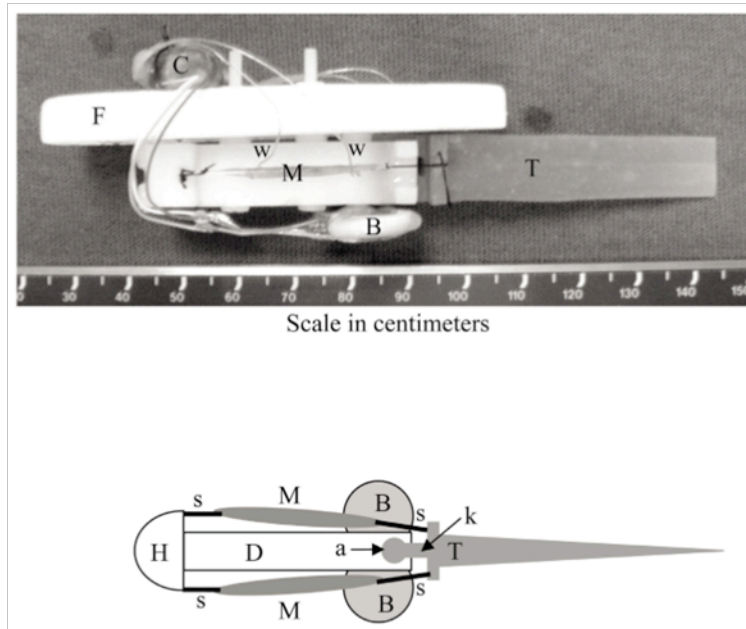


FIGURE 1.3 SWIMMING ROBOTIC DEVICE ACTUATED BY EXCISED FROG LEG MUSCLES. SIDE VIEW IMAGE (TOP) AND TOP VIEW SCHEMATIC (BOTTOM) TAKEN FROM HERR & DENNIS (2004). F = STYROFOAM FLOAT, C = MICROCONTROLLER, INFRARED SENSOR, AND STIMULATOR UNIT; W = ELECTRODE WIRES; M = SEMITENDINOSUS MUSCLES; B = LITHIUM BATTERIES; T = CAST SILICONE TAIL ASSEMBLY; H = RIGID DELRIN HEAD PIECE; S = SUTURE ATTACHMENTS; D = RIGID DELRIN BACKBONE; A = CYLINDRICAL TAIL MOUNTING BOSS; K = COMPLIANT HINGE SEGMENT.

Mammalian cardiomyocytes

Rat and mouse cardiomyocytes have been the most widely-used cell type for tissue engineered bioactuator studies. These cells are attractive for their synchronous and spontaneous contractile abilities (Horiguchi *et. al.*, 2009). Such constructs have mainly been used for basic studies of transport and response times, with the eventual goal of actuating of MEMS devices. For example, rat cardiomyocytes have been cultured on the surface of polydimethylsiloxane spheres and films to perform pumping or bending functions upon contraction (Figure 1.3A; Tanaka *et. al.*, 2007; Feinberg *et. al.*, 2007).

More recently, devices have begun to be developed that are structured using very thin elastomeric substrates or gels. In 2012, Nawroth *et. al.*

demonstrated bio-mimetic propulsion of a thin PDMS structure coated with rat cardiomyocytes (Figure 1.4B). Through the study of juvenile jellyfish structure and behavior, a synthetic, muscle-powered proof-of-concept of a micropump with simple repetitive behavior was designed. Electric fields were used to replace biological pacemakers in the animal. The elastic recoil of the recovery stroke was enabled by using a thin elastomer substrate. The geometry of the design served to achieve appropriate fluid boundary layers for efficient propulsion. Micropatterning of cells on the elastomer surface via microcontact printing yielded cellular alignment with functional syncytium for tissue-wide contraction. Although this was an effective proof-of-concept, the dimensions and lifetime of the device inhibit its long-term use as a functional pump. For example, the elastomer structure was only 22 μm thick, which is too thin for handleability and manipulation. Additionally, testing was performed at a single timepoint, four days after cell seeding, and prolonged cultivation of the cells and function were not demonstrated. It is likely that, since the cells are cultured on a coated silicone substrate, the cells would detach after around two weeks of culture, due to degradation of the fibronectin coating with time. As a result, this system would need significant design modifications if it were to be used as a long-term, functional device for real world applications.

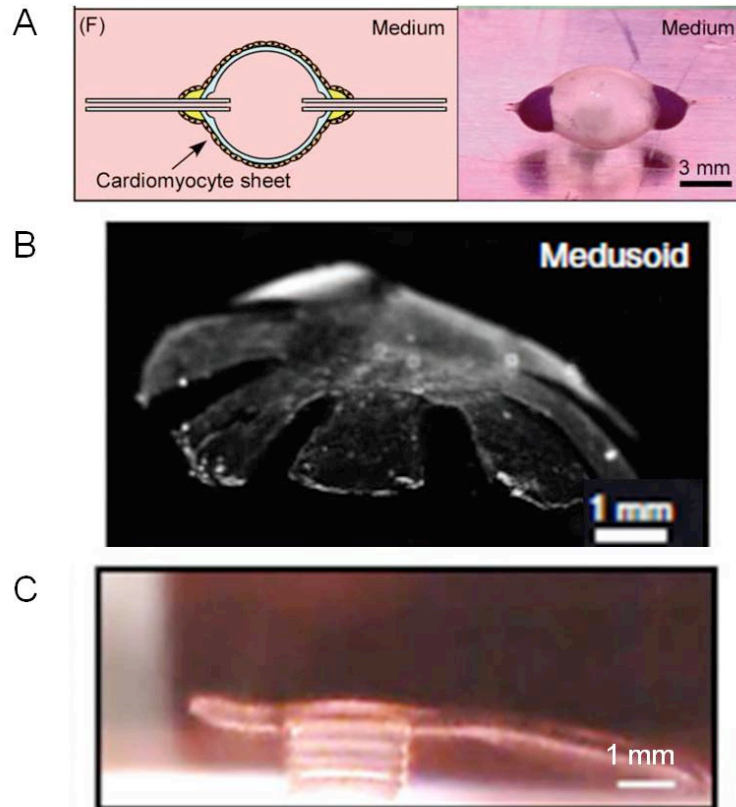


FIGURE 1.4 EXAMPLES OF MAMMALIAN CELL-BIOACTUATED DEVICES. A HOLLOW PDMS SPHERE COATED WITH CARDIOMYOCYTE SHEET TO PERFORM PUMPING ACTIONS (A, TAKEN FROM TANAKA *ET. AL.*, 2007). A JELLYFISH-LIKE PDMS SHEET COATED WITH CARDIOMYOCYTES TO MIMIC JELLYFISH SWIMMING AND FEEDING BEHAVIORS (B, TAKEN FROM NAWROTH *ET. AL.*, 2012). A 3D-PRINTED GEL “BIO-BOT” SEEDED WITH CARDIOMYOCYTES (C, TAKEN FROM CHAN *ET. AL.*, 2012).

Another example of a cardiomyocyte-powered micro-robot is the “Bio-bot” developed by Chan, *et. al.* (Figure 1.4C, 2012). Its fabrication takes advantage of 3D printing technology to generate poly(ethylene glycol) diacrylate gel Bio-bots with regionally-variable stiffness. When cells are applied to the structure, their traction forces alter the curvature of the cantilever “arm”, and overcome frictional forces of the dish by generating a power stroke when they contract. The force generated tilts the base forward and pushes it. This device was capable of locomoting at an average velocity of 236 $\mu\text{m/s}$ and traveled at total distance of 7.15 mm. While this is impressive for the state of the art, and the fabrication

process is much faster and readily iterated than conventional stereolithography techniques, the device only operates in aquatic environments. Additionally, the design of the robot, which consists of a bulky cubical base that the cell-coated arm pushes, could be improved to be more efficient and easy for the cells to effectively push forward. The robots are only able to perform work for 3 – 5 days, so longevity is also an issue that the group intends to address.

Controlling mammalian skeletal muscle-powered devices

All of the bioactuator examples described above undergo controlled contraction via bath stimulation or as a result of their natural rhythmic contractile properties. To date, a user-controllable bio-actuated device that can be steered via direct stimulation has not been developed outside of the Herr proof-of-concept robot described above. However, one can imagine a device whose body wall is made of a biomaterial printed with electrodes. The material properties of the device, including regional attachment point and adhesion protein coating, could promote cell attachment, growth and formation of muscle tissue in specified regions, allowing the actuators to form *in situ* and interface with the body wall and stimulating electrodes in precise locations. The long-term goal of the work initiated here is to develop such a device. Its benefits are that it could be biodegradable, and therefore used in applications such as exploratory surgery, reconnaissance, and unobtrusive observation of animals in their natural environments.

Other methods for stimulation include optogenetic control via genetic engineering of muscle cells to express light sensing channels (Sakar *et. al.*, 2012). The advantages to using this novel approach are that they are highly spatially controllable, which could aid in navigation, and do not lead to cellular

damage from high applied voltages and electrolysis. Additionally, an LED light source, rather than a current supply, is required for activation and could easily be incorporated into a light-weight, mobile robot. However, the structures generated in this work were very small, under 500µm in length and around 100µm wide. While this length scale allowed for detailed observation of myotube assembly, differentiation and output, such a structure would not be sufficient for powering meso-scaled devices. Chemical stimulation using pulses of compounds such as caffeine could also be used as an alternative to electrical stimulation.

1.4 Insect cells

1.4.1 Motivation and potential from organism-level

Despite the useful properties of the examples described in 1.2.4, stringent temperature, pH and osmotic pressure requirements impede the long-term use of such systems unless frequent media changes or a CO₂-regulated incubator are used. One potential application for tissue-engineered bioactuators is integration with meso-scaled robotic devices, which could lead to biomimetic locomotion and biodegradability of next-generation robots. However, bioactuators for this application would be expected to function in the real world, and would therefore require terrestrial locomotion at room temperature, robust and long-lasting function, and high force output.

Insect cells are excellent candidates to meet these challenges, as insects survive under a remarkable range of conditions and *in vitro* cultures may be maintained under ambient conditions (Lynn, 1996). Insect muscle systems are well-suited as linear actuators since they can have high power output (Josephson, *et. al.*, 2000), efficiency (Josephson, *et. al.*, 1991), and strain



(Woods, *et. al.*, 2008, Dorfmann, *et. al.*, 2007). For example, in a single work cycle, an isolated 5 mm muscle from the tobacco hornworm, *Manduca sexta* can pull a 3g weight a distance of 1.4 mm. The ability of these cells to function virtually maintenance-free for a long time highlights their potential as actuators for various devices such as micropumps or soft crawling robots.

Insects are known to adapt to environmental stresses by altering their use of metabolic pathways, a feature that may be helpful in future technological applications. For instance, the fruit beetle can endure long periods of starvation while still retaining the ability to fly by slowing glycolysis and synthesizing proline for use by the flight muscles (Auerswald & Gäde, 2000). Insulin-like peptides and insulin-like growth factor signaling (IIS) are important regulators of homeostasis and glucose metabolism in flies, as they are in humans. However, while IIS repression leads to disruption in glucose homeostasis and disease conditions such as diabetes in mammals, this same process incurs starvation management and lifetime extension in flies (Hull-Thomson *et. al.*, 2009). Longevity may be in part due to reduced organ deterioration, which is seen in flies with active insulin-like peptides pathways (Wu & Brown, 2006).

Additionally, fruit flies are able to endure hypoxic or anoxic conditions for several hours by reducing glycolysis and increasing dependence on pyruvate dehydrogenase over pyruvate carboxylase for conversion of pyruvate (Feala *et. al.*, 2009). Constraint-based modeling techniques were used to reveal the effects of the production of alternate metabolic byproducts in addition to lactate, such as alanine and acetate. Feala *et. al.*'s results demonstrated that acidification and glucose uptake were reduced and more ATP was produced than for the mammalian condition where lactate is the only anaerobic end-product (2007).

Similarly to IIS repression, this metabolic coping strategy results in smaller animals with longer lifespans.

Insect robustness to environmental conditions translates to insect-derived cells and tissues cultivated *in vitro* as well. A study of dorsal vessel cells (that act as an insect heart) isolated from Lepidopteran larvae demonstrated spontaneously contracting tissue could be maintained at room temperature for 18 days, with half-medium changes every two weeks (Akiyama *et. al.*, 2008). Although there was no attempt to describe the mechanism allowing for extended cellular survival, this result is consistent with experimental observations in the current work. Additional examples of the tolerance of insect cells to a range of environmental conditions are show in Table 1.3.

	Mammal	Insect
	 Bovine semitendinosus muscle	 <i>M. sexta</i> ventral interior medial muscle
Temperature	37°C	15 - 30°C ¹
pH	7.4	5 – 7
[Glucose]	4.5 g/L	1.23 g/L
Medium Refreshment	15X/month	0X/month

¹ *Drosophila* embryonic muscle observed to contract *in vitro* within this range, with optimal contraction between 25 – 27°C. Seecof & Donady (1972) *Mech. Of Ageing & Dev.* 1:165 – 174.

TABLE 1.3 COMPARISON OF *IN VITRO* CELL CULTURE CONDITIONS FOR MAMMALIAN AND INSECT CELLS.

1.4.2 Insect skeletal muscle physiology and function

The relative simplicity of insect tissues is also important for harnessing muscles for bioactuation applications. At the organ, cellular, and sub-cellular levels, insect skeletal muscle properties differ in some ways from vertebrate muscle.

Whereas most mammalian muscles contain thousands of fibers, arranged hierarchically and surrounded by ECM, *M. sexta* muscle usually consists of 2 – 14 single-celled myofibers, an arrangement which may be feasible to recapitulate *in vitro*. Surrounding each myofiber, there is very thin layer of basement membrane; however, the myofibers themselves are not bundled together into muscle units as in vertebrates (Rheuben & Kammer, 1980). Rather, a single muscle unit's myofibers are physically connected by their shared insertion points into the cuticle (Figure 1.5A) and electrically coupled through innervation by one shared neuron.

Insect muscles can be categorized in one of three classes: tubular, which comprise most adult muscles; fibrillar, which is a specialized class of adult muscles responsible for wing movements; and supercontracting, which includes visceral, heart, and larval intersegmental muscles, which are our muscle type of interest (Bernstein *et. al.*, 1993). Supercontractile muscles can contract beyond their resting length; their thin filaments have the ability to penetrate the Z-line. This remarkable capability allows for greater range of motion and flexibility, which is required for gut movements and for deforming the body wall. Furthermore, supercontractile muscles have 10 – 12 thin filaments surrounding each thick filament, which differs from both vertebrate muscle and adult insect muscle (Rheuben & Kammer, 1980).

In addition to undergoing thin filament-mediated contraction, which is described in Section 1.3.1, thick filament-mediated contraction can also occur in invertebrate skeletal muscle (Bernstein *et. al.*, 1993). During this process, calcium released upon neurotransmitter binding binds to calmodulin. This complex then binds to myosin light chain kinase, which phosphorylates myosin light-chain 2. This phosphorylation event permits actin binding to myosin, and the remainder of the contraction process carries out as for thin filament-mediated contraction. Additionally, while vertebrate skeletal muscles tend to have consistent thick and thin filament structure, invertebrate thick and thin filament structure varies widely across species, life stages, and even within the same animal (Hooper *et. al.*, 2008).

While most mammals use a lever system to generate large-scale motions from short, brief muscle contractions, soft-bodied insects such as *Manduca sexta* undergo body movements that more closely reflect the timing and contraction of the underlying muscles (Woods *et. al.* 2008). Larval body wall muscles contract seven times more slowly than fast adult muscles, and respond strongly to tetanic stimulation but not to single impulses, which further reflects how their properties suit the slower dynamics and greater force requirements for generating locomotion in soft-bodied hydrostats (Rheuben & Kammer, 1980). Consequently, the development of larval muscle *in vitro* would be advantageous for designing a bioactuated device, since the actuators would be expected to behave in the same way. As a result, the insect muscle system is well-suited for developing actuators for soft-bodied robots.

Larval muscle cells insert into the body wall cuticle via epithelial tendon-like cells (TCs, Figure 1.5B). TCs allow for force produced by the contracting muscle to be transmitted to the body wall, enabling deformation of the soft cuticle

and thereby generating locomotion. During development, these cells attract and assist in muscle patterning and development, which is very closely linked with their own development. Although specification of tendon cells occurs in a muscle-independent fashion, a later differentiation step requires contact from developing muscles in order to maintain TC-specific gene expression (Soustelle *et. al.*, 2004).

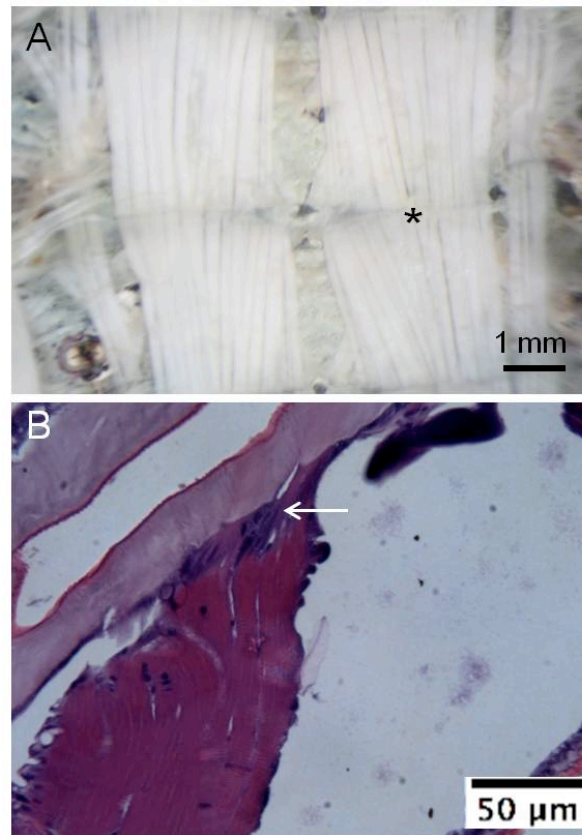


FIGURE 1.5 LARVAL MUSCLE STRUCTURE *IN VIVO*. IMAGE OF BODY WALL MUSCLES WITH GUT, FAT BODY, AND TRACHEA REMOVED (A). VIEW IS OF DORSAL SIDE, TOP OF THE IMAGE IS ANTERIOR. * = BODY SEGMENT BORDER, WHERE MUSCLE INSERTS INTO CUTICLE. HISTOLOGICAL SECTION STAINED WITH H&E, SHOWING LARVAL MUSCLE INSERTION (B). BRIGHT PINK INDICATES MUSCLE FIBERS, DARK PURPLE OVALS ARE NUCLEI. ARROW INDICATES TENDON-LIKE CELL MONOLAYER INTERFACING MUSCLE WITH CUTICLE (LT. PURPLE).

Mammalian muscle relies upon the transport of nutrients and gases through a complex vasculature; in contrast *M. sexta* does not have blood vessels and the transport of oxygen to tissues is mainly by passive diffusion through the tracheal system. Depending on the developmental stage of the insect, nutrients are delivered to muscle from the fat body in the form of the insect sugar trehalose, diacylglycerol, or proline. The fat body uses a shuttle system to transport diacylglycerol to the muscle, where it is then converted to free fatty acids. Trehalose is taken up by the muscle from the hemolymph. Proline is derived from protein stores.

1.4.3 Current research in insect cell cultivation *in vitro*

Insects have been widely-studied for a range of purposes, including understanding their development and physiology (Truman & Riddiford, 1999), using their cells for industrial protein production (Benslimane *et. al.*, 2005; Rhiel *et. al.*, 1997), and probing their genetics for clues into the mechanisms of human diseases (Beller *et. al.*, 2010; Law & Wells, 1989).

As a result of the benefits for use of insect cells in protein production, methods have been developed for culturing insect cells *in vitro*. The medium, which is often purchased commercially and supplemented with serum, peptones, and antibiotics, is often formulated to mimic the inorganic salt concentration, pH, amino acid concentration, among others, of the insect hemolymph for the species of interest (Lynn, 1996). Insect cells are kept in sealed, humidified containers and incubation temperatures usually range from 25 - 28°C.

Lepidopteran species are often selected for cell line initiation due to their ease of transfection and wide-spread use in baculovirus expression vector systems (Lynn, 1996). Cells are often sourced from immature tissue types such

as embryos, imaginal disks, and ovaries, due to their enrichment in stem cells (Baines, 1996). For example, Pan *et. al.* established cell lines from embryonic tissue of *Bombyx mori* (*B. mori*, 2007). The cell types appeared epithelial-like in morphology, and underwent exponential growth when analyzed at the 30th passage. Another epithelial-like embryonic cell line was developed in *Helicovera armigera*, another Lepidopteran species; these cells were found to be susceptible to baculoviral infection (Sudeep *et. al.*, 2002).

1.4.4 Insect bioactuators

Several studies by Akiyama *et. al.* have been performed to determine the feasibility of applying insect cells to a bioactuation application (2008, 2009, 2010, 2012). Initially, the researchers attempted to extract and dissociate heart cells from larvae to obtain cardiac muscle tissue (Akiyama *et. al.*, 2008).

Dorsal vessels, which act as hearts in insect larvae, were dissected and plated in culture dishes. Cells migrated from the tissues, which themselves were observed to beat spontaneously. When the concentration of fetal bovine serum (FBS), was increased from 10% to 20%, spontaneously contracting cells were observed, and their activity persisted for more than 18 days. The authors suggested that tissue engineering has the most potential for generating a bioactuated system, and that scaffold-free constructs, although not yet demonstrated in vertebrate tissue systems, would be ideal for this application. However, in a follow-up study, the group chose to move forward with excised tissue, rather than a tissue engineering approach, citing difficulties in the mass culturing of contracting cells as the major issue (Akiyama *et. al.*, 2009).

Researchers chose the dorsal vessel (DV) of *C. agnate* (inchworm); it is a tubular organ that serves to circulate hemolymph within the larva, and is

appealing for bioactuation applications because it contracts spontaneously when excised. After demonstrating the ability of excised dorsal vessel tissue to survive and contract *in vitro* for over 30 days, and successfully applying electrical stimulation, Akiyama *et. al.* constructed a simple bio-microrobot device actuated by dorsal vessel tissue (2009, 2010, 2012). The organ was placed onto a silicone elastomeric structure with micropillars, applying tension to the organ as it was intertwined in the pillars. Spontaneous shortening and torsional contractions of the DV caused locomotion of the elastomeric device at a velocity of 3.5 $\mu\text{m/s}$ over a 125 μm distance.

Despite the progress towards a room temperature operable functional device demonstrated in this study, several issues still need to be addressed. The structure only advanced 1% of the structure's total length over the course of the experiment. Additionally, the robot is limited in its dimensions due to the dimensions of the organ. The authors acknowledged that a future goal of theirs is to develop a protocol for dissociating the DV cells and forming a cell sheet, rather than using the excised tissue, to improve flexibility of structure design and control of functional outcomes.

In our present work, we seek a bottom-up approach by starting from muscle precursor cells and building functional muscle devices using techniques developed in mammalian tissue engineering research. By combining insect cells with tissue engineering techniques, we seek to overcome the current limitations in the field of bioactuation. Our overall goal is to demonstrate the ability of our tissue engineered insect muscle to function at room temperature, for extended period of time, and to have controllable dimensions, attachment features, and contractile properties. Eventually, this system will be integrated with current bioactuator designs to improve outcomes reported to date.

We have systematically investigated the isolation and characterization of embryonic muscle precursor cells from the *Lepidoptera Manduca sexta*. We then probed the metabolism of these cells to design cellular fuels for long-term power and to explain the extended cell survival we observed *in vitro*. We next attempted to apply skeletal muscle tissue engineering techniques to these cells, including micropatterning, incorporating biomaterials and cell adhesion proteins, and electrical stimulation. However, we often found that the cells developed most completely when we did not overly direct them using extracellular materials. We therefore developed a scaffold-free approach whereby the cell self-assemble in chambers. By closely investigating the cellular and metabolic properties of these cells, and by using cues from insect development and from the cells themselves, we have adapted mammalian tissue engineering techniques to create 3D, functional muscle structures that survive at room temperature and for months without medium replenishment. This improvement to current bioactuator cell sources will advance the capability of micro- and meso-scaled, cell-powered robots and could also lead to advances in *in vitro* meat production and *in vitro* soluble silk production from cultured *Bombyx mori* cells. Additionally, the methods developed here could be readily translated to other invertebrates with appealing muscle properties such as increased size, temperature tolerance, or muscle dynamics for an even wider range of bioactuator options.

1.5 References

- Adams A. (2004) *The Muscular System*. Westport, CT: Greenwood Press.
- Akiyama Y, Iwabuchi K, Furukawa Y, Morishima K. (2008) Culture of insect cells contracting spontaneously; research moving toward an environmentally robust hybrid robotic system. *J. Biotechnol.* 133: 261 – 266.
- Akiyama Y, Kikuo I, Furukawa Y, Morishima K. (2009) Long-term and room temperature operable bioactuator powered by insect dorsal vessel tissue. *Lab Chip* 9:140 – 144.
- Akiyama Y, Iwabuchi K, Furukawa Y, Morishima K. (2010) Electrical stimulation of cultured lepidopteran dorsal vessel tissue: an experiment for development of bioactuators. *In Vitro Cell. Dev. Biol. – Animal* 46:411 – 415.
- Akiyama Y, Hoshino T, Iwabuchi K, Morishima K. (2012) Room temperature operable autonomously moving bio-microrobot powered by insect dorsal vessel tissue. *PLoS ONE* 7(7):e38274.
- Allen RE, Rankin LL, Greene EA, Boxhorn LK, Johnson SE, Taylor RG, Pierce PR. (1991) Desmin is present in proliferating rat muscle satellite cells but not in bovine muscle satellite cells. *J. Cell. Physiol.* 149:525 – 535.
- Auerswald L & Gäde G. (2000) Metabolic changes in the African fruit beetle, *Pachnoda sinuate*, during starvation. *Journal of Insect Physiology* 46:343 – 351.
- Baines D. (1996) New approaches to insect tissue culture. *Cytotechnology* 20:13 – 22.
- Beller M, Bulankina AV, Hsiao H-H, Urlaub H, Jäckle H, Kühnlein RP. (2010) PERILIPIN-Dependent control of lipid droplet structure and fat storage in *Drosophila*. *Cell Metab.* 12:521 – 532.
- Benslimane C, Elias CB, Hawari J, Kamen A. (2005) Insights into the central metabolism of *Spodoptera frugiperda* (Sf-9) and *Trichoplusia ni* BTI-Tn-5B1-4 (Tn-5) insect cells by radiolabeling studies. *Biotechnol. Prog.* 21:78 – 86.
- Bernstein SI, O'Donnell PT, Cripps RM. (1993) Molecular genetic analysis of muscle development, structure, and function in *Drosophila*. *Int. Rev. Cytol.* 143:63 – 152.
- Bhisitkul RB & Keller CG. (2005) Development of microelectromechanical systems (MEMS) forceps for intraocular surgery. *Br J Ophthalmol* 89:1586 – 1588.

Borschel GH, Dennis RG, Kuzon WM. (2009) Contractile skeletal muscle tissue-engineered on an acellular scaffold. *Plast. Reconstr. Surg.* 113:595 – 602.

Bursac N, Parker KK, Iravanian S, Tung L. (2002) Cardiomyocyte cultures with controlled macroscopic anisotropy: A model for functional electrophysiological studies of cardiac muscle. *Circ. Res.* 91:e45 – e54.

Chan V, Park K, Collens MB, Kong H, Saif TA, Bashir R. (2012) Development of miniaturized walking biological machines. *Sci. Rep.* 2:857.

Choi JS, Lee SJ, Christ GJ, Atala A, Yoo JJ. (2008) The influence of electrospun aligned poly(ϵ -caprolactone)/collagen nanofiber meshes on the formation of self-aligned skeletal muscle myotubes. *Biomaterials* 29:2899 – 2906.

DARPA Broad Agency Announcement. (2010) Maximum mobility and manipulation (M3). DARPA-BAA-10-65

Das M, Wilson K, Molnar P, Hickman JJ. (2007) Differentiation of skeletal muscle and integration of myotubes with silicon microstructures using serum-free medium and a synthetic silane substrate. *Nature Protocols* 2(7):1795 - 1801.

Datar L & Betti M. (2010) Possibilities for an in vitro meat production system *Innov. Food Sci. Emerg. Tech.* 11:13 – 22.

Dennis RG & Kosnik PE. (2000) Excitability and isometric contractile properties of mammalian skeletal muscle constructs engineered *in vitro*. *In Vitro Cell. Dev. Biol. - Animal* 36:327 – 3.

Dorfmann A, Trimmer BA, Woods WA. (2007) A constitutive model for muscle properties in a soft-bodied arthropod. *J. R. Soc. Interface* 4:257 - 269.

Engler AJ, Griffin MA, Sen S, Bonnemann CG, Sweeney HL, Dischler DE. (2004) Myotubes differentiate optimally on substrates with tissue-like stiffness: pathological implications for soft or stiff microenvironments. *J. Cell Biol.* 166(6): 877 – 887.

Feala JD, Coquin L, McCulloch AD, Paternostro G. (2007) Flexibility in energy metabolism supports hypoxia tolerance in *Drosophila* flight muscle: metabolomic and computational systems analysis. *Mol. Syst. Biol.* 3:99.

Feala JD, Coquin L, Zhou D, Haddad GG, Paternostro G, McCulloch AD. (2009) Metabolism as means for hypoxia adaptation: metabolic profiling and flux balance analysis. *BMC Systems Biology* 3:91.

Feinberg AW, Feigel A, Shevkopyas SS, Sheehy S, Whitesides GM, et al. (2007) Muscular thin films for building actuators and powering devices. *Science* 317:1366 - 1370.

- Fujita H, Nedachi T, Kanzaki M. (2007) Accelerated *de novo* sarcomere assembly by electric pulse stimulation in C2C12 myotubes. *Exp. Cell Res.* 313:1853 - 1865.
- Gil ES, Park S-H, Tien LW, Trimmer B, Hudson SM, Kaplan DL. (2010) Mechanically robust, rapidly actuating, and biologically functionalized macroporous poly(*N*-isopropylacrylamide)/silk hybrid hydrogels. *Langmuir* 26(19):15614 – 15624.
- Gilbert PM, Havenstrite KL, Magnusson KEG, Sacco A, Leonardi NA, Kraft P, Nguyen NK, Thrun S, Lutolf MP, Blau HM. (2010) Substrate elasticity regulates skeletal muscle stem cell self-renewal in culture. *Science* 329(5995):1078 – 1081.
- Gilbert SF. (2006) *Developmental Biology 8th ed.* Sunderland, MA: Sinauer Associates.
- Gomis-Bellmunt O & Campanile LF. (2010) *Design Rules for Actuators in Active Mechanical Systems.* London: Springer-Verlag. pp 3 – 26.
- Grayson WL, Martens TP, Eng GM, Radisic M, Vunjak-Novakovic G. (2009) Biomimetic approach to tissue engineering. *Sem. Cell Dev. Biol.* 20:665 – 673.
- Greene EA & Allen RE. (1991) Growth factor regulation of bovine satellite cell growth in vitro. *J. Anim.Sci.* 69:146 – 152.
- Herr H & Dennis RG. (2004) A swimming robot actuated by living muscle tissue. *J. Neuroeng. Rehabil.* 1:1 – 6.
- Ho C-T, Lin R-Z, Chang H-Y, Liu C-H. (2005) Micromachined electrochemical T-switches for cell sorting applications. *Lab Chip* 5:1248 – 1258.
- Hooper SL, Hobbs KH, Thuma JB. (2008) Invertebrate muscles: Thin and thick filament structure; molecular basis of contraction and its regulation, catch and asynchronous muscle. *Progress in Neurobiol.* 86:72 – 127.
- Horiguchi H, Imagawa K, Hoshino T, Akiyama Y, Morishima K. (2009) Fabrication and evaluation of reconstructed cardiac tissue and its application to bio-actuated microdevices. *IEEE Trans. Nanobiosci.* 8(4):349 - 355.
- Huang Y-C, Dennis RG, Larkin L, Baar K. (2005) Rapid formation of functional muscle in vitro using fibrin gels. *J. Appl. Physiol.* 98:706 – 713.
- Hull-Thomson J, Muffat J, Sanchez D, Walker DW, Benzer S, Ganfornina MD, Jasper H. (2009) Control of metabolic homeostasis by stress signaling is mediated by the lipocalin NLaz. *PLoS Genet.* 5(4):e1000460

Josephson RK & Stevenson RD. (1991) The efficiency of a flight muscle from the locust *Schistocerca americana*. *J. Physiol.* 442:413.

Josephson RK, Malamud JG, Stokes DR. (2000) Power output by an asynchronous flight muscle from a beetle. *J. Exp. Biol.* 203(17):2667.

Kahane N, Cinnamon Y, Bachelet I, Kalcheim C. (2001) The third wave of myotome colonization by mitotically competent progenitors: regulating the balance between differentiation and proliferation during muscle development. *Development* 128:2187 – 2198.

Klute GK, Czerniecki JM, Hannaford B. (2002) Artificial muscles: Actuators for robotic systems. *Int. J. Robotics Res.* 21:295 – 309.

Koning M, Werker PMN, van Luyn MJA, Harmsen MC. (2011) Hypoxia promotes proliferation of human myogenic satellite cells: a potential benefactor in tissue engineering of skeletal muscle. *Tissue Eng. A* 17(13 – 14):1747 – 1758.

Kroehne V, Heschel I, Schügner F, Lasrich D, Brtsch JW, Jockusch H. (2008) Use of a novel collagen matrix with oriented pore structure for muscle cell differentiation in cell culture and in grafts. *J. Cell. Mol. Med.* 12(5A):1640 – 1648.

Lam MT, Huang Y-C, Birla RK, Takayama S. (2009) Microfeature guided skeletal muscle tissue engineering for highly organized 3-dimensional free-standing constructs. *Biomater.* 30:1150 – 1155.

Langer R, Cima LG, Tamada JA, Wintermantel E. (1990) Future directions in biomaterials. *Biomaterials* 11:738 – 745.

Langer R & Vacanti JP. (1993) Tissue engineering. *Science* 260:920 – 926.

Langer R, Vacanti JP, Vacanti CA, Atala A, Freed LE, Vunjak-Novakovic G. (1995) Tissue engineering: biomedical applications. *Tissue Eng.* 1(2):151 – 161.

Law JH & Wells MA. (1989) Insects as biochemical models. *J. Biol. Chem.* 264(28):16335 – 16338.

Lepper C, Conway SJ, Fan C-M. (2009) Adult satellite cells and embryonic muscle progenitors have distinct genetic requirements. *Nature* 460:627 – 631.

Levenberg S, Rouwkema J, Macdonald M, Garfein ES, Kohane DS, Darland DC, Marini R, van Blitterswijk CA, Mulligan RC, D'Amore PA, Langer R. (2005) Engineering vascularized skeletal muscle tissue. *Nat. Biotech.* 23(7):879 - 884.

Lieber RL. (2002) *Skeletal Muscle Structure, Function & Plasticity 2nd ed.* Baltimore, MD: Lippincott Williams & Wilkins.

Lin H-T, Leisk GG, Trimmer B. (2011) GoQBot: a caterpillar-inspired soft-bodied rolling robot. *Bioinsp. Biomim.* 6:026007.

Lovett ML, Rockwood D, Baryshyan A, Kaplan DL. (2010) Simple modular bioreactors for tissue engineering: A system for characterization of oxygen gradients, human mesenchymal stem cell differentiation, and prevascularization. *Tissue Eng. C* 16(6):1565 – 1573.

Lynn DE. (1996) Development and characterization of insect cell lines. *Cytotechnology* 20:3 - 11.

Machingal MA, Corona BT, Walters TJ, Kesireddy V, Koval CN, Dannahower A, Zhao W, Yoo JJ, Christ GJ. (2011) A tissue-engineered muscle repair construct for functional restoration of an irrecoverable muscle injury in a murine model. *Tissue Eng. A* 17(17 & 18):2291 – 2303.

Maidhof R, Tandon N, Lee EJ, Luo J, Duan Y, Yeager K, Konofagou E, Vunjak-Novakovic. (2012) Biomimetic perfusion and electrical stimulation applied in concert improved the assembly of engineered cardiac tissue. *J. Tissue Eng. Regen. Med.* 6(10):e12 – e23.

Merritt EK, Hammers DW, Tierney M, Suggs LJ, Walters TJ, Farrar RP. (2010) Functional assessment of skeletal muscle regeneration utilizing homologous extracellular matrix as scaffolding. *Tissue Eng. A* 16(4):1395 – 1405.

Mikos AG, Sarakinos G, Lyman MD, Ingber DE, Vacanti JP, Langer R. (1993) Prevascularization of porous biodegradable polymers. *Biotechnol. Bioeng.* 42:716 – 723.

Mikos AG, Herring SW, Ochareon P, Elisseeff J, Lu HH, Kandel R, Schoen FJ, Toner M, Mooney D, Atala A, Van Dyke ME, Kaplan D, Vunjak-Novakovic G. (2006) Engineering complex tissues. *Tissue Eng.* 12(12):3307 – 3362.

Nawroth JC, Lee H, Feinberg AW, Ripplinger CM, McCain ML, Grosberg A, Dabiri JO, Parker KK. (2012) A tissue-engineered jellyfish with biomimetic propulsion. *Nat. Biotech.* 30(8):792 – 797.

Najarian S, Dargahi J, Darbemamieh G, Farkoush SH. (2012) *Mechatronics in Medicine: A Biomedical Engineering Approach*. New York, NY:McGraw-Hill. pp 39 – 50.

Ouellette SE, Li J, Sun W, Tsuda S, Walker DK, Hersom MJ, Johnson SE. (2009) Leucine/glutamic acid/lysine protein 1 is localized to subsets of myonuclei in bovine muscle fibers and satellite cells. *J. Anim. Sci.* 87:3134 – 3141.

Pan, M-H, Xiao S-Q, Chen M, Hong X-J, Lu C. (2007) Establishment and characterization of two embryonic cell lines of *Bombyx mori*. *In Vitro Cell. Dev. Biol.* – *Animal* 43:101 – 104.

- Park H, Bhalla R, Saigal R, Radisic M, Watson N, Langer R, Vunjak-Novakovic G. (2008) Effects of electrical stimulation in C2C12 muscle constructs. *J. Tissue Eng. Regen. Med.* 2:279 – 287.
- Portier GL, Benders AAGM, Oosterhof A, Veerkamp JH, van Kuppevelt TH. (1999) Differentiation markers of mouse C2C12 and rat L6 myogenic cell lines and the effect of the differentiation medium. *In Vitro Cell. Dev. Biol. – Animal.* 35:219 – 227.
- Powell CA, Smiley BL, Mills J, Vandenburg HH. (2002) Mechanical stimulation improves tissue-engineered human skeletal muscle. *Am. J. Physiol. Cell. Physiol.* 283:C1557 – C1565.
- Qu Z, Balkir L, van Deutekom JCT, Robbins PD, Pruchnic R, Huard J. (1998) Development of approaches to improve cell survival in myoblast transfer therapy. *J. Cell Biol.* 142(5):1257 – 1267.
- Rheuben MB & Kammer AE. (1980) Comparison of slow larval and fast adult muscle innervated by the same motor neurone. *J. Exp. Biol.* 84:103 – 118.
- Rhiel M, Mitchell-Logean CM, Murhammer DW. (1997) Comparison of *Trichoplusia ni* BTI-Tn-5B1-4 (High Five™) and *Spodoptera frugiperda* Sf9 insect cell line metabolism in suspension cultures. *Biotechnol. Bioeng.* 55(6):909 – 920.
- Rossi C, Colorado J, Coral W, Barrientos A. (2011) Bending continuous structures with SMAs: a novel robotic fish design. *Bioinsp. Biomim.* 6:045005
- Sakar MS, Neal D, Boudou T, Borochin MA, Li Y, Weiss R, Kamm RD, Chen CS, Asada HH. (2012) Formation and optogenetic control of engineered 3D skeletal muscle bioactuators. *Lab Chip* 12:4976 – 4985.
- Saxena AK, Marler J, Benvenuto M, Willital GH, Vacanti JP. (1999) Skeletal muscle tissue engineering using isolated myoblasts on synthetic biodegradable polymers: Preliminary studies. *Tissue Eng.* 5(6):525 - 531.
- Scime A, Caron AZ, Grenier G. (2009) Advances in myogenic cell transplantation and skeletal muscle tissue engineering. *Frontiers in Bioscience* 14:3012 – 3023.
- Sheybani R, Gensler H, Meng E. (2013) A MEMS electrochemical bellows actuator for fluid metering applications. *Biomed Microdevices* 15:37 – 48.
- Shimizu K, Kawakami S, Hayashi K, Mori Y, Hashida M, Konishi S. (2012) Implantable pneumatically actuated microsystem for renal pressure-mediated transfection in mice. *J. Con. Rel.* 159:85 – 91.
- Siamak N, Dargahi J, Darbemamieh G, Farkoush SH. (2012) CHAPTER 3 Actuators and Feedback Sensors, from *Mechatronics in Medicine: A Biomedical Engineering Approach*. New York, NY: McGraw-Hill.

- Soustelle L, Jacques C, Altenhein B, Technau GM, Volk T, Giangrande A. (2004) Terminal tendon cell differentiation requires the glide/gcm complex. *Development* 131(18):4521 – 4532.
- Subramanian B, Rudym D, Cannizzaro C, Perrone R, Zhou J, Kaplan DL. (2010) Tissue-engineered three-dimensional *in vitro* models for normal and diseased kidney. *Tissue Eng. A* 16(9):2821 – 2831.
- Sudeep AB, Mourya DT, Shouche YS, Pidiyar V, Pant U. (2002) A new cell line from the embryonic tissue of *Helicoverpa armigera* HBN. (Lepidoptera: Noctuidae). *In Vitro Cell. Dev. Biol. – Animal.* 38:262 – 264.
- Takashima Y, Hatanaka S, Otsubo M, Nakahata M, Kakuta T, Hashidzume A, Yamaguchi H, Harada A. (2012) Expansion-contraction of photoresponsive artificial muscle regulated by host-guest interactions. *Nature Comm.* 3:1270.
- Tanaka Y, Sato K, Shimizu T, Yamato M, Okano T, et al. (2007) A micro-spherical heart pump powered by cultured cardiomyocytes. *Lab Chip* 7:207 – 212.
- Truman JW & Riddiford LM. (1999) The origins of insect metamorphosis. *Nature* 401:447 – 452.
- Vacanti CA, Langer R, Schloo B, Vacanti JP. (1991) Synthetic polymers seeded with chondrocytes provide a template for new cartilage formation. *Plast. Reconstr. Surg.* 88(5):753 – 759.
- Vacanti CA, Kim W, Upton J, Mooney D, Vacanti JP. (1995) The efficacy of periosteal cells compared to chondrocytes in the tissue engineered repair of bone defects. (1995) *Tissue Eng.* 1(3):301 – 308.
- Vandenburgh HH, Swasdison S, Karlisch P (1991) Computer aided mechanogenesis of skeletal muscle organs from single cells *in vitro*. *FASEB J.* 5:2860 – 2867.
- Vandenburgh HH, Del Tatto M, Shansky J, LeMaire J, Chang A, Payumo F, Lee P, Goodyear A, and Raven L. (1996) Tissue engineered skeletal muscle organoids for reversible gene therapy. *Human Gene Therapy* 7:2195-2200.
- Villanueva A, Smith C, Priya S. (2011) A biomimetic robotic jellyfish (Robojelly) actuated by shape memory alloy composite actuators. *Bioinsp. Biomim.* 6:036004.
- Woods WA, Fusillo SJ, Trimmer BA. (2008) Dynamic properties of a locomotory muscle of the tobacco hornworm *Manduca sexta* during strain cycling and simulated natural crawling. *J Exp. Biol.* 211:873 – 882.

- Wray LS, Rnjak-Kovacina J, Mandal BB, Schmidt DF, Gil ES, Kaplan DL. (2012) A silk-based scaffold platform with tunable architecture for engineering critically-sized tissue constructs. *Biomaterials* 33:9214 – 9224.
- Wu Q & Brown MR. (2006) Signaling and function of insulin-like peptides in insects. *Annu. Rev. Entomol.* 51:1 – 24.
- Xia Y & Whitesides GM. (1998) Soft lithography. *Annu. Rev. Mater. Sci.* 28:153 – 184.
- Xie T, Xie H, Fedder GK, Pan Y. (2003) Endoscopic optical coherence tomography with new MEMS mirror. *Electronics Letters* 39(21):20030998.
- Yaffe D & Saxel O. (1977) Serial passaging and differentiation of myogenic cells isolated from dystrophic mouse muscle. *Nature* 270:725 – 727.
- Yan W, George S, Fotadar U, Tyhovych N, Kamer A, Yost MJ, Price RL, Haggart CR, Holmes JW, Terracio L. (2007) Tissue engineering of skeletal muscle. *Tissue Eng.* 13(11):2781 – 2790.
- Zammit PS, Partridge TA, Yablonka-Reuveni Z. (2006) The skeletal muscle satellite cell: the stem cell that came in from the cold. *J. Histochem. Cytochem.* 54(11):1177 – 1191.
- Zatti S, Zoso A, Serena E, Luni C, Cimetta E, Elvassore N. (2012) Micropatterning topology on soft substrates affects myoblast proliferation and differentiation. *Langmuir* 28:2718 – 2726.

Chapter 2. Cell sourcing and isolation

2.1 Introduction

The model organism studied in this work is *Manduca sexta* (*M. sexta*). It has been selected because of its large size relative to other widely-studied insects such as *Drosophila melanogaster*. Additionally, since its larval stage is a soft-bodied, hydrostatic caterpillar, its muscles serve as actuators during crawling. As a result, muscles grown from *M. sexta* myoblasts have the potential to act as robust bioactuators in soft robotics applications. In future work, however, the techniques presented here may be extended to other organisms of interest in order to take advantages of desirable muscle properties such as size, freezing tolerance, and contractile frequency. The potential of these alternate systems is discussed in more detail in Section 2.2.

M. sexta is often used to study neuromuscular system formation and, more specifically, reorganization during metamorphosis. The motor neurons of adult muscles are the same as from the larvae, but have been respecified; this gives researchers a simple and interesting model system for investigating cell fate and hormonal control of metamorphosis (Bayline *et. al.*, 1998; Bayline *et. al.*, 2001; Champlin *et. al.*, 1999; Hegstrom & Truman, 1996). Muscle precursor cells have been cultured from *M. sexta in vitro*, however, they have all been myoblasts

in the pupae of developing adults (Kurtti & Brooks, 1970; Lehmann *et. al.*, 1985; Luedeman & Levine, 1996). Additionally, *M. sexta* embryonic cells have been reported; these cells were isolated from embryos well into development (dorsal closure, Eide *et. al.*, 1975). Embryos were individually dissected from eggs, and epithelioid, fibroblastic, neuron-like, and macrophage-like cells were observed. After 8 subcultures, the resulting cell line was stably fibroblastic in morphology.

Although there have not been examples of embryonic muscle cells cultured from *M. sexta*, studies have shown it is possible to derive these cells from *Drosophila* embryos (Seecof *et. al.*, 1971; Seecof & Donady, 1972; Bernstein *et. al.*, 1978). Seecof *et. al.* demonstrated that gastrulating *Drosophila* embryos could generate *in vitro* cultures of neurons and visceral muscle, but that the staging of these embryos was crucial to the differentiation of the appropriate cell types from the initially unspecialized embryonic cells (Seecof *et. al.*, 1971).

An invertebrate muscle cell line was also derived from the Chinese oak silkworm, *Antheraea pernyi* (Inoue *et.al.*, 1991). Researchers plated developing embryos, and cell masses were observed to develop rhythmic contractions after several months. Subsequent passaging of the cells also resulted in contracting masses and individual cells expressed tropomyosin. However, multinucleation, myosin heavy chain expression and distinct sarcomeres were not observed. Since invertebrate muscle is always striated, the researchers concluded that incomplete differentiation had occurred due to a lack of appropriate culture conditions. We therefore took these studies as a starting point from which to develop our techniques for generating embryonic muscle cell populations.

We have chosen to grow muscle tissues from muscle precursor cells rather than study the fully developed muscle for a device. Preformed muscles are terminally-differentiated, meaning that their development is complete and

manipulation of the size, shape, attachment points, and other characteristics are not feasible. Although they would presumably contract with many times higher force than *in vitro*-developed muscles, the dissection and removal of the tissue is labor-intensive and time-consuming. Excised tissues also vary widely in performance based on the individual, dissection technique, etc. Additionally, lifetimes from excised tissues are typically short, on the order of hours, while *in vitro* cultivated tissue can remain viable for months (Quinn *et. al.*, 2012). A tissue-engineered structure has the ability to self-assemble with little or no maintenance, and the size, shape, and end-point attachment materials may be custom-designed. Therefore, since our ideal cell source is a stem cell or muscle stem cell population capable of generating larval muscle tissue, we modeled our isolation methods and cell culture conditions from those developed for culturing cells from *Drosophila melanogaster* embryonic myoblasts (Bernstein, *et. al.*, 1978).

Muscle stem cells may be found in several of *M. sexta*'s life stages. During embryonic development, muscle stem cells are present following the onset of gastrulation, while rapid germ band extension is taking place. These myoblasts eventually form the larval muscles. During pupation, several larval muscles degenerate, with new muscles forming to enact the body plan of the adult. In order to accomplish this, regions of muscle stem cells are present at this stage as well. However, these cells are fated to become adult muscles, which have very different dynamic properties from larval muscles. Adult muscles, in order to power the rapid beating of the wings, contract with a much higher frequency than larval body wall muscles. The property differences arise from differences in the muscle fiber structure; for example, adult muscle sarcomeres are regularly spaced while larval muscles have irregular banding (Woods *et. al.*,

2008). Presumably, this feature might lead to a higher strain range and force production per contraction. Ideally, we would like our tissue-engineered muscle constructs to reflect the contractile properties of larval muscle, which perform as actuators during crawling. Therefore, we chose embryonic muscle precursor cells, which form the larval muscles, as our cell source.

Our methods for isolating and cultivating muscle cells were developed with the intent to allow for scalable collection, storage and usage of the cells, and subsequent self-assembly of muscle-based devices. We have therefore explored simple isolation methods, ambient culture conditions, medium development that allows for both muscle differentiation and maintenance, and cryopreservation techniques.

2.2 Cell sourcing and staging

Cells were isolated from embryos; this approach generated a high yield of usable cells and avoided the dissection of individual larvae. Additionally, embryonic cells have little developmental history, and thus a greater potential for manipulation than lineage-developed cells. Our aim was to collect muscle precursor cells, and to chemically induce their differentiation. Therefore, eggs were staged such that myogenesis had begun but muscle differentiation had not yet occurred, allowing us to harvest muscle precursor cells, which are readily able to become larval muscle.

The staging time for myoblast presence was determined from the myoblast staging strategy for *Drosophila*, which was to allow embryos to develop for four hours (Bernstein *et. al.*, 1978). At this point in the *Drosophila* program of development, gastrulation has begun and germ band extension is underway (Foe

et. al., 1993). These developmental events occur for *M. sexta* around nineteen hours post-ovipositioning; thus, a nineteen-hour staging time was chosen (Dorn *et. al.*, 1987). The staging time is a crucial factor in the generation of myogenic cultures; previous efforts to generate cell lines from *M. sexta* embryos, using staging times much further into development, resulted in cultures containing mainly fibroblastic cells (Eide *et. al.*, 1975). As terminally differentiated structures form, cell isolations disrupt these structures and damage their comprising cells; therefore, fibroblasts capable of migration are the primary populations that arise.

Our own experiments have further confirmed that a nineteen-hour staging time is optimal for muscle precursor collection. We harvested cells from eggs that had been allowed to develop for 8 hours, 19 hours, 50 hours, and 90 hours. Our hypothesis was that these staging times would correlate with the presence of stem cells, myoblasts, fat precursor cells, and differentiated tissues, respectively, based on reported timing of developmental events (Dorn *et. al.*, 1987). We indeed found enriched populations of the predicted cell types on the basis of staging time. An eight hour staging time resulting in a few stem cells, but mainly maternally-derived yolk cells were observed, as could be identified by their large size and lipid accumulation (Figure 2.1, top left). Some yolk cells were still present in cultures that had been staged for nineteen hours, but main cell type to appear from these cultures was muscle (Figure 2.1, top right). Fat populations were abundant in fifty hour-staged cultures, as indicated by lipid droplet staining (red, Figure 2.1, bottom left). Developed structures such as trachei and segments of the gut were found in ninety-hour staged cultures, but few dissociated cells were observed (Figure 2.1, bottom right). These results indicate that our approach not only allows us to target muscle precursor cells, but can be adjusted for harvesting other cell precursor types such as fat.

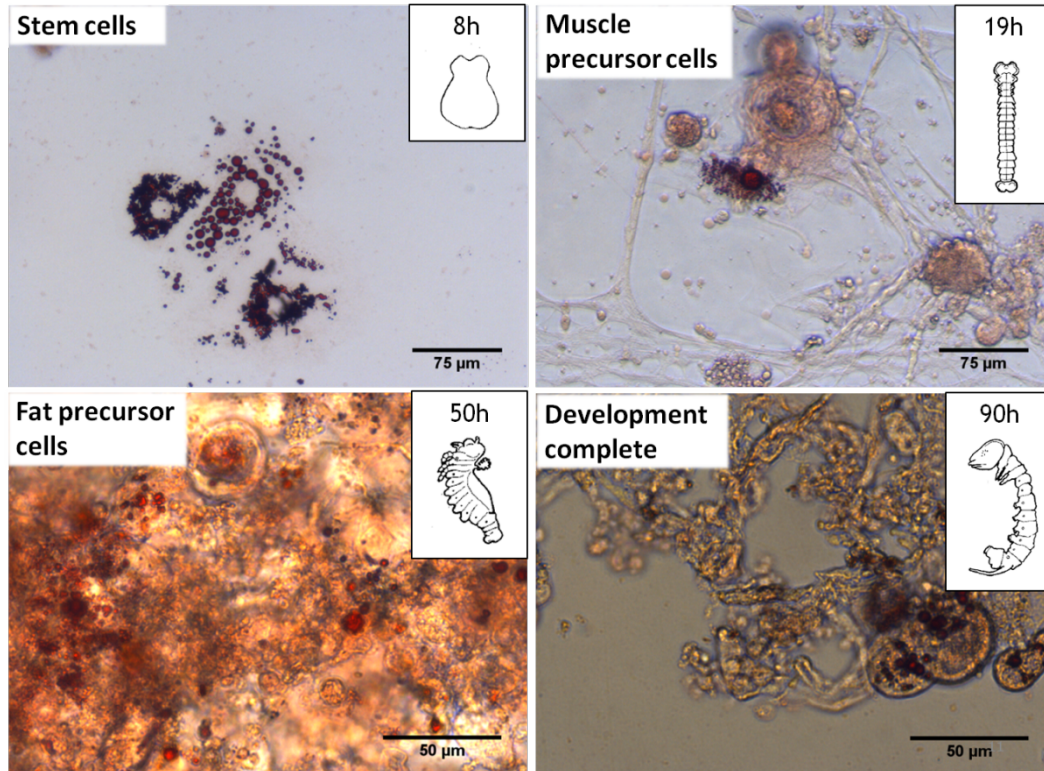


FIGURE 2.1. CELL POPULATIONS CULTIVATED *IN VITRO* FROM EMBRYONIC CELLS WITH VARYING STAGING TIMES. OIL RED O STAINING SHOWS PRESENCE OF LIPID DROPLETS IN YOLK CELLS PRESENT AFTER 8 HOURS OF DEVELOPMENT (RED, TOP LEFT), WHILE FEW YOLK CELLS AND MAINLY MUSCLE FIBERS GROW FROM 19 HOUR-STAGED EMBRYOS (TOP RIGHT). A HIGH ABUNDANCE OF LIPID STAINING IN 50 HOUR CULTURES INDICATED FAT CELL PRESENCE (BOTTOM LEFT). DEVELOPED STRUCTURES CAN BE OBSERVED IN 90 HOUR CULTURES (BOTTOM RIGHT).

This strategy does not only apply to *M. sexta*. *Drosophila* embryos staged in a similar way also produced fusion-competent muscle cells (Bernstein *et. al.*, 1978). A similar approach could be potentially taken to produce muscle with varying characteristics, reflecting the functional properties of the corresponding muscle *in vivo*. For example, cells have been isolated from shrimp, octopus, scallop, and lobster (Leudeman & Lightner, 1992; Necco & Martin, 1963; Odintsova & Khomenko, 1991; Panchin *et. al.*, 1993). Use of marine cells, in addition to obtaining new and interesting muscle properties, could lead to even broader applications, as these cells can tolerate lower temperatures than insect

cells. Furthermore, actively contractile and long-term viable muscle tissue has been cultured from *Mytilus trossulus* (mussel) larvae, and cardiomyocytes capable of dedifferentiation and regeneration have been isolated from adult zebrafish (Odintsova *et. al.*, 2010; Sander *et. al.*, 2013).

2.3 Cell isolation approach and culture conditions

Embryonic cells were isolated using a simple process by which embryos were lysed and the cells were collected by centrifugation, based on the method of Bernstein, *et. al.* (1978). As outlined in Figure 2.2, eggs were counted and washed to remove surface particulates, sterilized in bleach, and washed again under aseptic conditions. The embryos were then transferred to a Dounce homogenizer with a clearance smaller than the diameter of the eggs, but large enough to not lyse cells open (74 μm). After homogenization, the homogenate is collected and centrifuged twice to remove yolk material and collect the cells. The cells are then plated at a density of 5 eggs per square centimeter. Upon plating, cell masses containing myoblasts adhered to culture dishes. Due to the chelation of free calcium by ethylene glycol tetraacetic acid (EGTA), yolk material and most contaminating cell types did not attach; thus, an enriched culture of myogenic cells was generated (Bernstein *et. al.*, 1978).

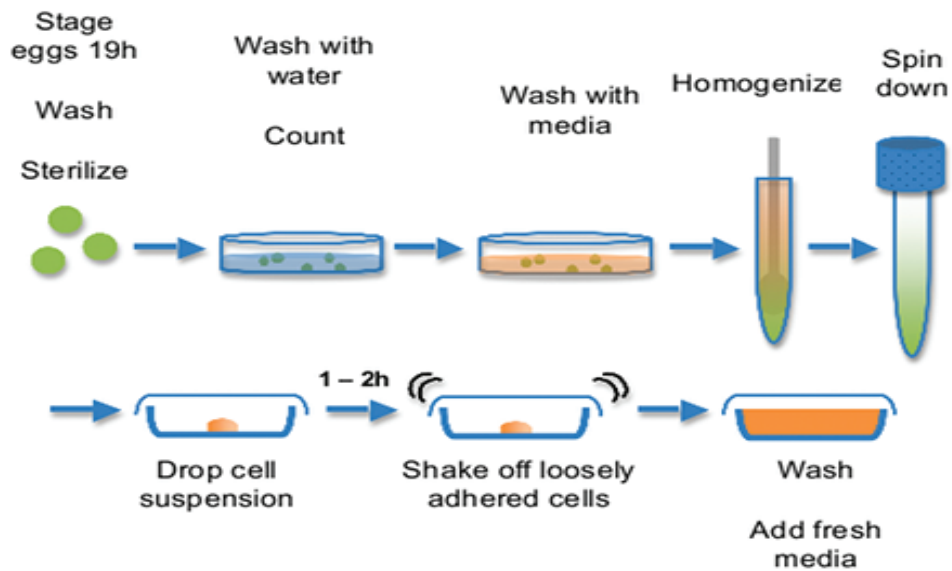


FIGURE 2.2. PROCESS DIAGRAM OUTLINING PROCEDURE FOR OBTAINING MUSCLE PRECURSOR CELLS FROM STAGED *M. SEXTA* EMBRYOS.

In addition to the process outlined above, several steps had to be adjusted to be optimally adapted to *M. sexta* eggs. These control points include the egg transfer process, centrifugation settings, removal of yolk, and media formulation.

M. sexta eggs are much larger than *Drosophila* eggs; they are approximately two millimeters in diameter. There are several steps in the isolation process that require transfer of eggs from one vessel to another. Depending on the experiment, several hundred eggs could be needed at once, and so the method for transferring eggs needs to be easy and efficient. Initially, 25mL sterile pipettes were used to move eggs from one vessel to another. However, the aperture of the 25 mL pipette is only three millimeters wide, and this closeness in size to the diameter of the eggs often led to clogging, which could greatly extend the duration of the isolation process. Several alternatives

have been explored, and the method which we have found the most success with is to use a sterile plastic transfer pipette, which has had the end cut off with a sterile razor.

We attempted to collect cells both by mechanical disruption of eggs and collection by centrifugation, and with manual dissection. We easily identified centrifugation settings that effectively pellet all of the cells; however, a large amount of yolk material was present as well. Manual dissections are often used in insect cell culture literature to obtain embryonic cells, however, we need high cell numbers for our studies, and the laborious method of individually dissecting embryos was found to be prohibitive. Additionally, our embryos were staged at an early point in development, and therefore the embryo fell apart into very small fragments when it was removed from the chorion. As a result, we chose to use mechanical disruption with a tissue homogenizer, and subsequent centrifugation for collecting large numbers of embryonic cells.

We attempted to adjust the centrifugation speed such that the cells were pelleted, yet the amount of yolk collected was minimal. The yolk material, which contains small vesicles of lipid, protein and carbohydrates, is less dense than the cells, and therefore we attempted to pellet the cells while leaving the yolk material in the supernatant. If the speed was set too high, a lot of yolk material would be included in the cell pellet. If the speed was too low, cells would be lost due to inefficient pelleting. We found that 200xg was the optimal speed to achieve a balance, with two rounds of centrifugation needed to most effectively remove yolk material. Even with this improvement, however, we found that washing the cells 24h post-plating was a necessary step as well.

The media formulation was based on that of Luedeman and Levine (1996). It was tested because the formula was developed specifically for muscle

precursor cell differentiation. Despite the ability of this media formulation to maintain the viability of our cells, the developmental stage of interest in Luedeman and Levine's study was developing legs during metamorphosis. Therefore, we hypothesized that a different level of the hormone 20HE, which is used to differentiate the muscle cells, would be required for our embryonic cultures. The optimization of 20HE levels is discussed in Section 2.4.1. Other changes that have been made from the original Luedeman and Levine media formulation are the replacement of fructose with additional glucose to simplify metabolism studies, the omission of niacin, and the replacement of vitamin and amino acid mixtures with commercially-available RPMI mixtures for ease of media preparation.

Insect cells are typically cultured at between 15 - 30°C and without a CO₂ incubator, as insect cells are generally more tolerant of pH changes. As with mammalian primary cultures, cell lines may be initiated from either dissociated cells or explants; however, unlike most mammalian cells, medium changes are only necessary every week or so, and it often takes months for cultures to reach confluence (Mitsubishi, 2002).

Under the culture conditions described above, myoblasts migrated from tissue masses and readily fused when exposed to low-level doses of 20HE (Figure 2.3). Within five days of plating, multinucleated myotubes began to contract spontaneously, possibly due to glutamate presence in the media. This activity persisted throughout the duration of the experiments (> 2 months). After one month, large muscle fibers and bundles could be observed (Figure 2.3).

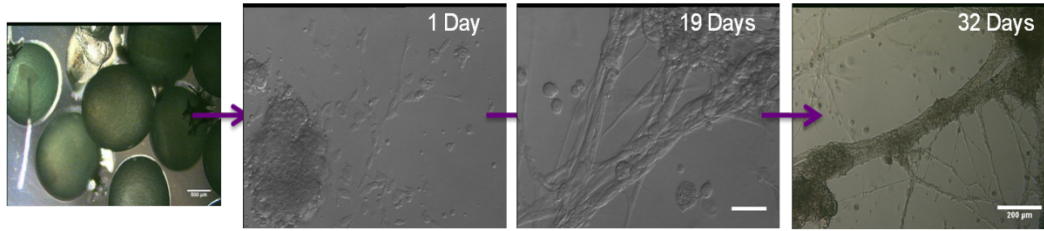


FIGURE 2.3. *IN VITRO* MUSCLE DEVELOPMENT FROM EMBRYONIC CELLS.

Since insect cells can tolerate a wider range of environmental conditions, and since our eventual application is robotic function under ambient conditions, we decided to probe the robustness of our cells by pushing the limits of the environmental conditions they were exposed to. For example, we found that our cells could tolerate media pH in the range of 5 – 7.5 (data not shown). In fact, the cells appeared to thrive at low pH (5 – 6.5). Additionally, the cells were subjected to mammalian medium and culture conditions, the results of which are shown in Figures 2.4 and 2.5. Greater than fifty percent of the cells remained viable after twenty-four hours in insect medium in either the insect or mammalian incubator, and in mammalian medium in the mammalian incubator. Cells did not survive in the insect incubator in mammalian medium, perhaps due to the presence of sodium bicarbonate without the maintenance of a CO₂ concentration for medium buffering. This result may indicate that although the cells thrive at low pH, they may be sensitive to alkaline pH greater than 7.5.

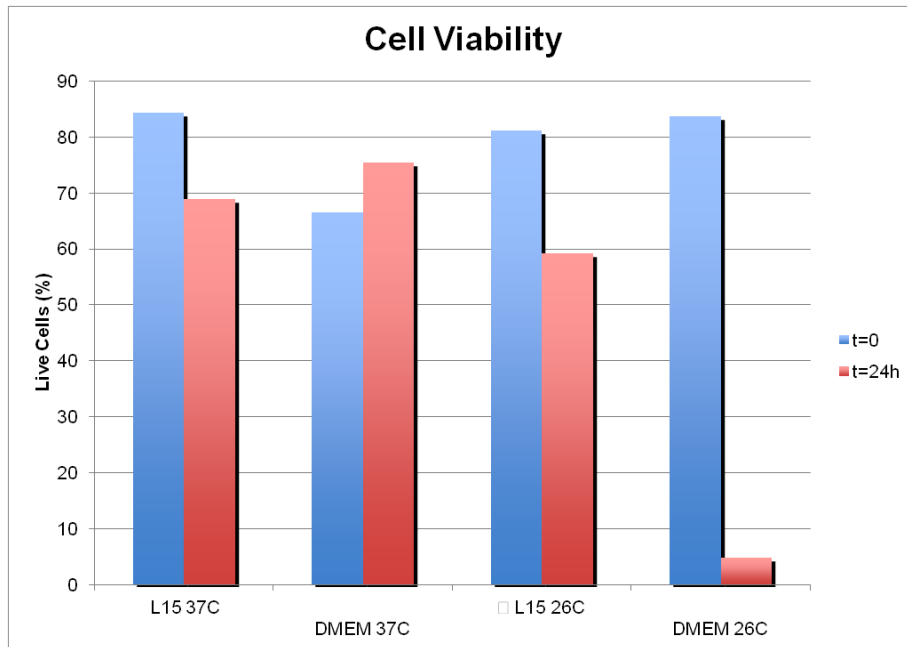


FIGURE 2.4. CELL VIABILITY AFTER 24 HOURS OF CULTURE IN EITHER INSECT MEDIUM (L15) OR MAMMALIAN MEDIUM (DMEM) UNDER INSECT CULTURE CONDITIONS (26C) OR MAMMALIAN CULTURE CONDITIONS (37C)

Additionally, besides the control condition (insect medium in insect incubator), the cells were most metabolically active in mammalian media in the mammalian incubator, as indicated by the steady increase in lactate production over a thirty-six hour period (Figure 2.5). As a result, future work could investigate potential interactions of insect muscle or fat with mammalian cell cultures. For example, we have found that insect yolk cells may sustain the viability of cultures for months without medium replenishment. If these cells could perform the same function with human cell cultures, this approach may have broad utility in cell cultivation and implant device development.

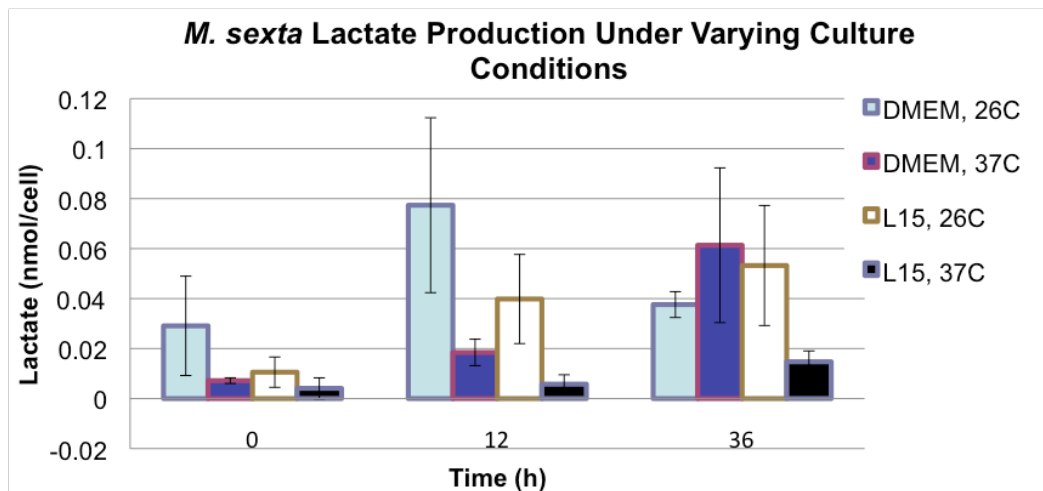


FIGURE 2.5. LACTATE PRODUCTION UNDER NORMAL AND MAMMALIAN (C2C12) CULTURE CONDITIONS. MEDIUM WAS EITHER FORMULATED FOR MOUSE (DMEM) OR INSECT CELLS (L15). THE TEMPERATURE APPLIED WAS EITHER SPECIFIC FOR MAMMALIAN CELLS (37°C) OR INSECT CELLS (26°C).

2.4 Hormonal regulation of differentiation and proliferation

2.4.1 Differentiation with 20-hydroxyecdysone (20HE)

Differentiated, functional muscle consists of long, multinucleated cells called myotubes. Myotubes form through the fusion of many mononucleated muscle precursor cells called myoblasts, as was described in more detail in Section 2.1. The identification and isolation of the point in development when these cells are present was our first step. We then designed a chemical environment to trigger the hormonal events that lead to myoblast differentiation into muscle.

Insect steroid hormone 20HE serves many roles in the coordination of development, larval molting, and metamorphosis (Wolfgang & Riddiford, 1986, Hegstrom & Truman, 1996, König, *et. al.*, 2011). At each of these stages, 20HE acts on several organ systems in a dose-dependent manner. The morphogenic

functions of 20HE occur partly through transcriptional upregulation of β -tubulin (Siaussat *et. al.*, 2007). This is significant for muscle development, since β 3 tubulin is transcribed by all somatic myoblasts, and β 1-tubulin expression is seen in the apodemes, or muscle attachment sites during embryogenesis (Buttgereit *et. al.*, 1996). 20HE also acts in the cell cycle to control proliferation through a G₂ phase control point requiring a suprathreshold level of ecdysteroid (Champlin *et. al.*, 1999). Researchers have described the effects of ecdysteroid dosage on myoblast proliferation and differentiation in *M. sexta* pupae (Champlin *et. al.*, 1999). Although the requirements for dosing may be different for embryonic myoblasts *in vitro*, it is likely that the actions of 20HE may be the same, namely regulating the cell cycle and initiating differentiation. Therefore, to promote muscle differentiation in embryonic myoblasts *in vitro*, it was necessary to optimize the concentration of 20HE.

Our goal was to establish appropriate dosing levels of 20HE for developing larval muscle *in vitro*. Medium concentrations higher than 1,000 ng/mL were observed to be detrimental to cell survival long term (data not shown), so a narrower range of ecdysteroid levels was chosen. Some muscle differentiation did occur in the absence of exogenous 20HE application (Figure 2.6A, D, G). In the animal, 20HE is synthesized from cholesterol derived from dietary sterols (Chapman, 1998). Additionally, 20HE may be produced in yolk cells from precursors in yolk granules, and subsequently released to signal gene transcription in embryonic cells starting during the gastrulation phase (Sonobe & Yamada, 2004). It is therefore possible that the muscle formation occurred in the absence of exogenous 20HE due to 20HE production by the cells themselves. This indicates that either the cells are capable of undergoing myogenic signaling and differentiation to some extent without genetic regulation via 20HE, or that

one or more populations of cells present in our cultures are capable of endogenously producing 20HE. However, the myotubes formed under this condition were small on day 10 and had deteriorated by day 19 (Figure 2.6D, G).

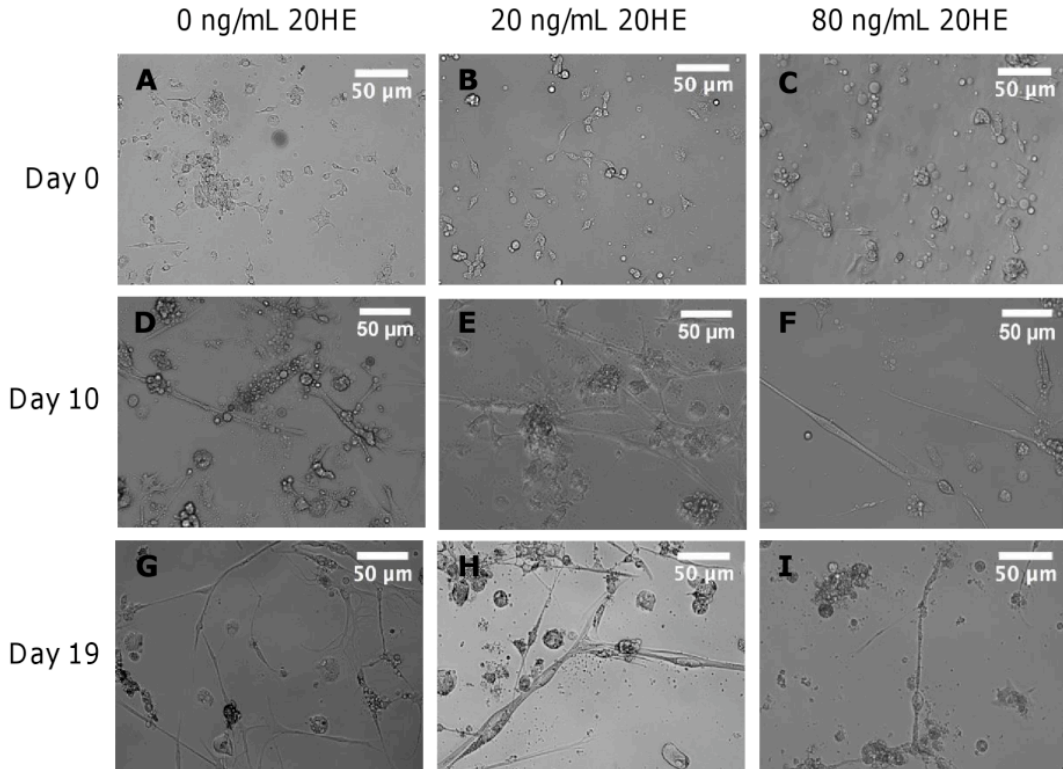


FIGURE 2.6. DOSAGE-DEPENDENT EFFECTS OF 20-HE ON MUSCLE DIFFERENTIATION. PHASE CONTRAST IMAGES SHOWING MYOTUBE FORMATION UNDER VARYING CONCENTRATIONS OF 20HE AT DAY 0 (A – C), DAY 10 (D – F) AND DAY 19 (G – I). REPRESENTATIVE IMAGES ARE SHOWN OF CELLS CULTURED IN 0 NG/ML (A, D, G), 20NG/ML (B, E, H) OR 80 NG/ML 20HE (C, F, I). SCALE BARS ARE 50 µM.

When cultured in media containing 20 ng/mL 20HE, myotube formation was evident by day 10, and maturation had continued through day 19, as evidenced by the increased size of the cells (Figure 2.6B, E, H). At 80 ng/mL 20HE, myotubes form by day 10 but did not mature further (Figure 2.6C, F, I). Additionally, when we analyzed images of the cells with varying levels of 20HE, we found that myotubes formed in 80 ng/mL media were thin, generally between

four microns and ten microns wide (Figure 2.7). In contrast, cells exposed to 20 ng/mL 20HE were generally in the range of eight to twenty-six microns wide, which indicates that these muscle cells were more mature. Based on these results, we concluded that low levels of 20HE promote muscle differentiation and contribute to maturation and maintenance of the tissue in larval *M. sexta* cells *in vitro*, and therefore 20 ng/mL 20HE was chosen as the optimal medium concentration.

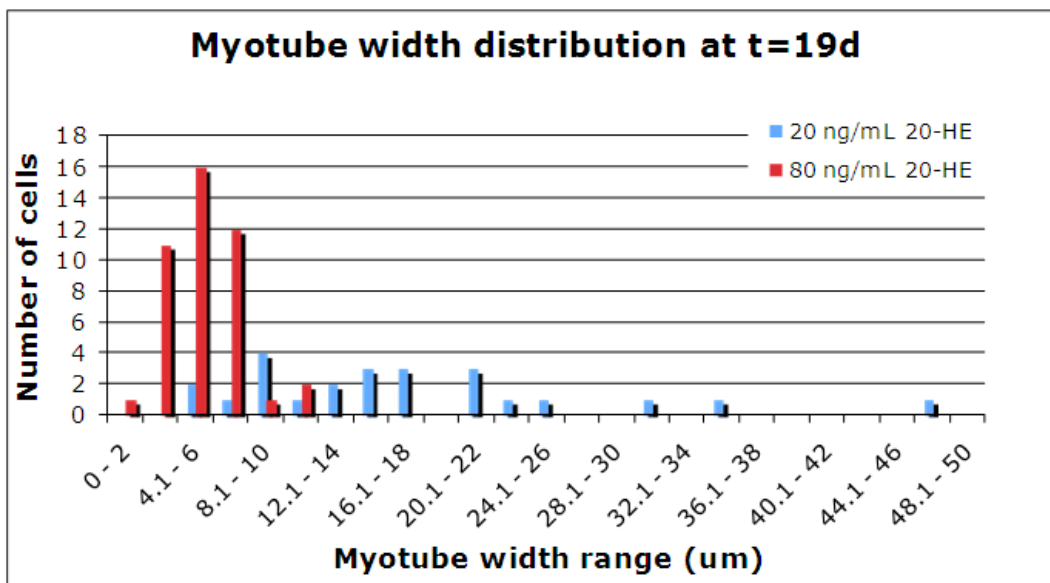


FIGURE 2.7. HISTOGRAM SHOWING DISTRIBUTION OF MYOTUBES WIDTHS UNDER VARYING 20HE LEVELS.

2.4.2 Proliferation with juvenile hormone (JH)

Although application of 20HE generated extensive myogenic differentiation, the control and timing of differentiation events is also important. Specifically, we would like to be able to induce proliferation in the myoblast population prior to triggering differentiation. This would allow for a larger and more uniform initial cell population, and would also bring us closer toward

generating a continuous cell line, which could be immortalized and cryopreserved for ease of experimental initiation and culture. To accomplish this, we chose to apply an insect juvenile hormone (JH) mimic, methoprene, which in many cases can modify the effects of 20HE; particularly, it has the ability to suppress 20HE-induced morphogenesis without interfering with 20HE-induced proliferation (Champlin *et al.*, 1999).

Cells were cultured in varying levels of JH, with 20ng/mL 20HE present in all conditions. On day 1, all cultures contained undifferentiated cells but by day 5, only cells cultured in the absence of methoprene underwent myogenic differentiation, as expected (Figure 2.8A – F). This result was further confirmed by cell counts and 5-bromo-2'-deoxyuridine (BrDU) incorporation and staining. The total number of cells was significantly higher on day 6 in cultures exposed to methoprene than cultures with no methoprene (Figure 2.8G). Cell counts were significantly higher for 500 ng/mL JH compared to 1000 ng/mL JH samples on day 2 but not day 6 (Figure 2.8G). There were significantly fewer proliferating cells on day 6 than day 2 for control samples; therefore methoprene exposure extends and maintains the proliferative phase in these cells (Figure 2.8H). Some studies suggest that juvenile hormone action in promoting proliferation is steroid independent (Truman & Riddiford, 2007), so this may be a direction to pursue in future studies.

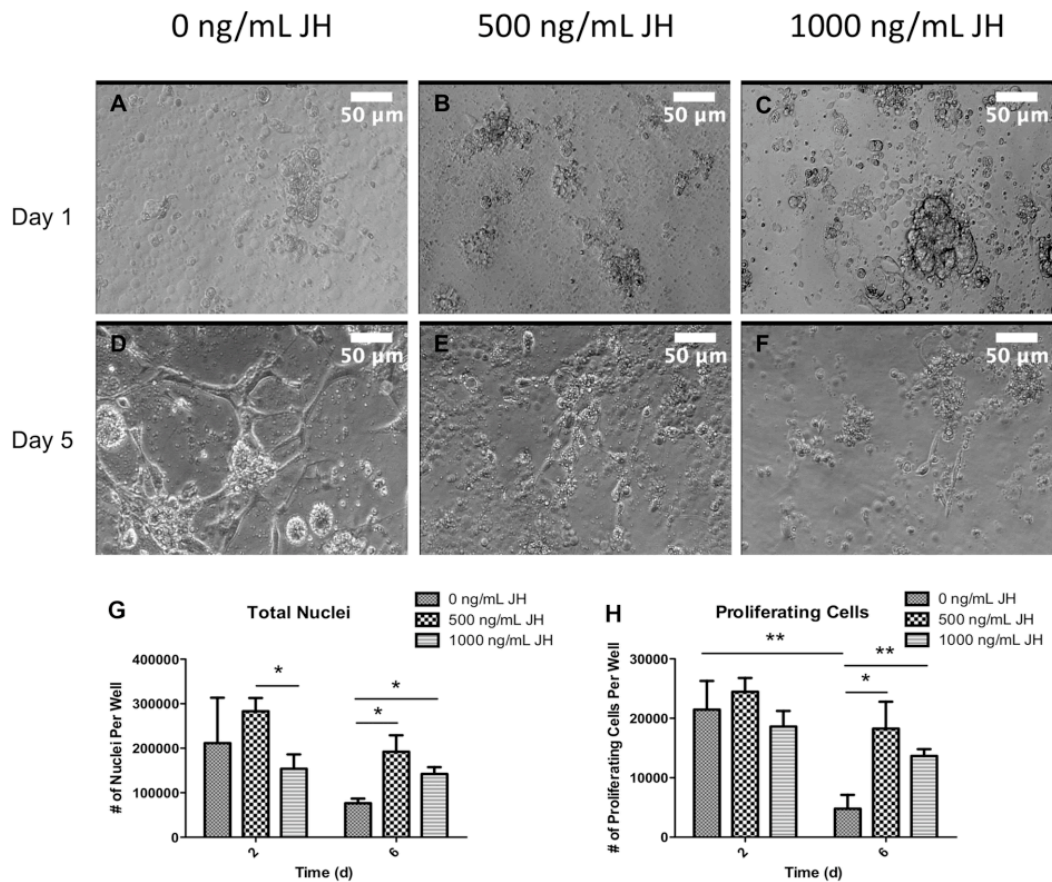


FIGURE 2.8. EFFECTS OF JUVENILE HORMONE (JH) MIMIC, METHOPRENE, ON 20HE ACTION AND CELL PROLIFERATION. PHASE CONTRAST IMAGES OF CELLS CULTURED IN 20NG/ML 20HE AND VARYING LEVELS OF METHOPRENE (A – F). TOTAL NUMBER OF NUCLEI AND BRDU-POSITIVE NUCLEI ON DAY 2 AND DAY 6 FOR VARYING METHOPRENE CONCENTRATIONS (G – H). *P<0.05, **P<.01. SCALE BARS ARE 50μM.

2.5 Summary

We have demonstrated that embryonic myoblasts from the insect *M. sexta* may be differentiated into functional muscle through the application of the molting hormone, 20-hydroxyecdysone. The resulting multinucleated cells express myosin heavy chain, and a subpopulation of cells exists, which contain lipid vesicles. Metabolic evaluations revealed that these cells do not appear to consume glucose, but they produce more lactate than mouse muscle on a per

cell basis. This indicates that the cells use an alternate energy source, such as glycogen reserves, amino acids, or lipids, to fuel cellular activity and spontaneous contractions. As a result, *M. sexta* muscle cells are able to thrive for extended periods of time without medium changes. We have demonstrated that the contractile ability of these cells exceeds that of conventional mammalian systems. Taken together, the larval muscle tissue we have generated from embryonic cells is a promising candidate for future bioactuation applications.

2.6 References

- Bayline RJ, Khoo AB, Booker R. (1998) Innervation regulates the metamorphic fates of larval abdominal muscles in the moth, *Manduca sexta*. *Dev. Genes Evol.* 208:369 – 381.
- Bayline RJ, Duch C, Levine RB. (2001) Nerve-muscle interactions regulate motor terminal growth and myoblast distribution during muscle development. *Dev. Biol.* 231:348 – 363.
- Bernstein SI, Fryberg EA, Donady JJ. (1978) Isolation and partial characterization of *Drosophila* myoblasts from primary cultures of embryonic cells. *J Cell Biol.* 78:856 – 865.
- Buttgereit D, Paululat A, Renkawitz-Pohl R. (1996) Muscle development and attachment to the epidermis is accompanied by expression of $\beta 3$ and $\beta 1$ tubulin isoforms, respectively. *Int. J. Dev. Biol.* 40:189 - 196.
- Champlin DT, Reiss SE, Truman JW. (1999) Hormonal control of ventral diaphragm myogenesis during metamorphosis of the moth, *Manduca sexta*. *Dev. Genes. Evol.* 209:265 - 274.
- Chapman RF. (1998) *The Insects: Structure and Function*, 4th ed. Cambridge University Press, Cambridge. p. 77, 303, 334, 350.
- Dorn A, Bishoff ST, Gilbert LI. (1987) An incremental analysis of the embryonic development of the tobacco hornworm, *Manduca sexta*. *Int. J. of Invert. Reprod. Dev.* 11:137 - 158.
- Eide PE, Caldwell JM, Marks EP. (1975) Establishment of two cell lines from embryonic tissue of the tobacco hornworm, *Manduca sexta* (L.). *In Vitro* 11(6):395 - 399.
- Foe VE, Odell GM, Edgar BA.et. al. (1993) *The Development of Drosophila melanogaster*. Bate M & Hartenstein V (editors). Cold Spring Harbor Laboratories: Long Island, NY. Ch. 3.
- Hegstrom CD & Truman JW. (1996) Steroid control of muscle remodeling during metamorphosis in *Manduca sexta*. *J. Neurobiol.* 29(4):535 - 550.
- Inoue H, Kobayashi J, Kawakita H, Miyazaki J-I, Hirabayashi T. (1991) Insect muscle cell line forms contractile tissue networks *in vitro*. *In Vitro Cell. Dev. Biol.* 27A:837 – 840.

- König A, Yatsenko AS, Weiss M, Sccherbata HR. (2011) Ecdysteroids affect *Drosophila* ovarian stem cell niche formation and early germline differentiation. *The EMBO Journal* 30:1549 - 1562.
- Kurtti TJ & Brooks MA. (1970). Growth and differentiation of Lepidopteran myoblasts *in vitro*. *Exp. Cell Res.* 61:407 – 412.
- Lehmann K, Zwadlo G, Pfeiffer P, Burger PM. (1985) Effect of hemolymph and nervous-tissue components on the *in vitro* development of flight-muscle myoblasts of *Manduca sexta*. *Differentiation* 30:92 – 97.
- Luedeman R & Levine RB. (1996) Neurons and ecdysteroids promote proliferation of myogenic cells cultured from the developing adult legs of *Manduca sexta*. *Dev. Biol.* 173:51 – 68.
- Luedeman RA & Lightner DV. (1992) Development of an *in vitro* primary cell culture system from the penaeid shrimp, *Penaeus stylirostris* and *Penaeus vannamei*. *Aquaculture* 101:205 – 211.
- Mitsuhashi J. (2002) *Invertebrate Tissue Culture Methods*. Springer-Verlag: Tokyo. Ch. 2.
- Necco A & Martin R. (1963) Behavior and estimation of the mitotic activity of the white body cells in *Octopus vulgaris*, cultured *in vitro*. *Exp. Cell Res.* 30:588 – 623.
- Odintsova NA, Dyachuk VA, Nezhlin LP. (2010) Muscle and neuronal differentiation in primary cell culture of larval *Mytilus trossulus* (Mollusca: Bivalvia). *Cell Tissue Res.* 339:625 – 637.
- Odintsova NA & Khomenko AV. (1991) Primary cell culture from embryos of the Japanese scallop *Mizuchopecten yessoensis* (Bivalvia). *Cytotechnology* 6:49 – 54.
- Panchin YV, Arshavsky YI, Selverston A, Cleland TA. (1993) Lobster stomatogastric neurons in primary culture I. Basic characteristics. *J. Neurophys.* 69(6):1976 – 1992.
- Quinn KP, Bellas E, Furligas N, Lee K, Kaplan DL, Georgakoudi I. (2012) Characterization of metabolic changes associated with the functional development of 3D engineered tissue by non-invasive, dynamic measurement of individual cell redox ratios. *Biomater.* 33:5341 – 5348.
- Sander V, Sune G, Jopling C, Morera C, Belmonte JCI. (2013) Isolation and *in vitro* culture of primary cardiomyocytes from adult zebrafish hearts. *Nature Protocols* 8(4):800 – 809.

Seecof RL, Alleaume N, Teplitz RL, Gerson I. (1971) Differentiation of neurons and myocytes in cell cultures made from *Drosophila* gastrulae. *Exp. Cell Res.* 69:161 – 173.

Seecof RL & Donady JJ. (1972) Factors affecting *Drosophila* neuron and myocyte differentiation *in vitro*. *Mech. Age. Dev.* 1:165 – 174.

Siaussat D, Bozzolan F, Porcheron P, Debernard S. (2007) Identification of steroid hormone signaling pathway in insect cell differentiation. *Cell. Mol. Life Sci.* 64:365 - 376.

Sonobe H & Yamada R. (2004) Ecdysteroids during early embryonic development in silkworm *Bombyx mori*: metabolism and functions. *Zoological Science* 21:503 - 516.

Truman JW & Riddiford LM. (2007) The morphostatic actions of juvenile hormone. *Insect Biochem. Mol. Biol.* 37:761 - 770.

Wolfgang WJ & Riddiford LM (1986) Larval cuticular morphogenesis in the tobacco hornworm, *Manduca sexta*, and its hormonal regulation. *Dev. Biol.* 113:305 - 316.

Woods WA, Fusillo SJ, Trimmer BA. (2008) Dynamic properties of a locomotory muscle of the tobacco hornworm *Manduca sexta* during strain cycling and simulated natural crawling. *J Exp. Biol.* 211:873 – 882.

Chapter 3. Cell population characterization

3.1 Introduction

Our eventual goal is to grow 3-dimensional tissues with the cell populations we have developed. However, the initial characterization, including cell type identification, survival tracking, and contractile activity analysis were examined in 2D for simplicity and ease of study.

Since we have chosen to isolate cells directly from whole embryos, it is likely that multiple cell types are present in the cultures. Preplating methods and hormonal application are used to preferentially cultivate muscle cells; however, epithelial cells, neurons, and developing fat, among others, are still likely to be present. In order to identify the presence of such cell types, we have chosen to use immunofluorescence staining. Our studies revealed that muscle differentiates with appropriate sarcomeric structures and protein expression by day 17 of culture. Additionally, populations of mesenchymal-derived stem cells persist over this time period. Neurons were identified in close proximity with muscle cells, and interconnect with one another. Maternally-derived yolk cells were determined to be present as well.

The literature and our experiments have demonstrated that insect cells, and particularly the *M. sexta* muscle cultures developed in the current work, are

able to survive in culture for extended periods of time without medium refreshment. The metabolic mechanisms behind this peculiar phenomenon are investigated and discussed in more detail in Chapter 4.

It is not uncommon for cells cultured *in vitro* to display different phenotypes and function from *in vivo* tissue. All the signals provided within the organism cannot fully be recapitulated in a 2D culture, and therefore we have observed some very unusual contractile outcomes with our cultured muscle. The cells and tissues we have generated *in vitro* contract spontaneously and for the entire duration of the culture. This is unexpected because the native muscle does not contract spontaneously when explanted. In future work, we will attempt to explain this phenomenon, as well as control contractions with electrical stimulation.

3.2 Cell type identification

3.2.1 Differentiated muscle (myotubes and myofibers)

Positive staining for insect muscle myosin heavy chain confirmed the myogenic identity of the dominant cell population in the cultures (Figure 3.1). Myosin heavy chain is a sarcomeric protein, and its expression indicates a mature skeletal muscle phenotype. Sarcomeric striations are visible in both actin and myosin staining (Figure 3.1). However, they are not as precisely aligned as in mammalian muscle. This is in agreement with the characteristics of larval muscle *in vivo*, where Z-bands are irregular compared to adult and mammalian muscle (Rheuben & Kammer, 1980). Furthermore, mammalian sarcomeres are typically spaced 2 μm apart; however, we observed spacing of 4 – 13 μm in our cells. Again, this is consistent with physiological studies of larval muscle, where

sarcomere lengths are longer than those of mammalian muscle (Rheuben & Kammer, 1980). These ultrastructural differences may contribute to differences we observed in contractile properties, which is discussed in more detail below.

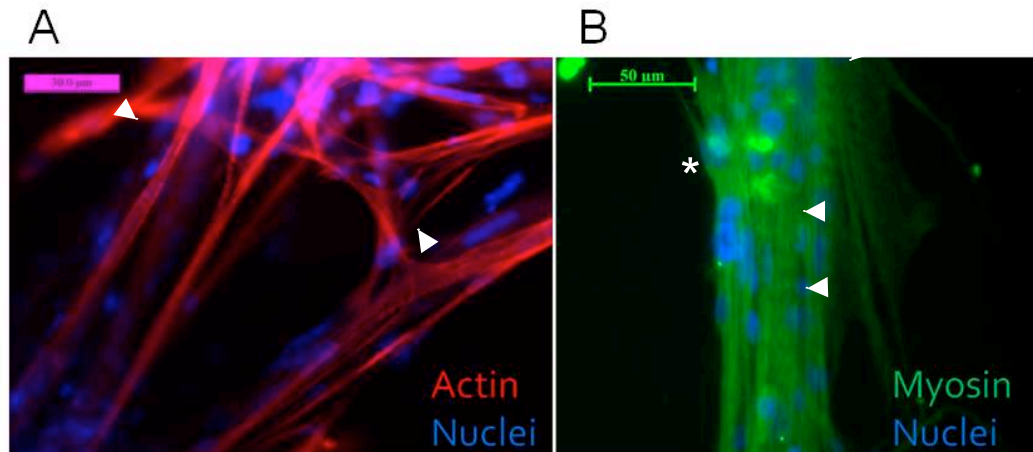


FIGURE 3.1 IMMUNOFLUORESCENCE IDENTIFICATION OF DIFFERENTIATED MUSCLE. ACTIN STAINING REVEALS SARCOMERIC STRIATIONS (ARRWOHEADS) IN A 100-DAY OLD CULTURE (RED, A). MYOSIN STAINING CONFIRMS MUSCLE PHENOTYPE AND ALSO REVEALS SARCOMERIC STRIATIONS (ARROWHEADS) AND MULTINUCLEATION (ASTERISK) IN A 48-DAY OLD CULTURE (GREEN, B). NUCLEI ARE SHOWN IN BLUE. SCALE BARS ARE 30 MICRONS AND 50 MICRONS, RESPECTIVELY.

We wanted to further evaluate the myogenic properties of these cells, so we stained for a wider range of skeletal muscle markers and probed their expression at early and later timepoints. These markers included α -actinin, connectin, myosin, and troponin-T (Figure 3.2). We found that α -actinin was expressed in our cultures both on day 0 and on day 17. α -actinin is an actin-binding protein that is expressed in both non-muscle and muscle cell types. In non-muscle cells, α -actinin binds to microfilament bundles and is localized at adherens junctions. In muscle cells, α -actinin is a sarcomeric protein found in the Z-discs of larval body wall muscles. Therefore, we can speculate that the

expression observed on day 0 was mostly in non-muscle cells, while the expression seen on day 17 was a combination of non-muscle cells and larval body wall muscles (Figure 3.2A – B).

Connectin expression was not observed at either time point (Figure 3.2C – D). While connectin, also known as titin, performs the crucial role of regulating the passive elasticity of muscle in vertebrates, it appears to be expressed in only specific muscles during insect development (Baylies *et. al.*, 1998). As a result, we can speculate that the founder cells of these specific muscles, and indeed the muscles themselves, are not generated by our *in vitro* culture methods. In future work, as described in Chapter 6, we will attempt to pinpoint founder cell populations and may be able to generate specific muscles from careful study of founder cell populations.

Myosin expression was seen only at the day 17 time point (Figure 3.2E – F). On day 17, muscle fibers could be seen that express myosin with sarcomeric striations (Figure 3.2F, arrowhead), and with diffuse fibers aligning with the axis of the cell (Figure 3.2F, arrow). This indicates either that the cells were still in the process of differentiating, or that some visceral (gut) muscles were present in addition to skeletal muscle. Troponin-T is another sarcomeric component and, similarly to myosin, its expression was observed on day 17, but not day 0, further confirming that differentiated muscle cells arise in our cultures from embryonic precursors (Figure 3.2G, H).

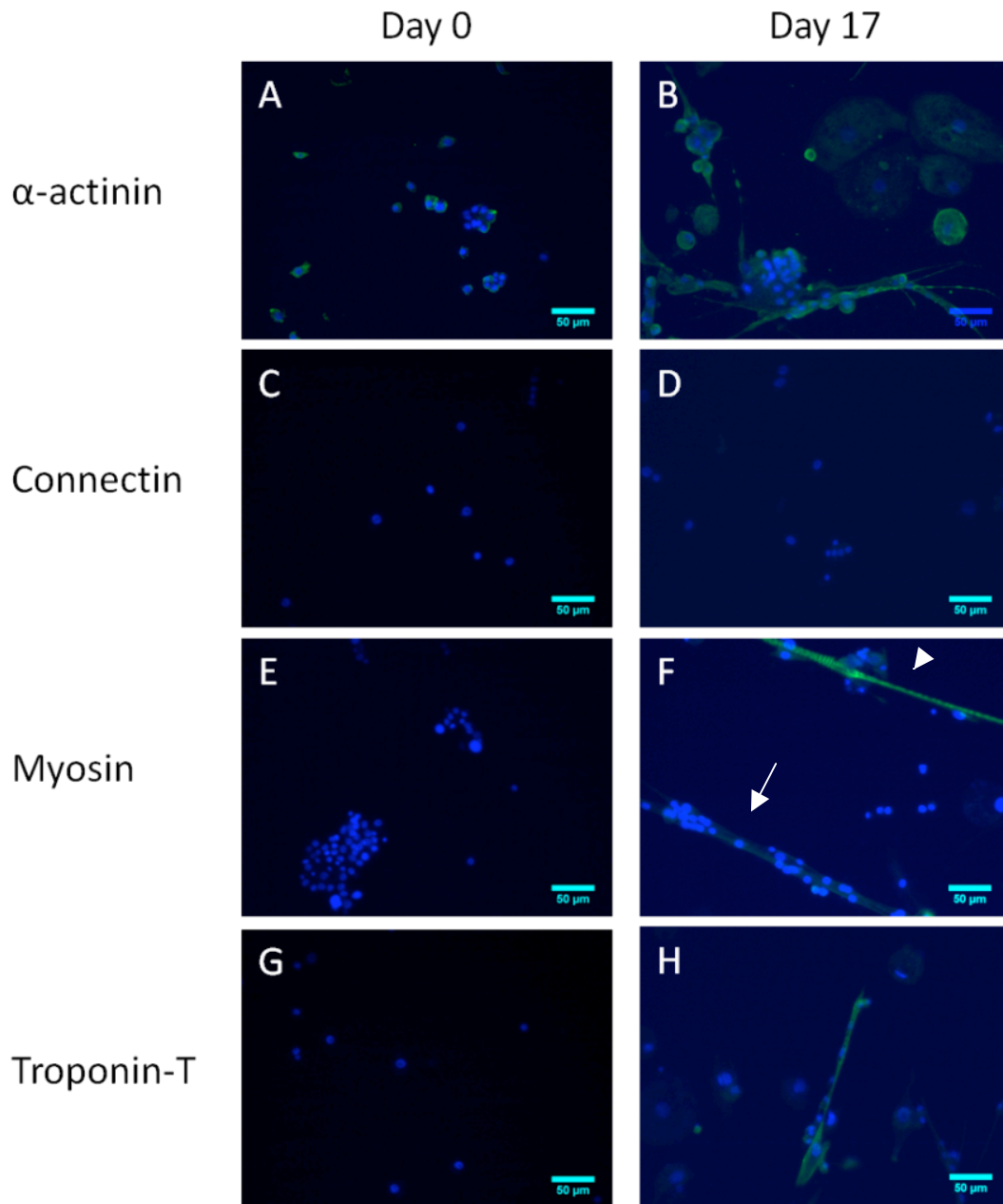


FIGURE 3.2 EXPRESSION OF MUSCLE CELL MARKERS OVER TIME IN DEVELOPING *IN VITRO* CULTURES. A-ACTININ IS EXPRESSED ON BOTH DAY 0 AND DAY 17 OF CULTURE (GREEN, A,B). CONNECTIN IS NOT EXPRESSED ON EITHER DAY 0 OR DAY 17 (C,D). MYOSIN AND TROPONIN-T ARE NOT EXPRESSED ON DAY 0, BUT ARE EXPRESSED ON DAY 17 (GREEN, E – H). MYOSIN STAINING CAN BE SEEN IN BOTH A STRIATED MUSCLE FIBER (ARROWHEAD) AND A NON-STRIATED MUSCLE FIBER (ARROW). BLUE INDICATES NUCLEI. SCALE BARS ARE 50UM.

3.2.2 Muscle precursor cells (myoblasts)

We wanted to verify that muscle precursor cells were present and if a population of these cells remains in an undifferentiated state over time. Initially, we used cell morphology to identify cell types, as other studies have used cell shape to claim the presence of myoblasts (Bernstein, *et. al*, 1978; Seecof *et. al.*, 1971). Spindle-shaped cells thirty to fifty micrometers in length, which were capable of fusing into multinucleated myotubes, were identified as muscle-specific stem cells, or myoblasts.

Additionally, we chose to probe the genetic expression of these cells using immunofluorescence staining. *Twist* is a transcription factor expressed by all early mesodermal cells during embryonic development (Baylies, *et. al.*, 1998). In addition to giving rise to somatic muscles, the mesoderm also produces visceral (gut) muscles, dorsal vessel (heart) muscle, and fat body. However, we may be able to specifically identify these other cell types by probing for differentially-expressed genes. For example, *even-skipped (eve)* is expressed in the progenitors of visceral muscle and fat, while *sloppy paired (slp)* is expressed in the progenitors of somatic muscle and heart (Baylies *et. al.*, 1998). This differential expression pattern serves to segment the mesoderm along the anterior-posterior axis. Furthermore, segmentation is amplified in the *slp* domain by high *twist* expression. Thus, high *twist* expression denotes muscle precursor cells.

We stained for *twist* on day 0 and day 17 of *in vitro* culture and found that *twist* expression was moderate on day 0, but high on day 17 (Figure 3.3). Thus, we may speculate that our cells are mainly unspecified mesodermal cells at the time of isolation, but proceed towards muscle-specific commitment in culture.

This may be due to our selected cultivation conditions, such as 20HE levels (discussed in 2.4.1). Indeed, high twist expression in the posterior segment of the mesoderm is known to be at Stage 10 of *Drosophila* development, and our *M. sexta* cells are isolated at the equivalent of *Drosophila* Stage 9 (Interactive Fly).

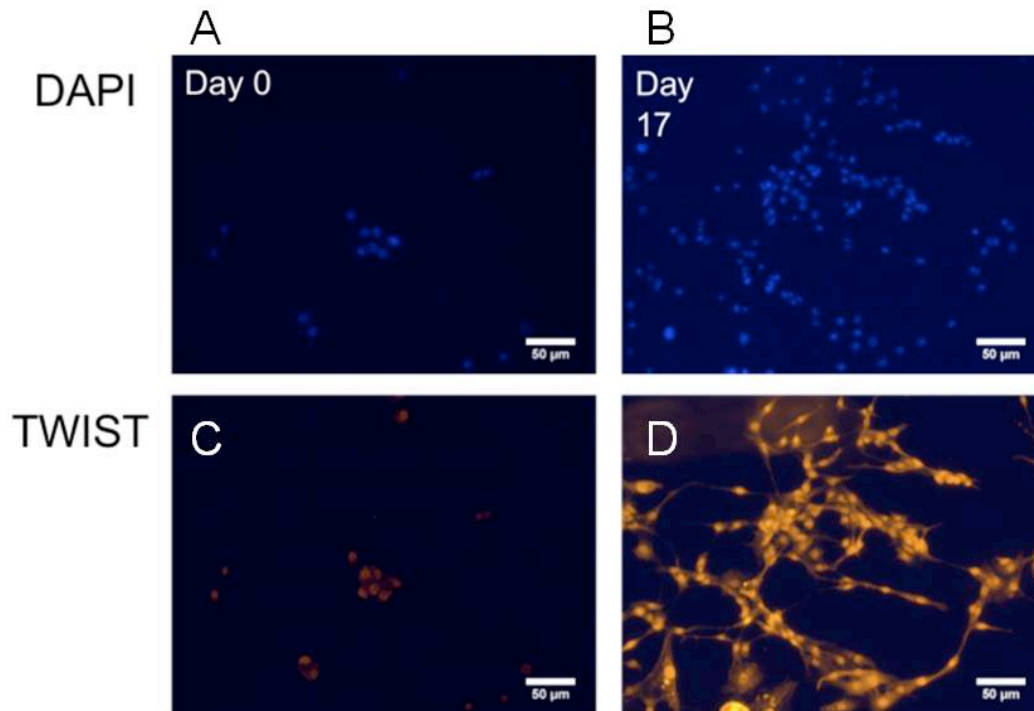


FIGURE 3.3 *TWIST* EXPRESSION IN EARLY AND LATE CULTURES. *TWIST* IS EXPRESSED BY ALL CELLS AT BOTH TIMEPOINTS, BUT IS MODERATE ON DAY 0 (RED, C) AND HIGH ON DAY 17 (RED, D). BLUE STAINING IN A AND B DENOTES CELL NUCLEI. ALL SCALE BARS ARE 50 MICRONS.

3.2.3 Neurons

Several reports have highlighted the importance of neuronal interactions for insect muscle development *in vitro* (Luedeman & Levine, 1996; Lehman *et al.*, 1985). One study demonstrated that the presence of neurons in myogenic cultures enhanced proliferation and improved the formation of multinucleated contractile fiber (Luedeman & Levine, 1996). Another group found that when pupal *M. sexta* muscle medium was supplemented with nervous tissue extract of nervous tissue, the structural development of the muscles improved (Lehman *et al.*, 1985). This is in concurrence with reports observing that denervation is devastating for muscle specification and repatterning during metamorphosis of *M. sexta* (Bayline *et al.*, 2001; Bayline *et al.*, 1998). Indeed, several studies that generated *in vitro* cultures of embryonic *Drosophila* muscle also found neuronal cells in their cultures, as the two cell types begin to emerge at similar stages of development (Bernstein *et al.*, 1978; Seecof *et al.*, 1971; Seecof & Donady, 1972).

As a result, we were interested to see if our heterogeneous cell populations also contained neurons. The identification of insect neurons *in vitro* is often accomplished by immunofluorescence staining of horseradish peroxidase (HRP; Küppers-Munther *et al.*, 2004; Lürer & Technau, 2009). Staining for this plant-derived glycoprotein is found in all neurons in the embryonic and larval stages of *Drosophila*, indicating that HRP, or neuron-specific glycoproteins similar to HRP, are found in the insect neuronal cytoplasm (Sun & Salvaterra, 1995). We saw positive staining for HRP, and the cells stained have typical neuronal features, such as long, slender axons that often run along muscle fibers, and the typical beaded appearance (Figure 3.4).

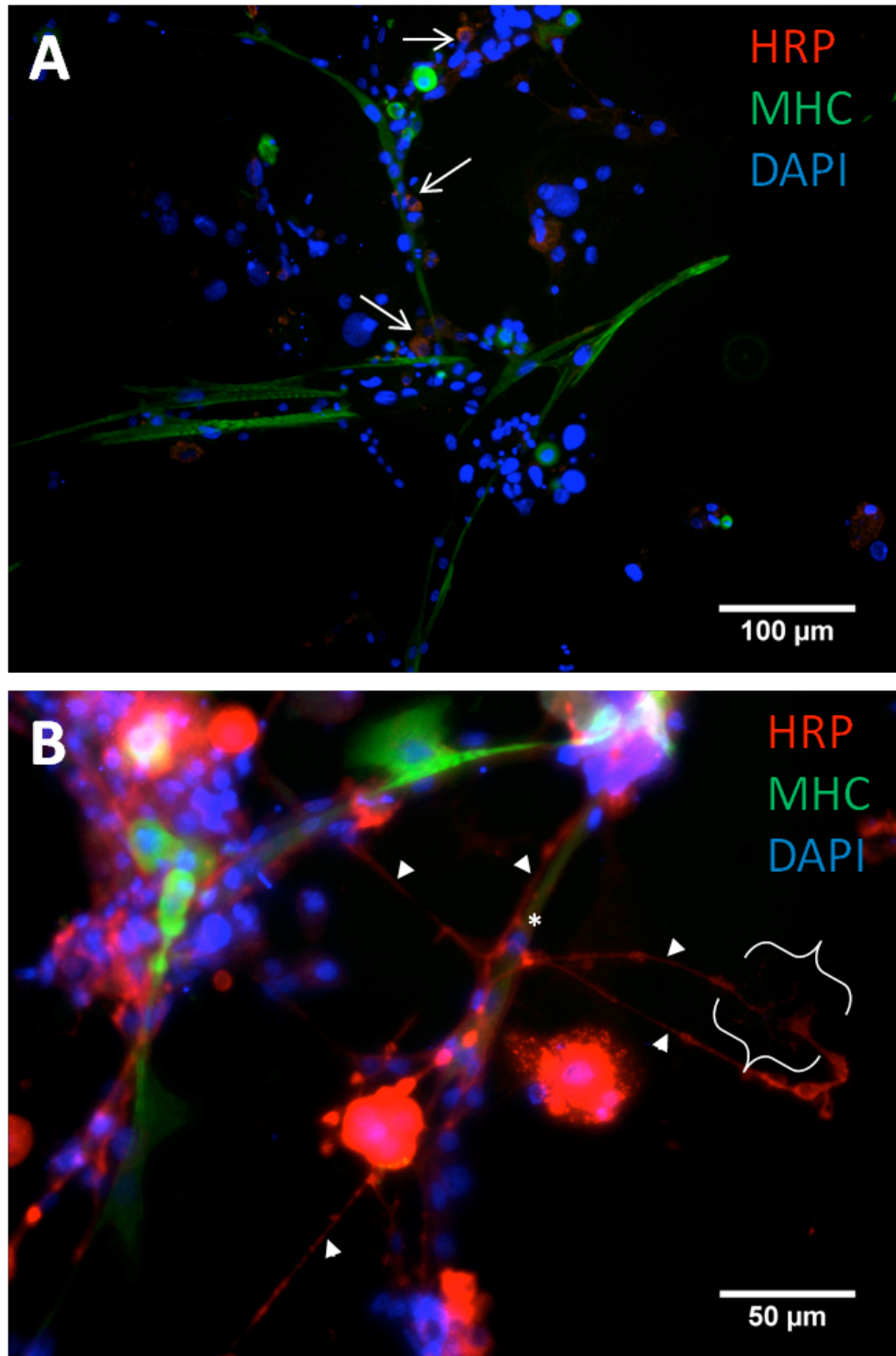


FIGURE 3.4 DOUBLE IMMUNOFLUORESCENCE STAINING FOR HRP (RED), WHICH INDICATES NEURONS AND MYOSIN (GREEN), WHICH INDICATES MUCLE. MUSCLE FIBERS SEEM TO GROW IN CLOSE PROXIMITY TO NEURONAL CLUSTERS (A). NEURONAL AXONS ARE SEEN SPREADING AROUND AND ALONG MUSCLE FIBERS (ARROWHEADS, B). * INDICATES MUSCLE FIBER. BRACKET INDICATES REGION WHERE TWO NEURONS ARE INTERACTING. BLUE INDICATES NUCLEI.

3.2.3 Yolk cells (vitellophages)

Although our resulting populations are enriched in myogenic cells, several contaminating cell types are present. In particular, cells containing lipid droplets are evident in every culture (Figure 3.4B). These cells tend to be large, typically 20 to 50 μm in diameter. Although it is possible that some are fat body cells known as trophocytes, which may have differentiated from mesodermal precursors in our cultures, it is more likely that they are yolk cells, or vitellophages, as we tend to observe such cells from the time of initial plating. Vitellophages are preexisting in the eggs at the time of cell isolation and serve to break down the embryonic yolk and may eventually become midgut epithelial cells as well (Fausto, *et. al.*, 1994; Chapman, 1998). To verify this hypothesis, we fixed and sectioned eggs developed to the staging time where we normally collect cells. When we stained these eggs with hematoxylin and eosin, we observed large extraembryonic cells containing many small vesicles and a single nucleus (Figure 3.4A, inset). These cells have a very similar morphology and size to the lipid droplet-containing cells we observe in culture (Figure 3.4B). It should be noted that the small droplets, while taking up hemotoxylin, do not stain positively for Oil Red O and thus do not contain lipid (Figure 3.4A - B). Yolk consists of lipids, mainly triacylglycerol, as well as proteins, and a small amount of carbohydrates stored as glycogen (Chapman, 1998). Therefore, the material in the remainder of the vitellophage vesicles is most likely protein or glycogen. Lipid droplet size, yolk cell contents and the overall metabolism of these yolk cells were tracked in further studies, which are discussed in Chapter 4.

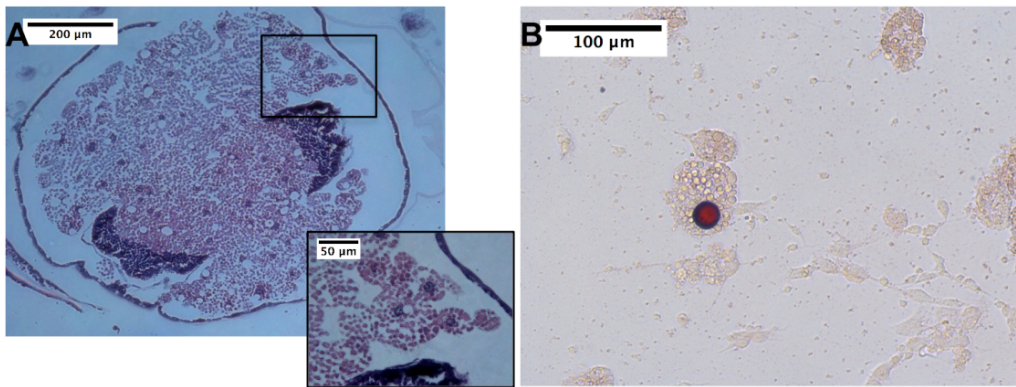


FIGURE 3.5 VITELLOPHAGE IDENTIFICATION IN STAGED EMBRYOS AND *IN VITRO*. HISTOLOGICAL SECTIONING AND STAINING OF A DEVELOPING EMBRYO 19H POST-OVIPOSITIONING (A). DARK REGIONS ARE CROSS-SECTIONS OF THE EMBRYO. THE REST OF THE EGG CONTAINS YOLK GRANULES AND VITELLOPHAGES (YOLK CELLS). YOLK CELLS ARE 20 – 50UM IN DIAMETER AND CONTAIN A SINGLE NUCLEUS, STAINED DARK PURPLE (INSET). THESE CELLS ARE ALSO OBSERVED IN OUR CULTURES, AND TEND TO CONTAIN A SINGLE, LARGE LIPID DROPLET, AS SHOWN IN RED BY OIL RED O STAINING (B).

3.3 Prolonged survival

Our cultures in differentiation media were observed to survive and contract continually for over 90 days (Figure 3.6). Cell fusion increased over the course of the culture, resulting in extensive, interconnected myotube networks by day 28, with no evident cell death (Figure 3.6A - B). These networks continued to develop in the absence of medium changes, and at day 44, cells achieved confluence and nearly all remained viable (Figure 3.6C - D). By day 75, highly developed bundles of muscle tissue were present and continued to survive and contract, while many of the undifferentiated cells in the culture were no longer viable (Figure 3.6E – F). This indicated a metabolic capability unique to the muscle tissue that allowed for extended cell survival under the closed system conditions of the cell culture well, perhaps through breakdown and mobilization of stored nutrients by vitellophages (yolk cells) or trophocytes (fat cells) (Figure B).

Indeed, researchers have cultured intact embryos *in vitro* and have found them to develop normally (Broadie *et. al.*, 1992).

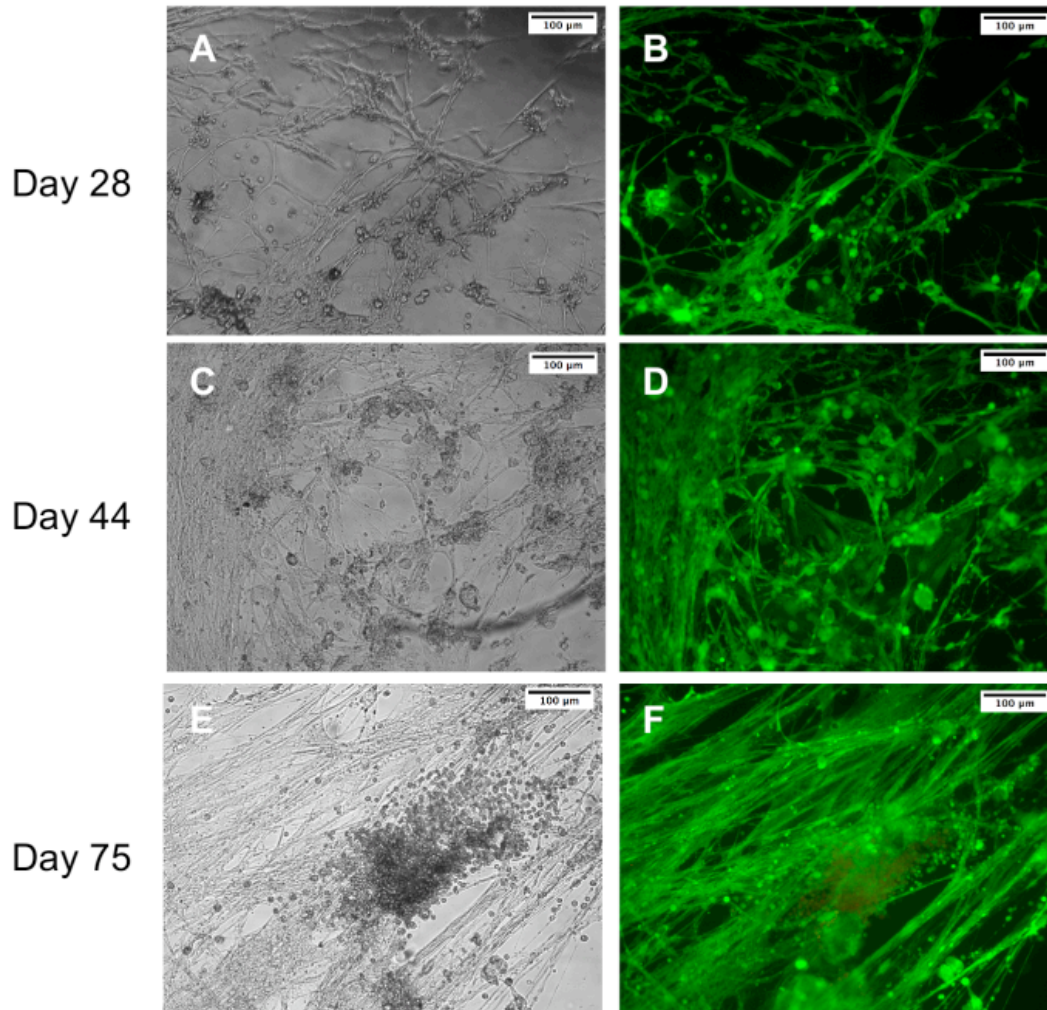


FIGURE 3.6 *M. sexta* MUSCLE CELL VIABILITY OVER TIME. PHASE CONTRAST (A, C, E) AND LIVE/DEAD STAINING (B, D, F) OF TYPICAL CULTURES GROWN IN THE ABSENCE OF MEDIUM CHANGES. FOR LIVE/DEAD IMAGES, GREEN STAINING INDICATES LIVE CELLS AND RED STAINING INDICATES DEAD CELLS. REPRESENTATIVE IMAGES TAKEN FROM CULTURES ON DAY 28 (A – B), DAY 44 (C – D), AND DAY 75 (E – F). SCALE BARS ARE 100 UM.

3.4 Spontaneous contractile activity

Qualitatively in culture, we observed that the frequency and displacement of cells undergoing spontaneous contractile activity varied dramatically between mouse C2C12 cells and insect *in vitro* developed muscle. C2C12 cells tend to have twitch-like contractions that are rapid, with a duration on the order of milliseconds, and have a regular frequency, with one or a region of cells pulsing synchronously for a short period of time, then shutting down permanently. *M. sexta* muscle cells, however, tend to contract with irregularity and more slowly than mammalian muscle, with the time scale for a single contraction duration on the order of hundreds of milliseconds. Additionally, contractions persist throughout the entire duration of the culture.

The spontaneous contractile activity of the cells was analyzed by evaluating the index of movement (IOM) for cultures over time. IOM is a measure of the changes in pixel intensity, and thereby the movements of cells, in a sequential set of frames taken from a video of contracting cells. First, we tracked the average pixel intensity for each frame of a video over time to reveal the contractile dynamics of spontaneously contracting insect muscle (Figure 3.7A). The results indicate that muscles contract with a frequency of approximately 0.2 Hz, with a 1 – 2s time to peak. We subtracted frames 700ms apart from an initial, baseline image to give differential maps showing the regions that differ in pixel intensity from the reference. We then summed these differential images to provide a snapshot of the cells' activity for a 2.8s period (Figure 3.7B, C). The average pixel values from these differential images is the IOM and can be used as a measure of how much the cells moved.

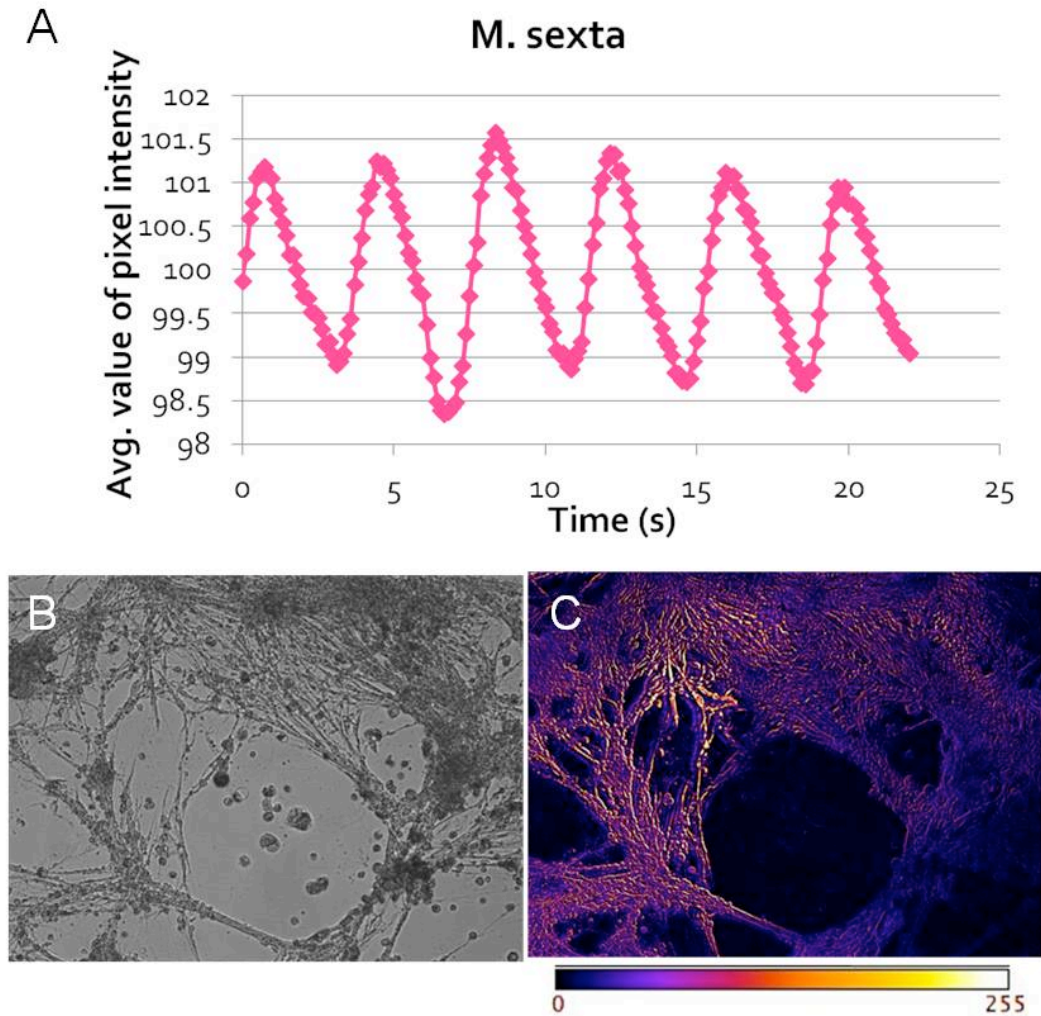


FIGURE 3.7 INDEX OF MOVEMENT ANALYSIS FOR *M. SEXTA* CULTURES. FOR A SINGLE VIDEO, THE AVERAGE PIXEL INTENSITY OF EACH FRAME MAY BE PLOTTED TO REVEAL CONTRACTILE DYNAMICS (A). PHASE CONTRAST STILL FRAME FROM VIDEO USED FOR ANALYSIS IN C. DIFFERENTIAL IMAGE DERIVED FROM VIDEO OF CONTRACTING CELLS (C). REGIONS WHERE NO CHANGE IN PIXEL INTENSITY OCCURRED ARE BLACK, WHILE REGIONS WHERE PIXEL INTENSITY CHANGED DRAMATICALLY ARE YELLOW TO WHITE.

We analyzed IOM for each condition at each time point to compare contractile activity of insect MSMY and mouse C2C12 cells over time without medium changes. Confluent C2C12 cells tended to only display contractions in single cells or small areas of the well. However for the insect cells, myocytes throughout the field contracted and, with the exception of a few non-myocytes,

nearly the entire field was displaced. Videos were taken from at least 3 regions in insect and mouse samples to track IOM with time (Figure 3.8). On the third day after contractions began, mouse muscle experienced a peak in movement intensity, followed by contractile arrest. Insect muscle cultures experienced a contractile peak on day 16, and continued to contract at all time points.

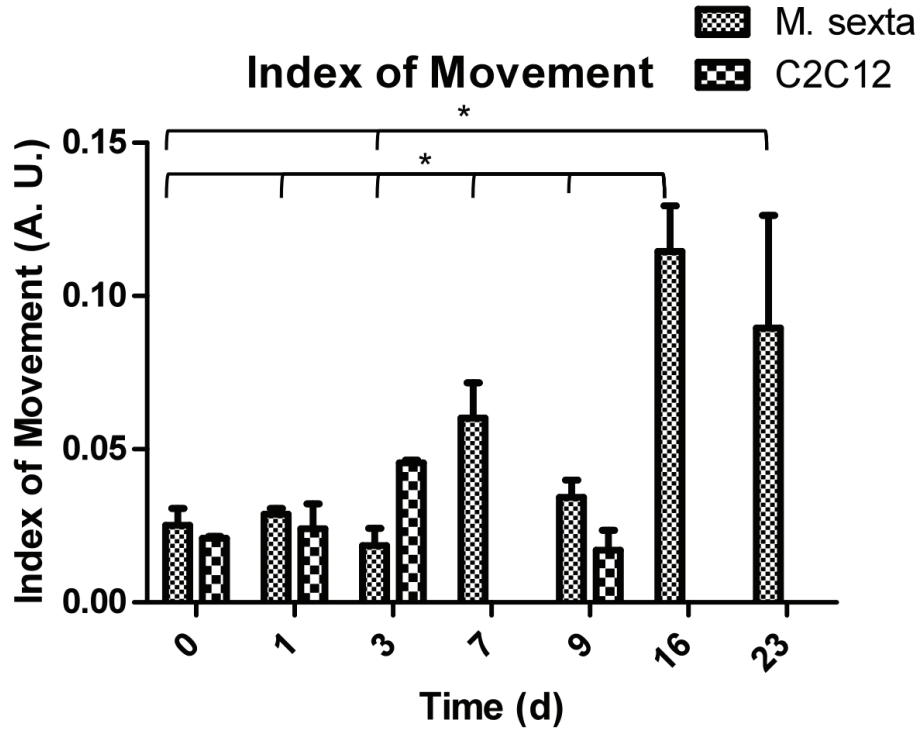


FIGURE 3.8 INDEX OF MOVEMENT TRACKING FOR *M. SEXTA* VS. C2C12 MUSCLE. PLOT OF AVERAGE INDEX OF MOVEMENT OVER TIME FOR BOTH CELL TYPES FOR 3 REGIONS PER CONDITION. VALUES ARE SIGNIFICANT FOR *M. SEXTA* T = 16D AND T = 23D COMPARED TO PREVIOUS TIME POINTS, AS INDICATED. *P<0.001.

One factor that plays a role in the enhanced contractile properties of *M. sexta* muscle is its limited adherence to tissue culture plastic. While C2C12 cells tend to attach to the cell culture substrate along their entire length, insect muscles tend to span from one cell mass to another, allowing them to be suspended with attachments to the cell masses at either end. The distribution of

integrins along the cell membrane may play a role in this phenomenon, as well as signaling occurring within the cell masses, which the muscle cells extend from. The mechanical properties of the cells themselves also contribute to their contractile behavior. *In vitro* mouse cells often tear themselves apart during contractile activity, presumably due to their adhesion to the tissue culture plastic and inability to undergo large deformations. However, insect muscle has the ability to stretch more than 160% its resting length, and has been compared to particle-reinforced rubber in terms of its material properties (Woods, *et. al.*, 2008, Dorfmann, *et. al.*, 2007).

Muscle contractions occur through changes in sarcomere length, with thin and thick filaments sliding over one another and thus creating shortening in myofibrils. The fact that insect larval muscle has less organized and often longer sarcomeres may allow it more freedom in range of shortening and may favorably influence the material properties. Indeed, sarcomeric striations in *M. sexta* cultures consist of domains space between 4 and 13 μm , rather than the 2 μm spacing typically observed in mammalian striated muscle (data not shown). Contractile properties may also be affected by active zone distribution. Mammalian muscle has a single region of concentrated active zones per cell, while insects tend to have more widely distributed active zones.

In a bioactuated system, we would like to be able to operate for extended periods of time without the need for tissue repair or replacement. Additionally, the force generated by the contractions must persist long enough to perform locomotion or pumping work. Therefore, since insect muscle cell contractions persist over the course of months, and a single contraction produces force for seconds rather than milliseconds, they are well-suited for bioactuation applications. However, in future work, we will develop stimulation regimes such

that spontaneous activity may be overridden and force production may be precisely controlled.

Whereas for most mammalian systems, the length of a typical sarcomere is around $2\mu\text{m}$, for larval *M. sexta* muscle it is much longer and variable (Rheuben & Kammer 1980, Greenhalgh *et. al.*, 2008). This may have important consequences for the contractile properties of the cell. We have observed sarcomeric spacings that are longer than $2\mu\text{m}$, and appeared to vary in regions along the myofiber (Figure 3.9). The cause for this variation in sarcomere length may be due to the myofibers still undergoing development, as several muscles in the larva do not develop sarcomeres until the second instar or later (Bernstein *et. al.*, 1993). It may also be attributed to the activity of the cell at the time of fixation, as active contraction causes a dynamic change in sarcomere spacing. Additionally, sustained contractions can cause changes in sarcomere ultrastructure (Greenhalgh *et. al.*, 2007). In mollusks, researchers have found that muscle cells undergo a shift with time from striated muscle to visceral muscle; this process may also be at play here, but additional studies are needed to track cell ultrastructure over time (Odintsova *et. al.*, 2010).

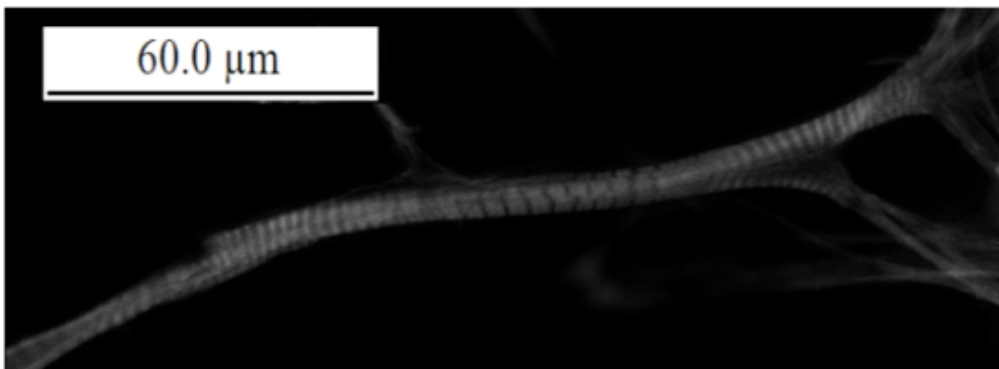


FIGURE 3.9 ACTIN STAINING REVEALING DOMAINS OF VARYING SARCOMERIC SPACING IN A 96-DAY OLD CULTURE.

3.5 Summary

We characterized our cultures using immunofluorescence staining and found that the majority of cells differentiated with time to functional myotubes. Despite the lack of purity in the cultures, there are several benefits to leave these supportive cell types in the culture, rather than use further purification steps such as FACS, including the positive influence of neurons on muscle development, and potential contributions of vitellophages to extended survival.

Our cells survived and contracted for greater than three months without medium refreshment. This is a very exciting and puzzling observation; our studies in Chapter 4 attempt to address the mechanisms for long-term cell survival. Additionally, cultivated muscle cells display long-term, spontaneous contractions with dynamics on the order of seconds, which is suitable for bioactuation applications. Furthermore, the long sarcomere observed within the cells are consistent with the ultrastructure of larval *M. sexta* muscle.

3.6 References

Bayline RJ, Khoo AB, Booker R. (1998) Innervation regulates the metamorphic fates of larval abdominal muscles in the moth, *Manduca sexta*. *Dev. Genes Evol.* 208:369 – 381.

Bayline RJ, Duch C, Levine RB. (2001) Nerve-muscle interactions regulate motor terminal growth and myoblast distribution during muscle development. *Dev. Biol.* 231:348 – 363.

Baylies MK, Bate M, Gomez MR. (1998) Myogenesis: A view from *Drosophila*. *Cell* 93:921 – 927.

Bernstein SI, Fryberg EA, Donady JJ. (1978) Isolation and partial characterization of *Drosophila* myoblasts from primary cultures of embryonic cells. *J Cell Biol.* 78:856 – 865.

Bernstein SI, O'Donnell PT, Cripps RM. (1993) Molecular genetic analysis of muscle development, structure, and function in *Drosophila*. *Int. Rev. Cytol.* 143:63 – 152.

Broadie K, Skaer H, Bate M. (1992) Whole-embryo culture of *Drosophila*: development of embryonic tissues *in vitro*. *Roux's Arch. Dev. Biol.* 201:364 - 375.

Chapman RF. (1998) *The Insects: Structure and Function*, 4th ed. Cambridge University Press, Cambridge. p. 77, 303, 334, 350.

Dorfmann A, Trimmer BA, Woods WA. (2007) A constitutive model for muscle properties in a soft-bodied arthropod. *J. R. Soc. Interface* 4:257 - 269.

Fausto AM, Carcupino M, Mazzini M, Giorgi F. (1994) An ultrastructural investigation on vitellophage invasion of the yolk mass during and after germ band formation in embryos of the stick insect *Carausius morosus* *Br. Develop. Growth & Differ.* 36(2):197 - 207.

Greenhalgh C, Prent N, Green C, Cisek R, Major A, Stewart B, Barzda V. (2007) Influence of semicrystalline order on the second-harmonic generation efficiency in the anisotropic bands of myocytes. *Applied Optics* 46(10):1852 – 1859.

Interactive Fly 67th edition <http://www.sdbonline.org> © 2013 Thomas B. Brody, Ph.D.

- Küppers-Munther B, Letzkus JJ, Lürer K, Technau G, Schmidt H, Prokop A. (2004) A new culturing strategy optimizes *Drosophila* primary cell cultures for structural and functional analyses. *Dev. Biol.* 269:459 – 478.
- Lehmann K, Zwadlo G, Pfeiffer P, Burger PM. (1985) Effect of hemolymph and nervous-tissue components on the in vitro development of flight-muscle myoblasts of *Manduca sexta*. *Differentiation* 30:92 – 97.
- Luedeman R & Levine RB. (1996) Neurons and ecdysteroids promote proliferation of myogenic cells cultured from the developing adult legs of *Manduca sexta*. *Dev. Biol.* 173:51 – 68.
- Lürer K & Technau GM. (2009) Single cell cultures of *Drosophila* neuroectodermal and mesectodermal central nervous system progenitors reveal different degrees of developmental autonomy. *Neural Dev.* 4(1):30.
- Odintsova NA, Dyachuk VA, Nezhlin LP. (2010) Muscle and neuronal differentiation in primary cell culture of larval *Mytilus trossulus* (Mollusca: Bivalvia). *Cell Tissue Res.* 339:625 – 637.
- Rheuben MB & Kammer AE. (1980) Comparison of slow larval and fast adult muscle innervated by the same motor neuron. *J. Exp. Biol.* 84:103 - 118.
- Seecof RL, Alleaume N, Teplitz RL, Gerson I. (1971) Differentiation of neurons and myocytes in cell cultures made from *Drosophila* gastrulae. *Exp. Cell Res.* 69:161 – 173.
- Seecof RL & Donady JJ. (1972) Factors affecting *Drosophila* neuron and myocyte differentiation *in vitro*. *Mech. Age. Dev.* 1:165 – 174.
- Sun B & Salvaterra PM. (1995) Characterization of Nervana, a *Drosophila melanogaster* neuron-specific glycoprotein antigen recognized by anti-horseradish peroxidase antibodies. *J. Neurochem.* 65(1):434 – 443.
- Woods WA, Fusillo SJ, Trimmer BA. (2008) Dynamic properties of a locomotory muscle of the tobacco hornworm *Manduca sexta* during strain cycling and simulated natural crawling. *J. Exp. Biol.* 211:873 - 882.

Chapter 4. Metabolic analyses

4.1 Introduction

Muscle is a highly metabolic tissue. As such, it requires sufficient nutrients and oxygen to carry out its contractile functions. Mammalian muscle can function through specific metabolic pathways, depending on the fiber type. However, larval insect muscle does not have the same classification for different muscles. Alternatively the tissues, and indeed the organism itself, have evolutionarily developed the ability to cope with environmental stresses by adapting their metabolism. Muscle metabolism can occur using three different energy sources as substrates. These include carbohydrates, proline, and lipids. The substrate selected by the insect depends on the species and/or life stage.

Vitellogenesis, or yolk cells, have not been widely studied. They are, however, maternally-derived and exist in developing embryos to provide nutrition to the cells. Studies of lipid transfer from yolk cells to embryos have cited inclusion of yolk cells into the gut at dorsal closure, and ingestion by the embryo as the mechanism for two of the three main phases of lipid uptake, but the mechanism of lipid transfer to the embryo during the earliest phase is unknown (Yamahama *et. al.*, 2008). The presence of yolk cells in our cultures prompted us to question whether these cells could be behaving similarly to the cells of the fat body, whereby diacylglycerol is shuttled to the muscle for fuel in the form of free

fatty acids (Figure 4.1). Other possible processes could be glycogen breakdown to glucose, and protein breakdown to amino acids, both of which can be used for fuel, and both of which we have found to be produced in our cultures (Figure 4.1).

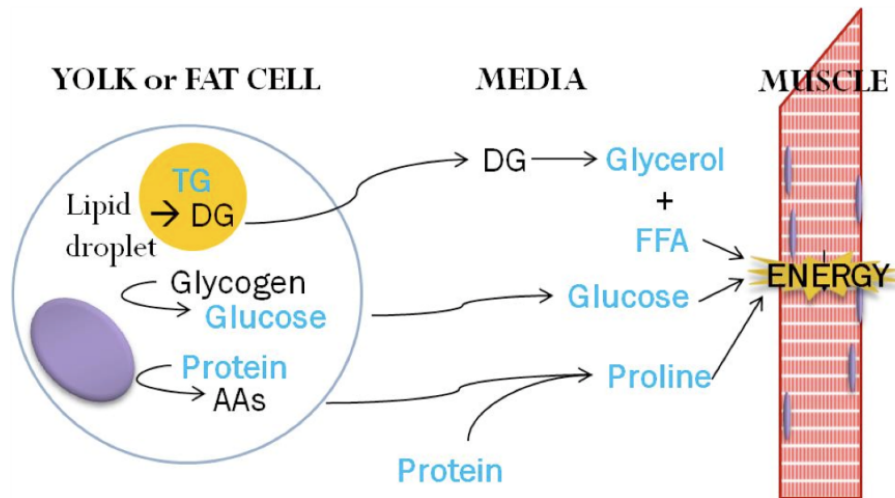


FIGURE 4.1 POTENTIAL INTERACTIONS BETWEEN FAT OR YOLK CELLS AND MUSCLE FIBERS *IN VITRO*. BLUE INDICATES METABOLITES THAT MAY BE TRACKED *IN VITRO* USING ASSAY KITS OR HPLC. TG = TRIGLYCERIDE, DG = DIACYLGLYCEROL, AAS = AMINO ACIDS, FFA = FREE FATTY ACID. PURPLE ARE NUCLEI, YELLOW CIRCLE IS A LIPID DROPLET.

We were interested in studying the differences between mouse muscle cell line C2C12 and our insect muscle cells, in terms of metabolism. We tracked metabolite concentrations in the medium of both cell types over time, in the absence of medium changes. As expected, mammalian cells used glucose and produced lactate before reaching senescence around day 3 due to lack of medium replenishment. However, we were surprised to find that although insect cells produced large amounts of lactate, they did not appear to be consuming glucose.

To test if glucose was necessary for metabolism, and to probe for the medium component that was, we performed subtractive medium experiments whereby a single, critical medium component was removed. We were further puzzled by the fact that glucose and amino acids seemed to be unnecessary for muscle metabolism. We discovered that maternally-derived yolk cells are present in our cultures, and this led us to hypothesize that the influence of yolk cells could be contributing to extended cell survival and could account for the production of nutrients such as glucose and amino acids *in vitro*. We tested this hypothesis by attempting to separate myoblasts from yolk cells and track their viability and metabolism.

4.2 Comparison with mouse

One of our hypotheses was that caterpillar muscle, given its ability to function without a closed circulatory system and with transport of oxygen arising mainly from passive diffusion, could function under nutrient-deprived conditions. Vascularization is a major limiting factor in engineering dense tissues such as muscle (Levenberg *et. al.*, 2005). Therefore, if this obstacle could be bypassed, it would be a major advantage for the development of bioactuators from insect muscles. Metabolic profiles of *M. sexta* and mouse C2C12 myotubes were evaluated under normal (1.23 g/L and 4.5 g/L, respectively) and low glucose (0.27 g/L and 1 g/L, respectively) conditions. Glucose consumption, lactate production, and cell numbers were quantitatively tracked over time (Figure 4.2A – B).

C2C12 mouse control and low glucose conditions resulted in steady glucose consumption and lactate production over the first three days, as

expected. After this time, activity plateaus, presumably due to nutrient limitations leading to senescence and cell death (Figure 4.2A – B). Surprisingly, insect control and low glucose cultures do not appear to consume glucose throughout the duration of the experiment. However, after three days, a dramatic increase in lactate production occurs (Figure 4.2A – B). Despite the high levels of lactate produced, cells remain viable and contractile. Insect cells are able to tolerate a wide range of pH environments, and therefore acidosis was not an issue. The approach utilized by these cells to tolerate pH lowering is unknown, however a mechanism for maintaining intracellular pH, such as a H⁺-V-ATPase in the plasma membrane, may be at play (Harrison, 2001).

The data suggest that, while mouse cells rapidly consume glucose and produce lactate, insect cells have different metabolic activity on a per cell basis. The control group of C2C12 cells consumed nearly 40% of their initial glucose within 3 days and low glucose cultures depleted all of their glucose supply within 5 days. Insect cells, however, did not consume significant amounts of glucose throughout the duration of the culture, which was extended to 14 days for *M. sexta* groups. It is possible that glucose consumption was affected by the action of 20HE, as the hormone may block glycolysis (Tian *et. al.*, 2010).

Mouse cells rapidly produced lactate when cultured for several days without medium changes, which was not surprising. Lactate is produced under anaerobic conditions, when cells are starved for a crucial metabolite such as glucose and are forced to convert pyruvate to lactate. The insect cells, after a 3-day lag phase, produced lactate at a rapid rate. The fact that a large amount of lactate was produced in the absence of glucose consumption led us to consider what energy source the cells were using.

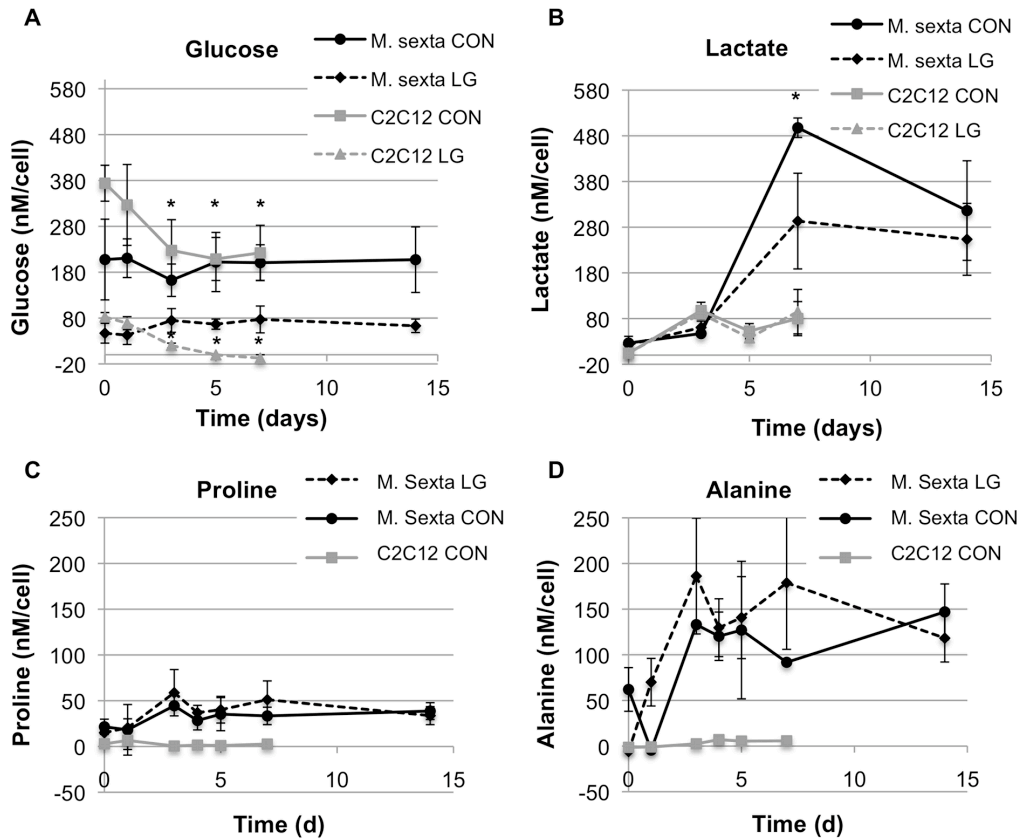


FIGURE 4.2 MEDIUM CONCENTRATIONS OF METABOLITES TRACKED OVER TIME IN INSECT AND MOUSE C2C12 CELL CULTURES, ON A PER CELL BASIS. GLUCOSE CONSUMPTION AND LACTATE PRODUCTION WERE ANALYZED FOR *M. SEXTA* CONTROL (CON, BLACK CIRCLES) AND LOW GLUCOSE (LG, BLACK DIAMONDS) CONDITIONS, ALONG WITH C2C12 CON (GRAY SQUARES) AND LG (GRAY TRIANGLES) SAMPLES FOR COMPARISON (A – B). STATISTICALLY DIFFERENT VALUES ARE COMPARED WITH CORRESPONDING TIME 0 VALUES FOR GLUCOSE (A), AND BETWEEN *M. SEXTA* CON AND LG FOR LACTATE (B). FOR AMINO ACID ANALYSIS, C2C12 LOW GLUCOSE CONDITION WAS OMITTED (C – D). * P<0.05.

Insects have the ability to utilize carbohydrates, amino acids, lipids, or a combination of these for changes in energy demand during flight (Suarez *et al.*, 2005; Auerswald & Gäde, 2000; Haunerland, 1997). Therefore, we investigated whether proline metabolism was fueling metabolic activity in the cells. Amino acid profiles were obtained from HPLC analysis of cell culture media, and normalized

to amino acid levels in the starting media. C2C12 low glucose samples were omitted from this analysis. For C2C12 control cells, proline was consumed by day 3, at which time a slight increase in alanine concentration was observed (Figure 4.2C – D). For both insect control and low glucose conditions, alanine levels increased dramatically with respect to starting medium concentrations and proline levels did not significantly decrease; rather, they remained stable (Figure 4.2C – D). This response is similar to the steady increase in lactate concentration while the levels of glucose remained constant (Figure 4.2A – B). These data suggest that there may be a mechanism in the cultured cells for producing energy sources such as glucose and proline, allowing their concentrations in the medium to remain stable while generating metabolic end products including energy, lactate, and alanine.

This result was further confirmed by analyzing amino acid levels on culture day 0, in comparison to medium levels (Figure 4.4). We found that, after a 1 hour incubation period on the day the cells were plated, both control and low glucose insect cultures had produced all of the amino acids we probed for (Figure 4.4). This was in stark contrast to the mammalian controls, where amino acid levels are the same, or slightly lower, than their concentrations in the media, after a 1 hour incubation. Therefore, on a fairly rapid basis, amino acids were being produced in the cultures, likely by the breakdown of proteins, and this process did not occur in mammalian cells.

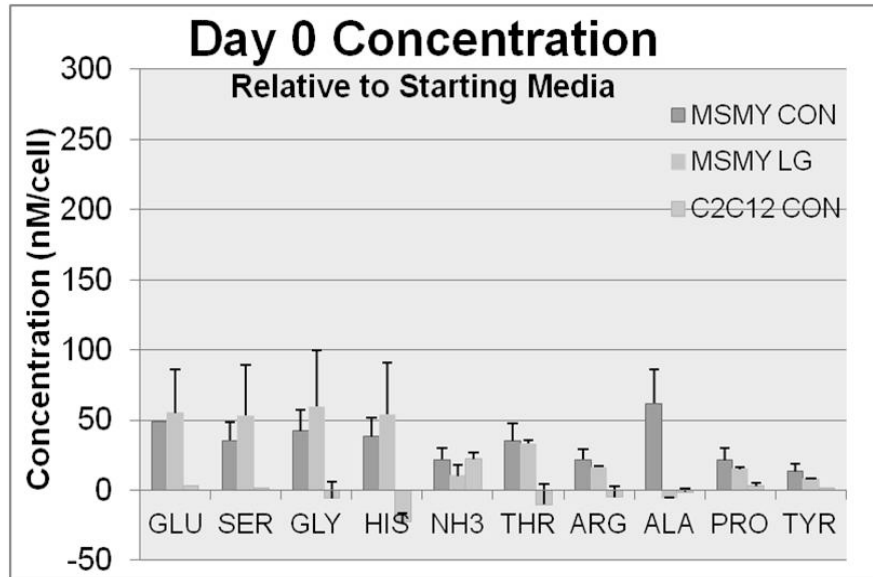


FIGURE 4.4 AMINO ACID CONCENTRATIONS, NORMALIZED TO CONCENTRATIONS IN MEDIA ALONE, IN CONDITIONED MEDIA FROM DIFFERENT CELL CULTURES AFTER APPROXIMATELY ONE HOUR OF INCUBATION.

Our next step was then to challenge the system, and see if the cells could survive when deprived of certain crucial nutrients, given the fact that their appeared to be producing their own energy substrates.

4.3 Culture responses to subtractive media

Our metabolic analyses thus far suggested that nutrients such as glucose and amino acids were being produced in the cultures, a result that was unique to insect cells. In order to further probe this theory, we conducted a study in which various essential medium components were excluded from the media formulation, and the cells were subsequently evaluated on the basis of morphology over a long time course (2 months).

We identified glucose, amino acid mix, yeast extract and FBS as media components that are likely required for metabolism and cell survival. Cells were grown in either control or subtractive media for a period of two months, with imaging time points collected at regular intervals. Within two weeks of culture without FBS, all the cells had died (Figure 4.5N). The remaining conditions all appeared viable and relatively similar at this point (Figure 4.5B, E, H, K). However, after two months of culture, cells deprived of yeast extract had died as well (Figure 4.5I). Control cells looked normal, surviving and contracting continuously as they typically do at this time point (Figure 4.5C). Cultures lacking glucose or amino acids appeared even healthier than the control condition (Figure 4.5F, L). The muscle fibers had larger widths and were more abundant than control cells, and the contractions appeared stronger and were observed with a higher frequency, qualitatively. This result, while not readily explainable, was nonetheless exciting and intriguing.

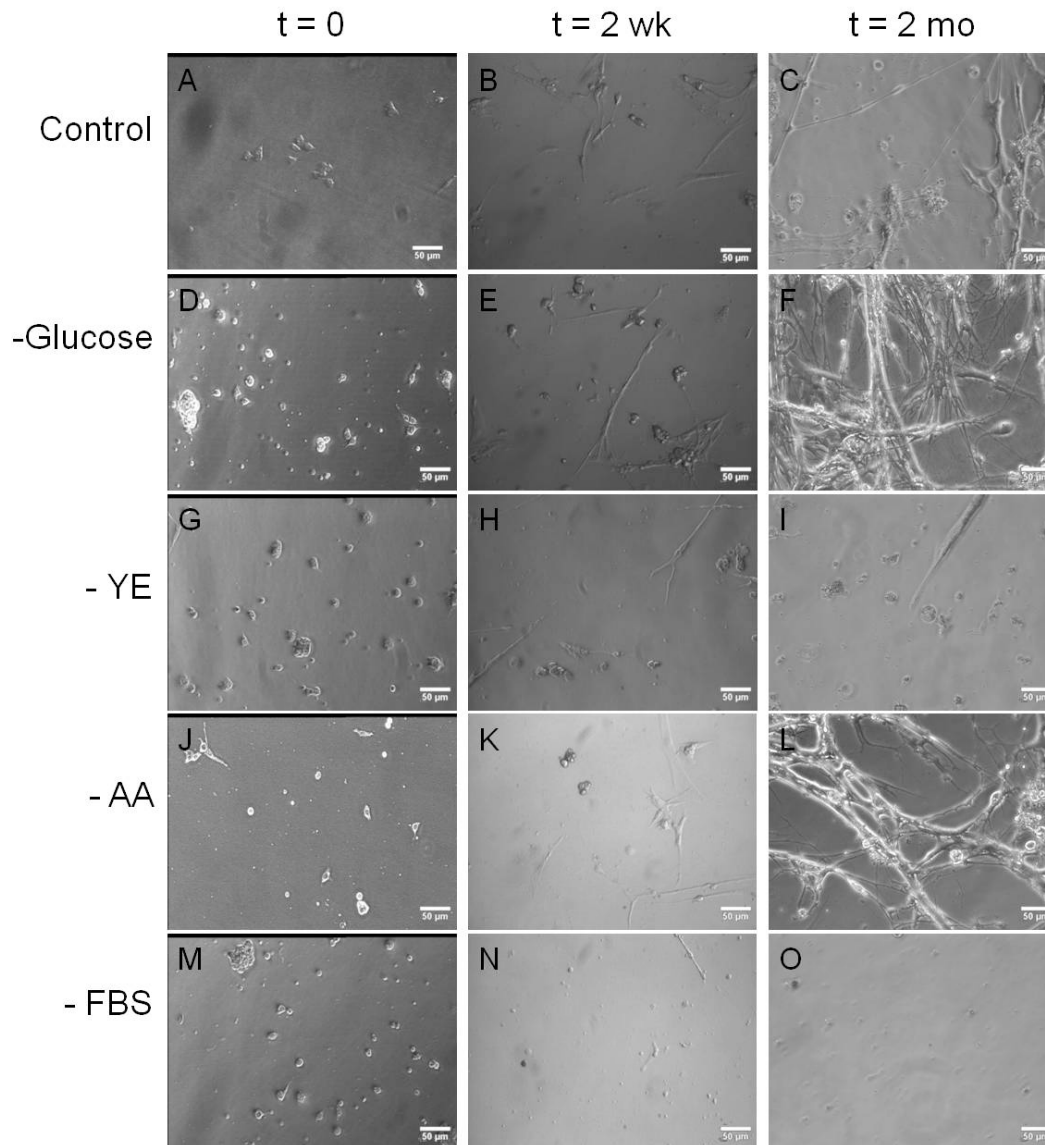


FIGURE 4.5 CELL MORPHOLOGY AND SURVIVAL IN SUBTRACTIVE MEDIA EXPERIMENTS OVER TIME. CELLS WERE GROWN EITHER IN CONTROL MEDIA (A – C), WITHOUT GLUCOSE ADDED (D – F), WITHOUT YEAST EXTRACT (YE) ADDED (G – I), WITHOUT AMINO ACIDS ADDED (J – L), OR WITHOUT FBS ADDED (M – O). SCALE BARS ARE 50 UM.

It was not very surprising that the cells required FBS for survival. Since cell culture practices were first developed, animal sera have been used to supplement media, and often required for cells to survive. However, the precise composition of these sera is not known and varies from batch to batch. For insect

cells, it has been found that egg extract promotes cell growth more effectively than FBS, and it is therefore likely that the combination of FBS and factors derived from the eggs in our cultures contribute to their vitality and long-term growth (Akiduki, 2010). Similarly, yeast extract is also undefined medium component, which provides the cells with additional vitamins, amino acids and carbohydrates, so it was also not surprising that the cells required this ingredient to thrive.

We were, however, very surprised to find that cells survived and thrived without glucose, and similarly without amino acids. In fact, it appeared as though cultures without supplemental glucose and amino acids developed better than control cultures. This result further convinced us that a component or components of our cell cultures derived from embryos were able to sustain themselves without needing significant supplementation.

4.4 Metabolic influence of vitellophages

Yolk cells derived from the developing eggs may be responsible for such processes, as their role in development is to provide nutrition to the developing embryo (Yamahama *et. al.*, 2008). It is possible that yolk cells accomplish transfer of nutrients to embryonic cells in a similar way to the fat body in later insect life stages. Triglyceride breakdown to diacylglycerol (DG) occurs in the fat body of adult *M. sexta* and other insects, and subsequent transport of DG to muscle tissues provides substrates for free fatty acid metabolism and energy production (Law & Wells, 1989; Patel *et. al.*, 2006). Additionally, yolk cells are known to have glycogen stores and protein granules as well, potentially allowing them to provide amino acids and carbohydrates to cells as well. We investigated

the role of yolk cells in our cultures to determine if extended cell survival was resulting from their influence.

4.4.1 Vitellophage metabolism

We studied yolk cells, specifically their intracellular lipid droplets, to see if lipid mobilization was occurring. We stained cells using Oil Red O and took images on day 1 and day 6 of culture. From the images, we performed analysis on the number and size of lipid droplets, and total lipid area at both time points. Qualitatively from our imaging, we can see that yolk cells initially contain only one or two lipid droplets per cell (Figure 4.7A). After 6 days, we found that the one or two large droplets remain, but many smaller droplets are present as well (Figure 4.7B). Our analysis confirmed this observation, as the number of lipid droplets per cell significantly increased (Figure 4.7C). The analysis further revealed that this was from the breakdown, rather than accumulation of lipid, as the largest lipid droplet size significantly decreased, and the overall lipid area decreased, though not significantly (Figure 4.7D, E). We were therefore encouraged that the cells were producing energy substrates for the muscles in the culture, and decided to further probe the system by separating yolk cell from the other cell types in the culture.

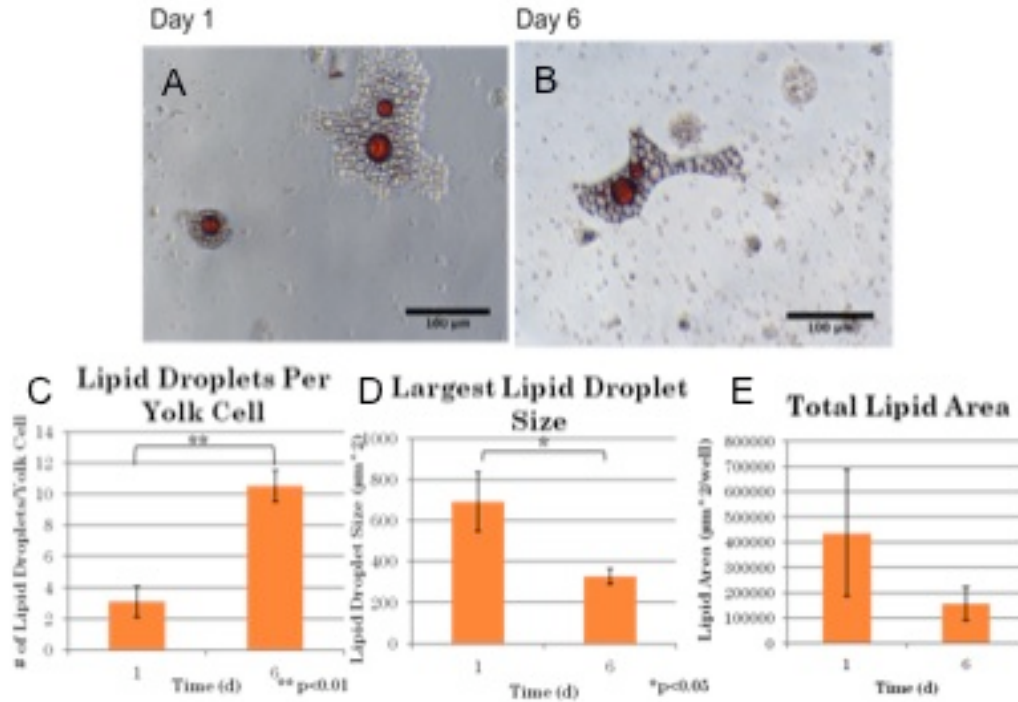


FIGURE 4.7 LIPID MOBILIZATION FROM YOLK CELLS. YOLK CELLS ON DAY 1 CONTAIN 1 OR 2 LIPID DROPLETS (A). BY DAY 6, SMALLER DROPLETS ARE SEEN WITHIN THE CELL (B). IMAGING ANALYSIS CONFIRMS THIS RESULT, AS NUMBER OF LIPID DROPLETS PER CELL SIGNIFICANTLY INCREASES (C). THE LARGEST LIPID DROPLET SIZE SIGNIFICANTLY DECREASES (D), AND OVERALL LIPID AREA DECREASES (E).

4.4.2 Cell separation methods

Percoll separation

In order to examine yolk cell and myoblast metabolism separately, we sought to develop an approach for collecting and purifying populations of each. One method we explored to accomplish that was separation by density gradient. Percoll is a commercially-available solution of silica particles with high density in a salt solution. By diluting the Percoll in saline and layering the solutions from high density at the bottom to low density at the top of a conical vial, cells may be separated on the basis of density and size by their ability to migrate through the layers, accumulating at layer interfaces, upon centrifugation.

In initial studies, we examined cell migration through a range of Percoll concentrations. From these experiments, we determined that yolk cells, which are larger but likely less dense than embryonic cells due to their high lipid content, could pass through a 15% Percoll solution but not 25%. We found that embryonic cells could migrate through a 25% Percoll solution, but not 60%. Therefore, for cell separations, we used discontinuous gradients as depicted in Figure 4.9A. For control cells, we wanted to keep yolk and embryonic cells together, but still pass them through a Percoll gradient to account for any changes in viability that the Percoll process might have. For this, we used a 60/15% discontinuous gradient, collecting a mixture of cell types at the interface of the two layers. To separate embryonic from yolk cells, we used a 60/25/15% discontinuous Percoll gradient. We collected embryonic cells at the 60/25 interface, and yolk cells at the 25/15 interface.

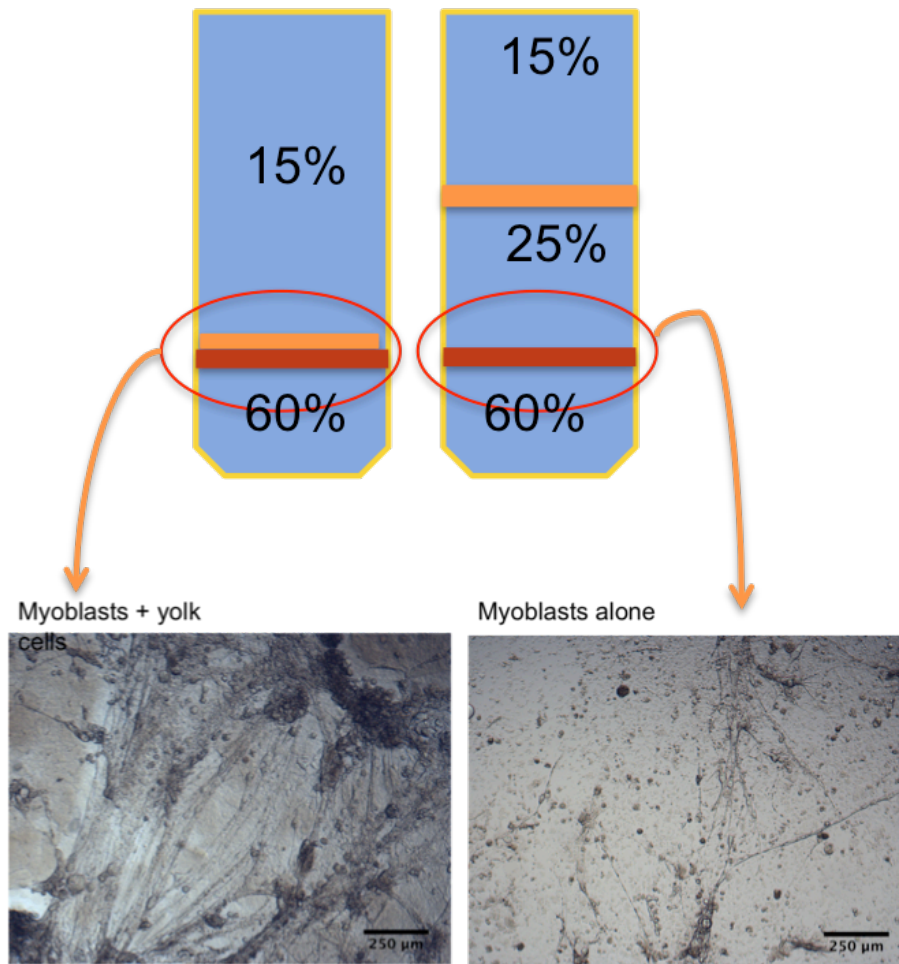


FIGURE 4.8 MUSCLE CELL PURIFICATION USING PERCOLL GRADIENTS.

The control and separated cell types were cultured for 90 days. We found that, although mixed cultures of embryonic and yolk cells survived and formed mature, dense, active muscle networks, embryonic cells alone failed to develop to maturity and lost viability (Figure 4.8B, C). LIVE/DEAD staining around mid-way through the culture revealed that embryonic cell cultures alone underwent significant cell death (Figure 4.9A, red staining), in comparison to cell cultures of the same age that had not had yolk cells removed (Figure 4.9B). Lower cell densities in the separated cultures versus control cultures could have contributed to reduced muscle network formation. Therefore, in future work, this experiment

will be refined such that cell numbers are collected to have equivalent cell densities in both experimental and control conditions.

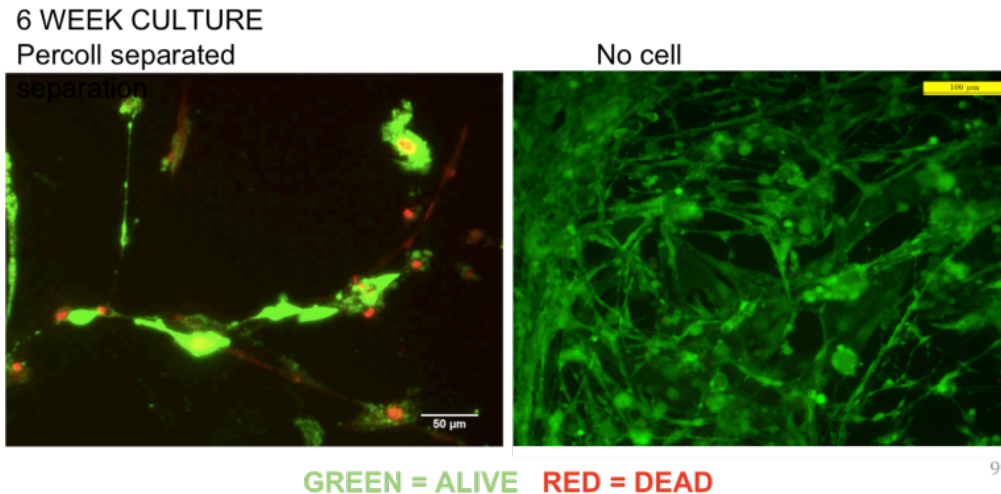


FIGURE 4.9 LIVE/DEAD STAINING OF PERCOLL SEPARATED (LEFT) AND NONSEPARATED (RIGHT) INSECT MUSCLE CULTURES AFTER 6 WEEKS.

We sought to additionally track the metabolism of the separated cell populations; however, due to limited yolk cell numbers we were unable to collect a pure population of yolk cells from the Percoll gradient interface. Therefore, although this is an effective method for collecting embryonic cells free from yolk, it is less useful for collecting yolk cells alone. We thusly chose to investigate other methods of cell separation.

Manual separation

Yolk cells and embryonic cells were manually separated by dissection. With the use of a dissecting microscope, yolk cells, which are large, round and contain 1 – 2 large lipid droplets, could be clearly identified. Similarly, fragments of the embryo were observed as well. A 1mL syringe was used to separately

collect yolk cells and embryonic cells from staged embryos; control conditions used a mixture of yolk cells and embryonic cells from the same number of eggs (Figure 4.10A).

The resulting populations were characterized with Oil Red O staining. Yolk cells were readily identified in yolk cell populations, and were not found in embryonic cell cultures (Figure 4.10B, C). We further analyzed the cultures by imaging and quantifying the lipid area and lipid droplet sizes using ImageJ. The results of this analysis indicated that yolk cell populations had significantly more lipid and significantly larger intracellular lipid droplets than cells in embryonic cultures (Figure 4.10D, E). Thus, we were confident in using these cell populations to analyze both yolk cell and embryonic cell metabolism alone, and when cultured together.

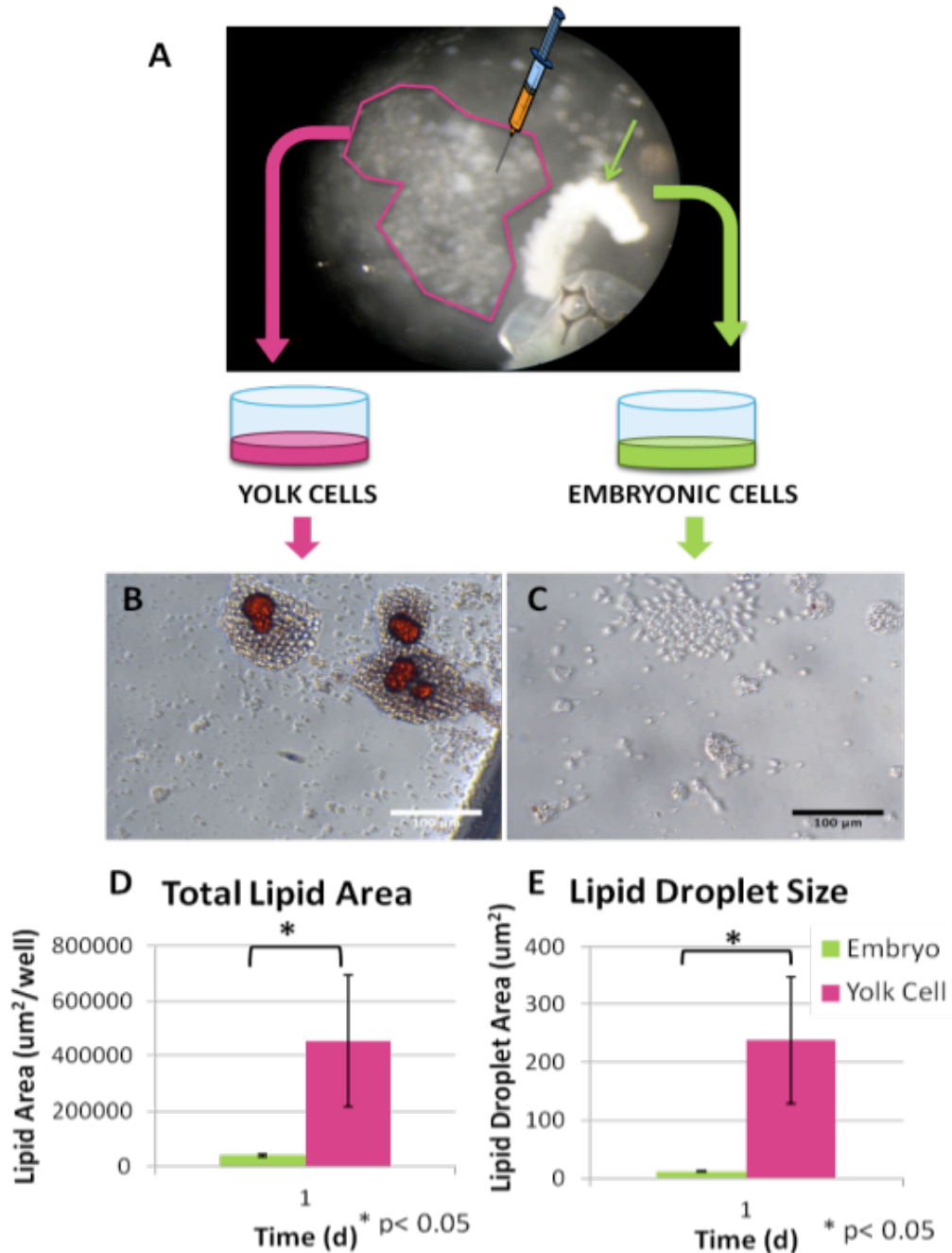


FIGURE 4.10 CELL SEPARATION BY MANUAL DISSECTION. YOLK CELLS AND EMBRYONIC TISSUE FRAGMENTS WERE COLLECTED SEPARATELY USING A SYRINGE (A). YOLK CELLS COULD BE CLEARLY IDENTIFIED IN YOLK CELL CULTURES (B), BUT NOT IN EMBRYONIC CULTURES (C), USING OIL RED O STAINING FOR LIPID DROPLETS (RED). TOTAL LIPID AREA WAS QUANTIFIED FROM THE IMAGES AND FOUND TO BE SIGNIFICANTLY HIGHER IN YOLK CELL CULTURES (D). LIPID DROPLET SIZES WERE ALSO QUANTIFIED AND FOUND TO BE SIGNIFICANTLY HIGHER IN YOLK CELL CULTURES (E).

4.4.3 Cell separation metabolism

Using the cultures generated by manual dissection, we tracked extracellular metabolism over time. Medium samples were taken from each culture at regular timepoints and analyzed for concentration of various metabolites. Results of glucose and protein analysis are shown in Figure 4.11.

For yolk cell only cultures, concentration of glucose remained fairly constant with time (Figure 4.11A). Embryonic and mixed cell cultures tracked together for the first week. Subsequently, embryonic only cultures leveled off for the remainder of the experiment. However, combined cell cultures experienced and increase in cel concentration between days 8 and 18. It is possible that myogenic cells use glucose for the first few days, then switch to another energy source, as the levels of glucose in cultures containing muscle cells increase after day 3, however, the mechanism by which glucose is produced in these cultures is still unknown, given that yolk cell only cultures do not appear to produce glucose. Even so, it should be noted that yolk cell cultures have an initially higher level of glucose than cultures containing myogenic cells.

Protein concentration in yolk cell cultures increases initially, then decreases and somewhat levels off (Figure 4.11B). Again, protein levels for both myogenic and combined cultures track closely to one another for the first week. This could indicate that combined cultures are using protein early on, since they should have a higher level than myogenic only due to protein production by yolk cells. However, it appears as though after the first week, protein is no longer used, given that protein concentrations gradually increase with time after the first week.

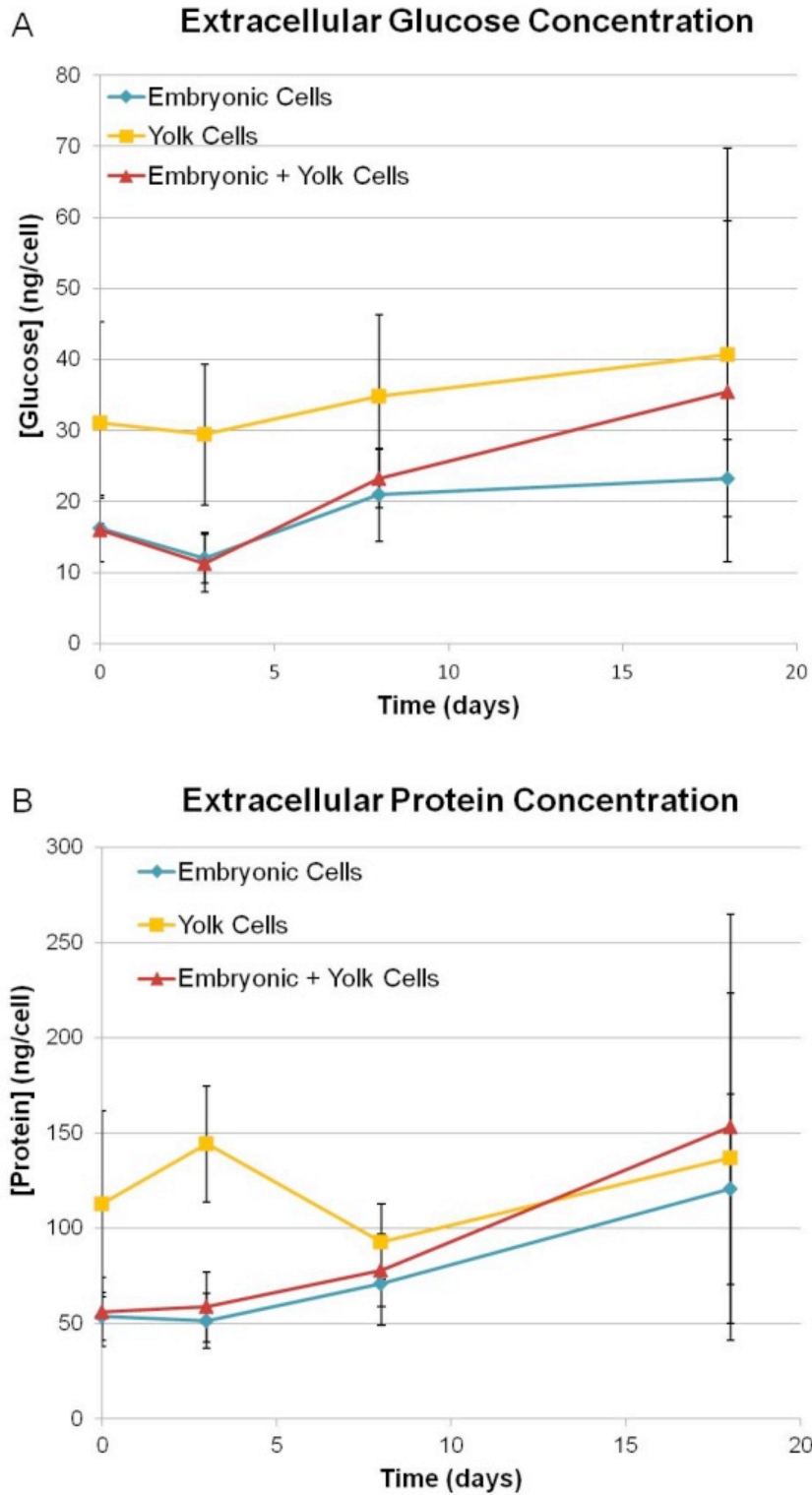


FIGURE 4.11 METABOLIC PROFILES FOR SEPARATED AND CONTROL CULTURES. GLUCOSE (A) AND PROTEIN (B) CONCENTRATIONS WERE QUANTIFIED AND NORMALIZED TO CELL NUMBERS.

We have not yet investigated triglyceride, proline, alanine, and lactate profiles for this system. We anticipate that lipid may be the energy source the muscle cells use after the first week, as it is clearly mobilized in yolk cells in culture. Studies have analyzed yolk cell lipid droplets in the embryo, and have found that the majority of the contents of yolk cells is transferred to the embryo by incorporation of the cells into the gut during dorsal closure, and by ingestion once the embryos mandibles have developed (Yamahama *et. al.*, 2008). However, there is an initial interval before these developmental events occur when the embryo takes on lipid, and the extraembryonic yolk concentration decreases. The mechanism for this transfer is unknown. We are presently working to elucidate the mechanism of energy transfer that is at play in our cultures, and very well could be at play in the early stages of embryonic development.

4.5 Summary

We evaluated the metabolism of our embryonic muscle cell populations in comparison to the widely-used mouse C2C12 muscle cell line. We found that our insect cells did not appear to use glucose over the course of the experiment. Similarly, we did not observe proline usage, although the end products for both of these metabolites, lactate and alanine, were produced at high levels. An additional observation from these experiments was that amino acids were produced in the cultures, as their levels were higher than medium concentrations. As a result, we performed subtractive medium experiments, which showed that neither supplemental glucose nor amino acids were required for cell survival and development, although yeast extract and FBS were.

We identified extraembryonically-derived yolk cells in our cultures, as discussed in Chapter 3, and hypothesized that these cells may be responsible for metabolite production in the cultures, and thereby extended survival. After determining an appropriate method for yolk cell and embryonic cell separation, we analyzed metabolism of both cultures, in comparison to combined cultures. Our results are not entirely conclusive, as we still need to analyze triglyceride profiles, among others, but we did find that embryonic cells alone do not survive and develop into active muscle as cultures containing yolk cells do. This result supports our hypothesis that yolk cells may be able to provide long-term nutrition and support survival and development of insect muscle cells *in vitro*. Interestingly, since these phenomena have not been closely studied *in vivo*, our work may also aid to explain nutrient delivery to developing embryos during the early stages of embryogenesis.

4.6 References

- Akiduki G. (2010) Egg extract promotes cell migration and growth in primary culture of early embryos in the silkworm, *Bombyx mori* (Lepidoptera: Bombycidae). *Appl. Entomol. Zool.* 45(1):153 – 161.
- Auerswald L & Gäde G. (2000) Metabolic changes in the African fruit beetle, *Pachnoda sinuata*, during starvation. *J. Insect Physiol.* 46:343 - 351.
- Harrison JF. (2001) Insect acid-base physiology. *Annu. Rev. Entomol.* 46:221 - 250.
- Hauerland NH. (1997) Transport and utilization of lipids in insect flight muscle. *Comp. Biochem. Physiol.* 117B(4):475 – 482.
- Law JH & Wells MA. (1989) Insects as biochemical models. *J. Biol. Chem.* 264(28):16335 – 16338.
- Levenberg S, Rouwkema J, Macdonald M, Garfein ES, Kohane DS, et al. (2005) Engineering vascularized skeletal muscle tissue. *Nature Biotech.* 23(7):879 - 884.
- Patel RT, Soulages JL, Arrese EL. (2006) Adipokinetic hormone-induced mobilization of fat body triglyceride stores in *Manduca sexta*: Role of TG-lipase and lipid droplets. *Arch. Insect Biochem. Physiol.* 63:73 – 81.
- Suarez RK, Darveau C-A, Welch KC, O'Brien DM, Roubik DW, et al. (2005) Energy metabolism in orchid bee flight muscles: carbohydrate fuels all. *J. Exp. Biol.* 208:3573 - 3579.
- Tian L, Guo E, Wang S, Liu S, Jiang R-J, et al. (2010) Developmental regulation of glycolysis by 20-hydroxyecdysone and juvenile hormone in fat body tissues of the silkworm, *Bombyx mori*. *J. Mol. Cell Biol.* 2:255 - 263.
- Yamahama Y, Seno K, Hariyama T. (2008) Changes in lipid droplet localization during embryogenesis of the silkworm, *Bombyx mori*. *Zool. Sci.* 25(6):580 – 586.

Chapter 5. 3D construct formation

5.1 Introduction

As the fields of robotics and MEMS develop, the need for an actuator platform on a meso-scale has emerged. The advantages of using muscles as actuators include flexibility, silence, biomimetic action, along with the potential for facile production scale-up. Most interesting perhaps, are the potential for such constructs and devices to self-assemble, regenerate or heal, and biodegrade, properties that have yet to be imagined in current robotic systems.

Though issues of sterility, temperature sensitivity, and real-world robustness have yet to be addressed, we believe that robotic and microsystem actuation may be achieved via bioactuation using the insect muscle cell system presented in this thesis. In order to achieve this goal, we sought to generate 3-dimensional muscle tissue constructs from our insect cell populations, which may serve as linear actuators.

We first investigated a number of cell-guidance and biomaterial formats with the widely-used mouse myoblast cell line, C2C12. These formats included micropatterned PDMS, silk-glycerol films, electrospun silk mats, and silk sponges. Though many of our techniques were highly amenable to mammalian cells, for the most part these approaches did not readily translate to the insect cell system. This is likely due to the structural and organizational differences between mammalian muscle and insect muscle.

As a result, we used developmental and anatomical cues from the insect muscle system to develop a more physiologically-relevant approach for generating functional insect muscle structures *in vitro*. These strategies include a scaffold-free format, incorporation of adhesion proteins that are present in the insect muscle attachment sites, and constraining the dimensions of the structures for optimal alignment, and therefore force output. Interestingly, the cells did not require additional gel or scaffold-based reinforcement; they were able to self-assemble into scaffold-free, spontaneously contractile tissues that were viable for months without medium replenishment.

Once tissue structures were successfully developed, we sought to measure their contractile output to aid in the design of compatible abiotic devices. The most widely-used method for directly measuring force production from muscle explants is with the use of a force transducer. In this approach, the muscle fiber is clipped or attached to a stiff material at either end; one end of the muscle is affixed in place and the other is attached to a sensor. Upon stimulation, the muscle contracts and applies force to the sensor. The mechanical output is converted to an electrical signal, filtered, and read through appropriate software (Fujita *et. al.*, 2007). Often times, tissue-engineered muscle structures are too small to achieve force detection on this type of system, and therefore smaller scale approaches are evaluated using microfabricated devices including tissue gauges and atomic force microscopy (AFM) (Legant *et. al.*, 2009; Shimizu *et. al.*, 2012). Additionally, several methods have been developed for estimating forces based on imaging analysis of contracting tissues (Hayakawa *et. al.*, 2011). Electrogenic activity and calcium flux may also be monitored using microelectrode arrays and calcium-sensing dyes, respectively (Herron *et. al.*, 2011).

5.2 C2C12 construct development

5.2.1 Silk-glycerol films

Silk films have been used in various tissue engineering systems, and are advantageous for their strength, tunable mechanical properties, and ability to be micropatterned (Lawrence *et. al.*, 2009, Gil *et. al.*, 2010). Glycerol incorporation enhances the flexibility of the silk material (Lu *et. al.*, 2010). We aimed to create a thin, flexible silk film to serve as a backing for a monolayer of mouse muscle cells, which would otherwise flake off from a hard surface such as plastic.

The silk solution was cast directly into well plates, rather than being cast separately and transferred to well-plate wells. Initially, our motivation for taking this approach was to avoid wrinkles in the film and to prevent cells from crawling under the film to the tissue culture plastic. However, our experimental results reveal that well-plate casting has a dramatic effect on cell orientation on the film.

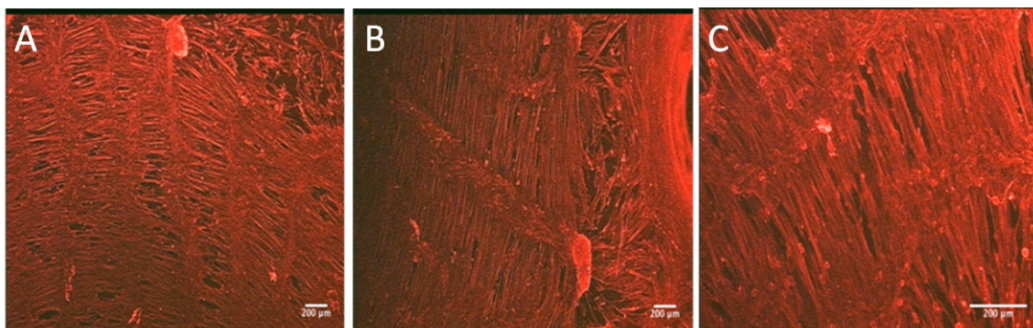


FIGURE 5.1 ACTIN-STAINED (RED) C2C12 CELLS GROWN ON FIBRONECTIN-COTED SILK-GLYCEROL FILMS. THE CELLS ALIGN CONCENTRICALLY WITHIN THE CIRCULAR WELL (A), AND MUSCLE FIBERS CAN BE SEEN ALIGNING BETWEEN REGIONS OF HIGHLY DENSE CELLS (B, C).

Figure 5.1 shows actin-stained C2C12 cells on silk-glycerol films. The cells aligned concentrically in the wells, forming highly organized muscle cell regions in between regions of high cell density. This effect may have been due to

the silk films drying within the wells from the outside in, forming micropatterned rings. However, the films were too thin to remove intact for analysis. Additionally, regions on the films had incomplete or no cell adhesion, and with time, the cell began to flake off from the films. We also did not observe cellular contractions. This was either due to strong adhesion to the films, or the cells did not reach developmental maturity. However, Figure 5.1 shows that the cells appeared healthy and continuous, so the lack of contractile activity is likely due to an inability of the cells to deform the silk substrate. Although silk glycerol films are less rigid and stiff than pure silk films, we decided to explore alternative scaffold types that may be less of an impedance on mechanical output.

However, in future work, we may be able to incorporate this system back into the design of a biodegradable robot. For example, we could cast thin silk-glycerol films with silk suture end point embedded. The cells could grow on the films in contact with the end points, and when they eventually lift off from the film, they will remain attached to the end points, thus providing a mechanism for deformation of the entire film without contractile impedance. In order to develop such a system, we would need to identify suitable methods for handling very thin silk-glycerol films.

5.2.2 Silk sponges

In order to fully explore the available formats for engineering muscle tissue structures in our lab, we decided to use silk sponge scaffolds, to investigate the possible advantages of a fully-three dimensional structure, which would potentially double as the structural component, or body wall, of the robot.

Silk sponges are formed by exposing a silk solution to sodium chloride crystals. The size of the salt crystals determines the size of the scaffold pores.

Incubation of the silk solution with the salt induces beta sheet formation in the protein, causing it to become insoluble. The salt is then removed and the scaffolds may be sterilized by soaking in ethanol, coated, and seeded with cells.

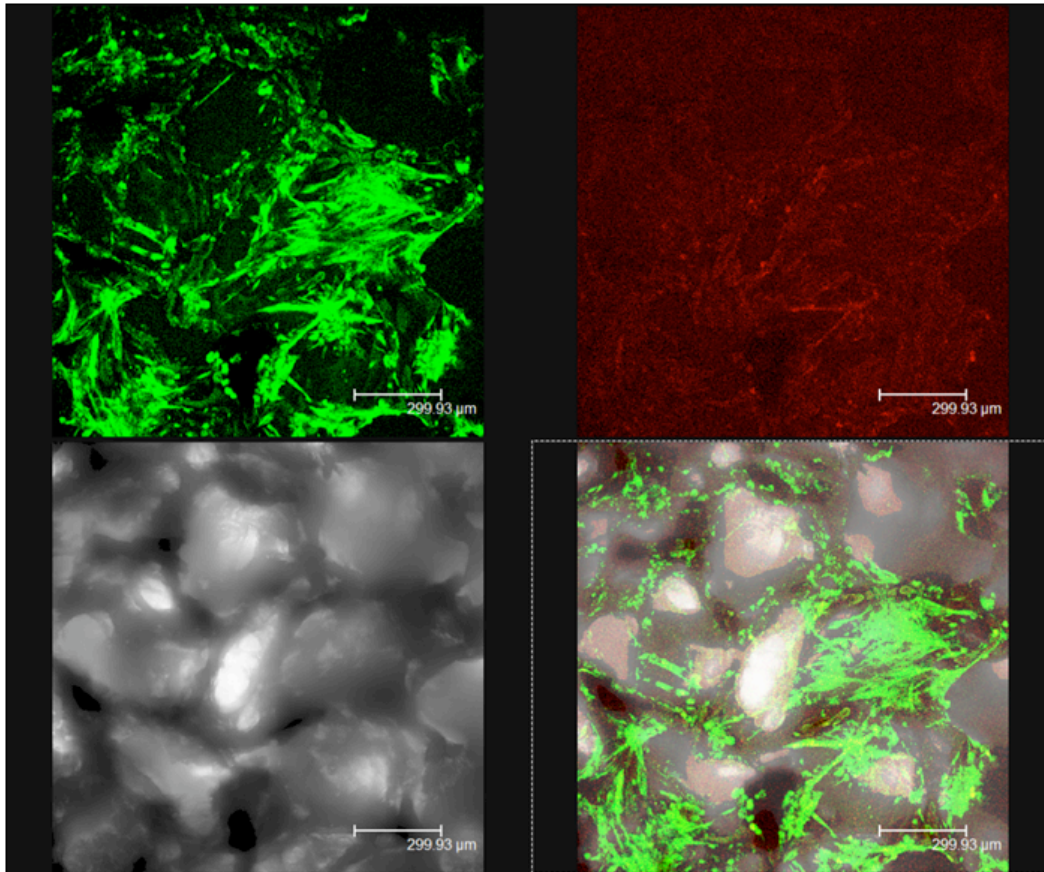


FIGURE 5.2 MAX 2D PROJECTION OF A 337UM SCAN 6C5 2MM HEIGHT, COATED WITH FIB 20UG/ML, 2.5 MILLION CELLS, TOP, 7.82% SILK, 9D DIFF

Using this method, C2C12 cells proliferated and differentiated well within the porous structure of the scaffolds, as shown in Figure 5.2. Very little cell death was observed, and viable muscle fibers spanned across the width of the pores. Although the cells thrived in these scaffolds, the internal structure of the scaffolds was not optimal for directing cellular alignment throughout.

The development of lamellar silk scaffolds allowed for similar porous structure to result; however, the pores in these scaffolds run parallel to the long axis of the scaffold (Mandal, *et. al.*, 2012). Whereas the pores in the randomly-oriented sponges are generated by leaching salt particles from the structure, lamellar scaffolds are made by freezing a silk solution in a unidirectional fashion by equipping the freezing chamber with a heat-conductive plate at one end, and exposing the opposing side of the plate to liquid nitrogen or other low-temperature solution. The scaffold is subsequently lyophilized to remove the aligned ice crystals, and a water-insoluble structure comprised only of silk results.

For this study, we did not coat the scaffolds. Additionally, we used a double seeding method whereby we seeded cells on one side of the scaffold, flipped the structure over, then seeded cells again on the other side, for a total of 1 million cells per scaffold. After allowing cells to proliferate, muscle differentiation was induced and tissue formation could be observed qualitatively within one week (Figure 5.3). The differentiation phase lasted 11 days before the scaffolds were analyzed.

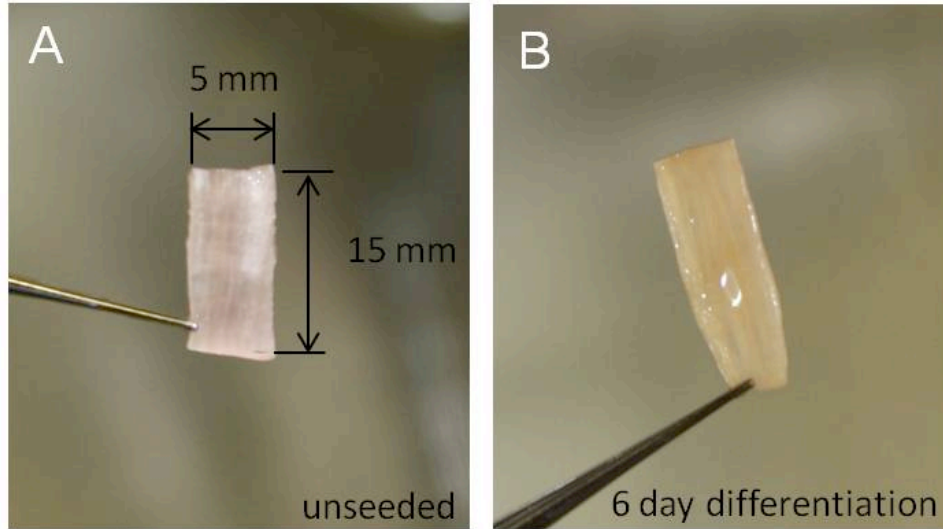


FIGURE 5.3 GROSS MORPHOLOGY OF TISSUE ENGINEERED MUSCLE CULTURED ON LAMELLAR SILK SCAFFOLDS. SCAFFOLD DIMENSIONS WERE 5MM X 15 MM X 1 MM (A). AS MUSCLE MATURED ON AND WITHIN THE SCAFFOLDS, THEY TOOK ON A GLOSSY APPEARANCE (B).

LIVE/DEAD staining and confocal imaging revealed extensive differentiation and cellular alignment (Figure 5.4). Cells were densely packed within the 100 μm depth we imaged. However, we observed more cell death in the lamellar scaffolds than the randomly-aligned porous scaffolds. Although our differentiation phase was two days longer for the anisotropic scaffolds, the difference in viability was likely due to an increased seeding density, compounded by the fact that the lamellar scaffolds have pore sizes around 100 μm in diameter, which is about five times smaller than those of the randomly-oriented porous scaffolds.

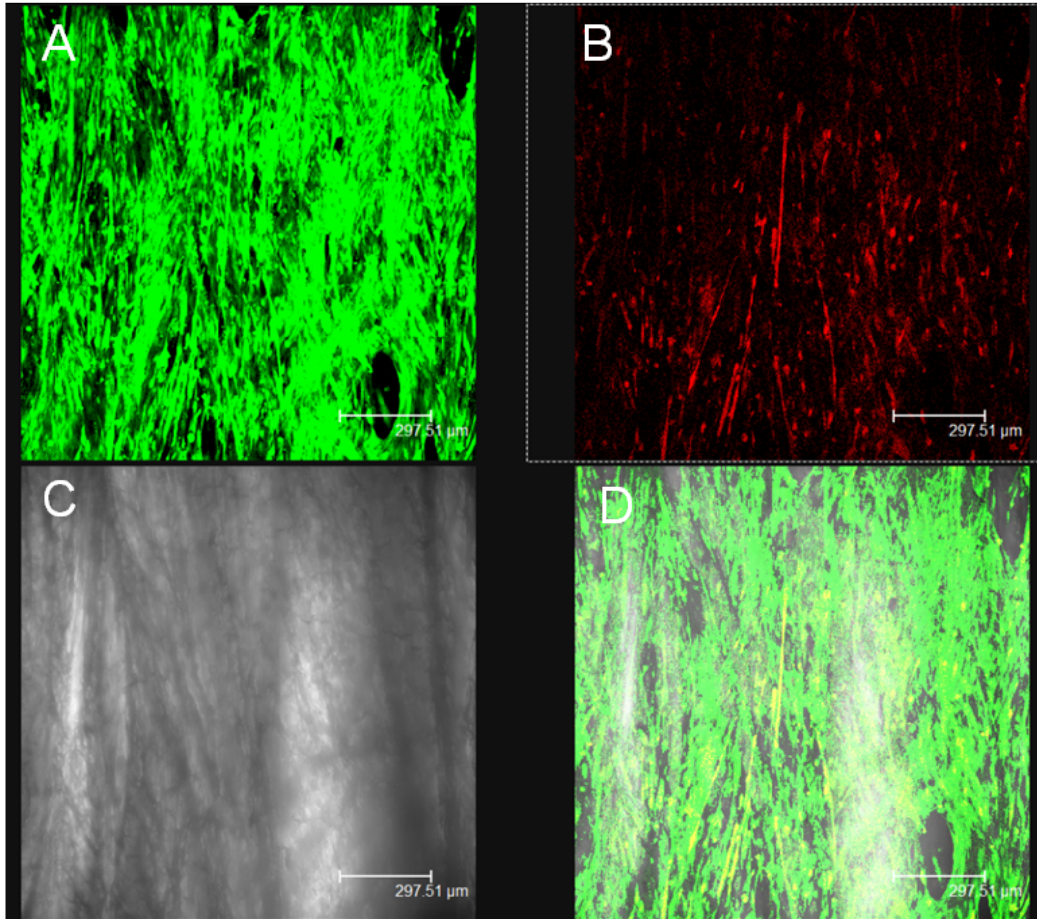


FIGURE 5.4 LIVE/DEAD MAX 2D PROJECTION OF A 112 μM SCAN THROUGH A 1-MM THICK LAMELLAR SILK SCAFFOLD SEEDDED WITH C2C12 CELLS AND DIFFERENTIATED FOR 11 DAYS. VIABLE CELLS (GREEN) WERE DENSELY PACKED AND WELL ALIGNED (A). SIGNIFICANT CELL DEATH WAS OBSERVED (B). PHASE CONTRAST (C) AND MERGED (D) IMAGES SHOW THE CELLS' ALIGNMENT IN THE DIRECTION OF SCAFFOLD PORE ORIENTATION. SCALE BARS ARE 297.51 μM .

In future studies, it would be advantageous to increase the pore size of the scaffolds. This has been achieved by slowing the freezing process, and through incorporation of larger channels by casting the scaffolds around wire arrays (Wray, *et. al.*, 2012). Additionally, the application of a perfusion bioreactor system would increase the viability of cells within the interior of the scaffolds (Lovett *et. al.*, 2010). Further improvements to this system and the previously

described 3D muscle systems could be made by incorporating electrical and mechanical stimulation during the course of the culture.

For our specific purposes in bioactuation, we would like for the muscle tissue to be able to deform the scaffold. In addition to the future directions recommended above, the scaffolds should be less than 1mm in thickness, and the elasticity of the scaffolds could be enhanced by incorporating tropoelastin. These modifications are addressed using insect cells in Section 6.3. Furthermore, in order to simultaneously use silk scaffold-based tissue engineered muscles as actuators and structural components, a “skin” layer would be required to ensheath the scaffold and prevent media leakage. A hollow cylindrical conformation would likely be preferred. However, these future directions are outside the scope of this thesis.

5.2.3 Electrospun silk-gel constructs

In order to organize the cells into larger, more 3-dimensional structures, we moved away from silk films and began to work with electrospun silk-PEO mats that had an open structure, with more volume and thickness than the films. The strategies of Dennis et. al. informed our approach, and we made further modifications for our system and end goals (2000).

For example, we used fibronectin as opposed to laminin for our PDMS coating material, as our past experiments had demonstrated improved outcomes with fibronectin. Additionally, we rotated the silk suture “artificial tendons” so that their long axes were perpendicular to the long axis of the muscle structure. This allowed us to form thin, flat sheets, as opposed to cylindrical, string-like structures. Our hope was that this modified morphology would lead to a greater force output and organization in our constructs.

Silk was blended with poly ethylene oxide (PEO) at a 4:1 ratio, in order to improve the silk's ability to be electrospun. Grounded collectors were fashioned from aluminum foil. They were folded such that two parallel walls of defined spacing were generated. When the collector was used, silk fibers formed anisotropically between the walls (Figure 5.5).

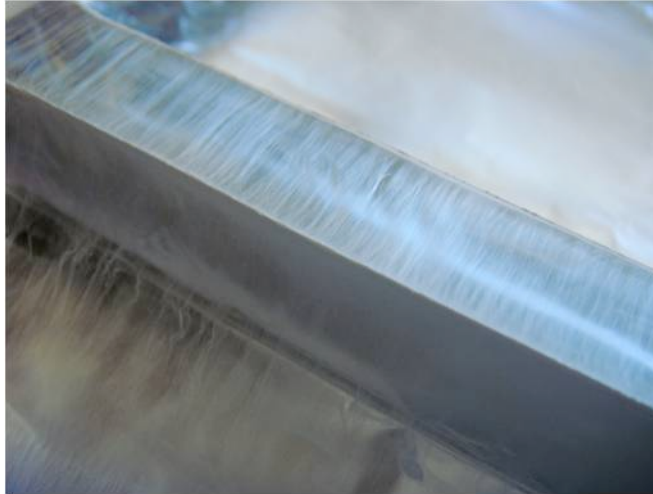


FIGURE 5.5 ALIGNED ELECTROSPUN SILK SUBSTRATES WERE FORMED BY USING TWO PARALLEL ALUMINUM WALLS AS A COLLECTOR.

Substrates were prepared from the electrospun silk fibers as outlined in Figure 5.6. Briefly, silk fibers were electrospun as described above. Sections of the electrospun material were cut out and placed in a 35-mm Petri dish, which had been precoated with a thick layer of PDMS. Silk suture end points were pinned in place, and the entire dish was sterilized by incubating in 70% ethanol, and by UV exposure. The dishes were then washed in PBS for at least 2 days. Next, the fibers were coated with fibronectin solution at room temperature for one hour. The substrates were then seeded with C2C12 cells, which were mixed into a neutralized collagen I solution prior to gelation. The collagen gelled around the

electrospun fibers, with the cells embedded; the dishes were then flooded with medium and incubated.

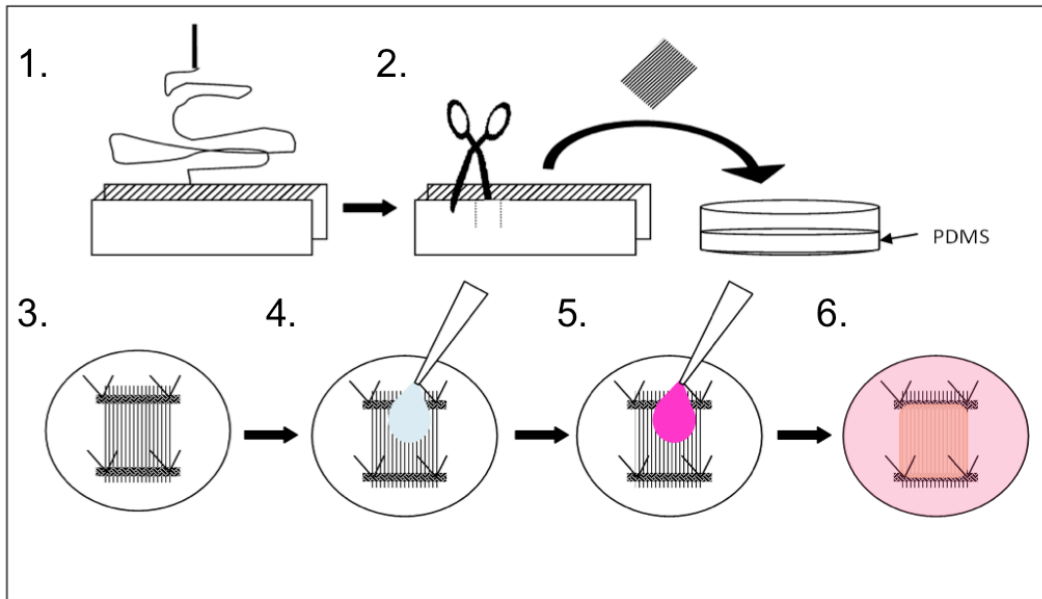


FIGURE 5.6 PROCESS FOR GENERATING SILK FIBER-GEL CONSTRUCTS. 1. SILK-PEO FIBERS ARE ELECTROSPUN ANISOTROPICALLY. 2. SECTIONS OF ELECTROSPUN MATERIAL ARE CUT OUT FROM THE COLLECTOR AND PLACED IN A PETRI DISH COATED WITH PDMS. 3. SILK SUTURES ARE PINNED AT THE ENDS OF THE ELECTROSPUN FIBER SEGMENTS. 4. FIBERS ARE COATED WITH FIBRONECTIN. 5. CELLS ARE SEEDING IN A COLLAGEN GEL. 6. CELLS ARE CULTURED AND FORM CONTRACTILE MUSCLE CONSTRUCTS.

As the cells grew to confluence on the silk fibers, alignment was guided, and the cells fused readily when placed in differentiation medium. Figure 5.7A shows that while cells were organized on the fibers, they were oriented randomly outside of the fibers. After 10 days of differentiation, the collagen gels had contracted, but their dimensions were maintained by the embedded fiber arrays. Differentiated muscle cells were well organized, and regions of contractile activity were observed (Figure 5.7B). Furthermore, the cells and collagen formed strong attachments to the artificial tendons we provided (silk sutures, Figure 5.7C). Overall, this method provided an excellent way of generating organized,

contractile muscle tissue structures of a large size (generally 5mm x 15mm), yet limited thickness due to the silk suture end points constraining the structure to a sheet (Figure 5.7D). This modification to the roll-up method of forming myooids (discussed in Section 1.3.2) avoided the issues of disorganization and transport limitation encountered using the reported method.

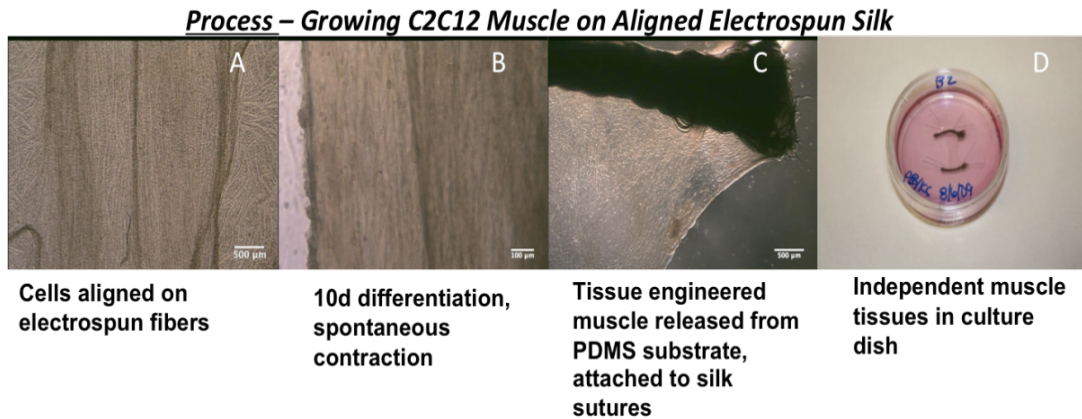


FIGURE 5.7 CELL DEVELOPMENT ON ALIGNED ELECTROSPUN SILK. WHEN CELLS ARE INITIALLY SEEDED, THEY PROLIFERATE AND ALIGN ALONG SILK FIBERS, WHILE CELLS OUTSIDE OF THE ELECTROSPUN MAT HAVE RANDOM ORIENTATIONS (A). AFTER CULTURING IN DIFFERENTIATION MEDIA FOR 10 DAYS, THE CONSTRUCTS ARE COMPACT, AND ALIGNED MUSCLE FIBERS ARE CLEARLY VISIBLE (B). THE CELLS AND COLLAGEN GEL INTERPENETRATE AND ADHERE STRONGLY TO SILK SUTURE END POINTS (C). FURTHERMORE, THE GEL RELEASES FROM THE PDMS SUBSTRATE BY DAY 14 OF DIFFERENTIATION. PHOTOGRAPH OF ELECTROSPUN SILK-GEL CONSTRUCT (D).

We performed immunofluorescence staining and confocal imaging of electrospun silk- gel constructs (Figure 5.8). Myosin heavy chain was coexpressed with filamentous actin towards the periphery of the constructs. This is consistent with our observed spontaneous contractions taking place only towards the edges of the structures. The advantages to using this format are the cells are allowed a more open structure to fill as compared with silk scaffolds, they are thin and thus viability is not an issue, they can easily be integrated with

attachment points, and the resulting tissues are contractile. We therefore chose to attempt to apply this approach to our insect cells, in the hope of generating contractile insect bioactuators.

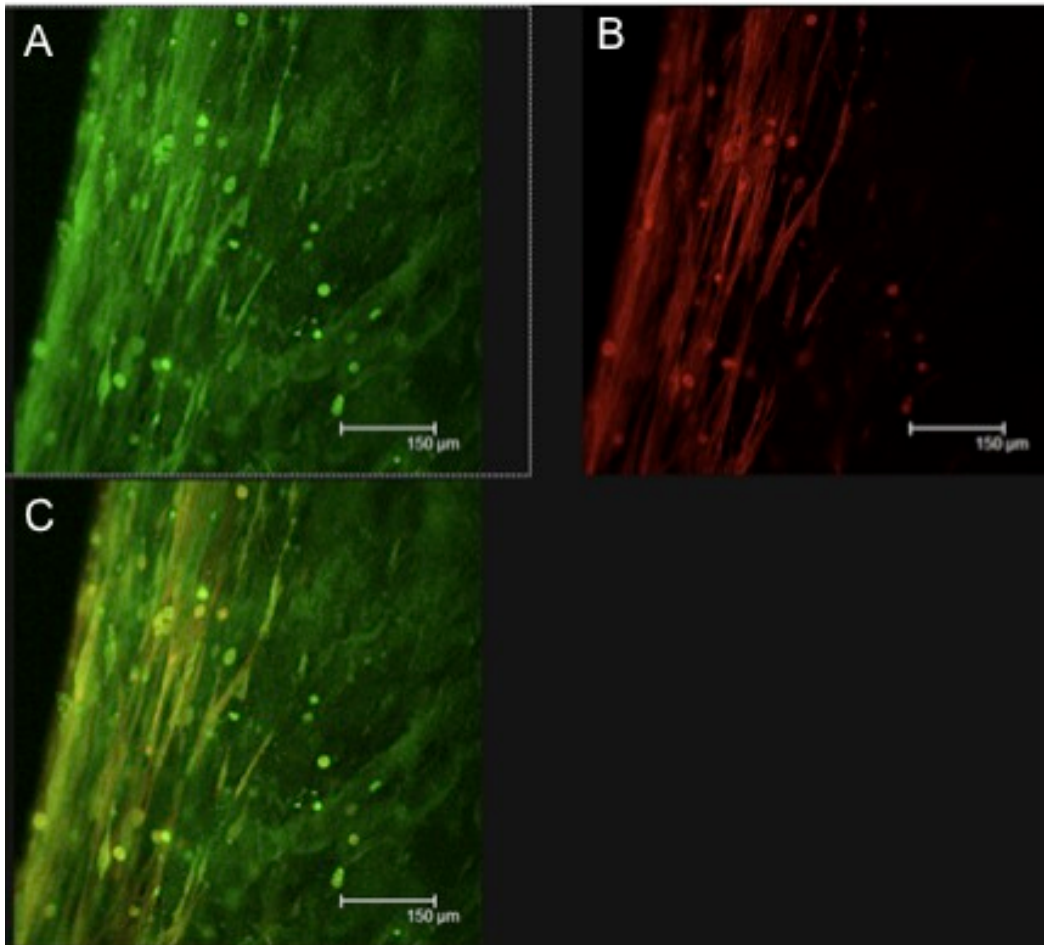


FIGURE 5.8 IMMUNOFLUORESCENCE STAINING OF ELECTROSPUN SILK-GEL CONSTRUCTS SEEDED WITH C2C12 CELLS. MYOSIN HEAVY CHAIN (GREEN, A), ACTIN STAINING (RED, B), AND MERGED (C) IMAGES SHOW ALIGNMENT OF MUSCLE FIBERS TOWARDS THE PERIPHERY OF THE CONSTRUCT.

5.3 Insect construct development

5.3.1 Application of mammalian approaches

We developed our mammalian cell-based 3D muscle systems concurrently with the development of our insect muscle cell cultures. Once we

had an understanding of muscle cell development from *M. sexta* embryos, we attempted to incorporate these cells with our previously described biomaterial systems. Specifically, we investigated insect muscle cell interactions with silk-glycerol films, electrospun silk fibers, and collagen gels. Application of insect cells to silk scaffolds will be discussed in Section 6.3. We chose to omit silk-glycerol films due to the limitations described in our conclusions for Section 5.2.1.

We seeded *M. sexta* myoblasts at high densities on aligned electrospun silk mats in PDMS-coated dishes. Our hope was that the PDMS would deter cell adhesion to the dish and encourage the cells to interact with the fibers instead. However, these cultures never matured; rather, the cells remained as dense clumps and did not show signs of cell migration onto, along or around the fibers (Figure 5.9A). We then attempted to embed the cells in a collagen gel, as this provided our mammalian electrospun silk constructs with greatly improved outcomes by retaining the cells in close proximity to the fibers and allowing them to be surrounded by an appropriate gel matrix. Again, our insect cells remained within dense cell masses and never migrated out into the surrounding gel (Figure 5.9B).

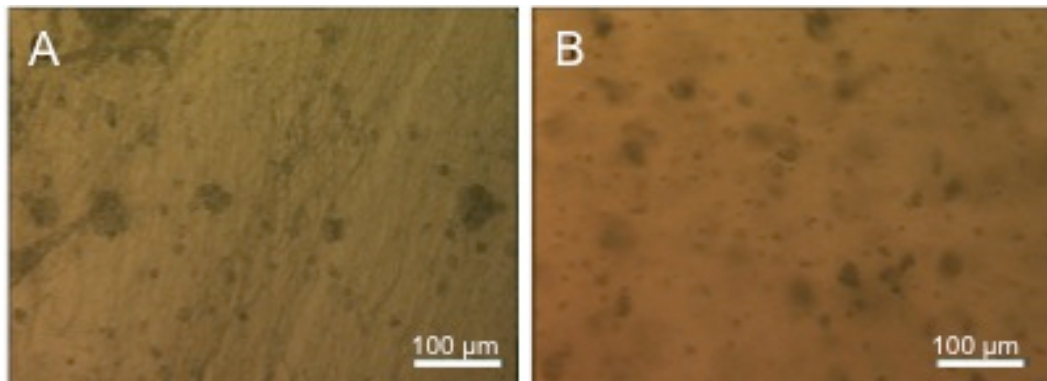


FIGURE 5.9 INSECT CELLS IN ELECTROSPUN SILK (A) AND COLLAGEN GEL (B) MATRICES. CELLS REMAIN CLUMPED AND DO NOT MIGRATE OUT FROM CELL MASSES.

Since our initial attempts at recreating the structures in Section 5.2.2 with insect cells were not successful, we took a step back and re-evaluated the biochemical and structural differences between mammalian muscle and insect muscle in order to design a more appropriate system for cultivating functional 3D insect muscle tissue.

5.3.2 PDMS micropatterned channels

Insect muscle has a very simple structure, with 2 – 14 muscle fibers per unit, each of which is a single, large myofiber. Each myofiber has a diameter of approximately 300 μ m. The cells have no surrounding ECM, except at each end of the muscle, where laminin and thrombospondin aid in cell-cell interactions between the muscle cells and tendon-like epithelial cells lining the body wall. Therefore, a simple array of several fibers would sufficiently mimic the native structure of larval body wall muscles, and enable us to regenerate this tissue *in vitro*.

One of the most straight-forward ways to replicate this structure is soft lithography, a well-established method frequently used in muscle tissue engineering to generate patterned PDMS substrates (Xia & Whitesides, 1998). Briefly, this process involves spin-coating a silicon wafer with SU-8 photoresist to a thickness of 100 μ m. The photoresist is exposed to UV light through a photomask, which allows UV light only through the desired pattern (Figure 5.10A). The areas of photoresist exposed to UV are cross-linked, and the remaining photoresist can then be removed, leaving a master mold with raised topology. Uncured PDMS is poured over the master mold features and is allowed to cure (Figure 5.10B). The PDMS may then be delaminated from the master mold, sterilized, and seeded with cells (Figure 5.10C).

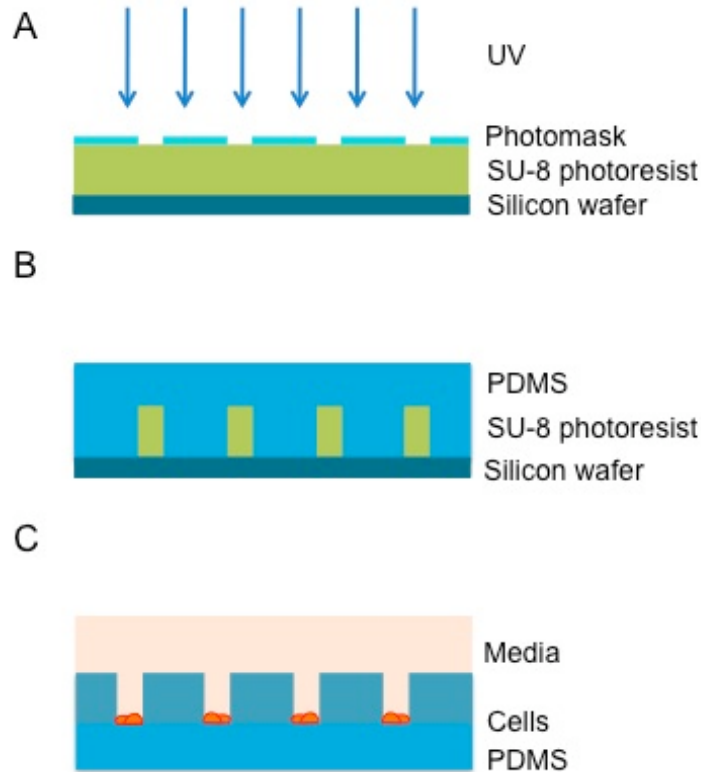


FIGURE 6.10 SOFT LITHOGRAPHY PROCESS FOR GENERATING CHANNELED SUBSTRATES FOR MUSCLE FORMATION. STANDARD LITHOGRAPHY METHODS ARE USED TO SPIN-COAT A SILICON WAFER WITH SU-8 PHOTORESIST. UV EXPOSURE CROSS-LINKS THE SU-8 THROUGH A PHOTOMASK WITH THE DESIRED PATTERN (A). UNCROSSLINKED PHOTORESIST IS REMOVED AND PDMS IS POURED OVER THE PHOTORESIST TOPOGRAPHY AND ALLOWED TO CURE (B). CURED PDMS IS STERILIZED, SILANIZED, AND SEEDED WITH CELLS BATHED IN MEDIA (C).

We fabricated PDMS channel structures with varying widths and tested the cell adhesion, muscle development and alignment of cells cultured within the channels (Figure 5.11A). For these initial studies, we first applied mouse cells to the channels. We found that, when coated with fibronectin prior to seeding, C2C12 mouse myoblasts formed aligned and contractile myotubes and myotube bundles within the structures (Figure 5.11B, C). At widths of 400 μ m per channel, bundles of myotubes formed with an overall angle of alignment that closely paralleled the channel walls. At widths of 50 μ m per channel, single myotubes formed (Figure 5.12).

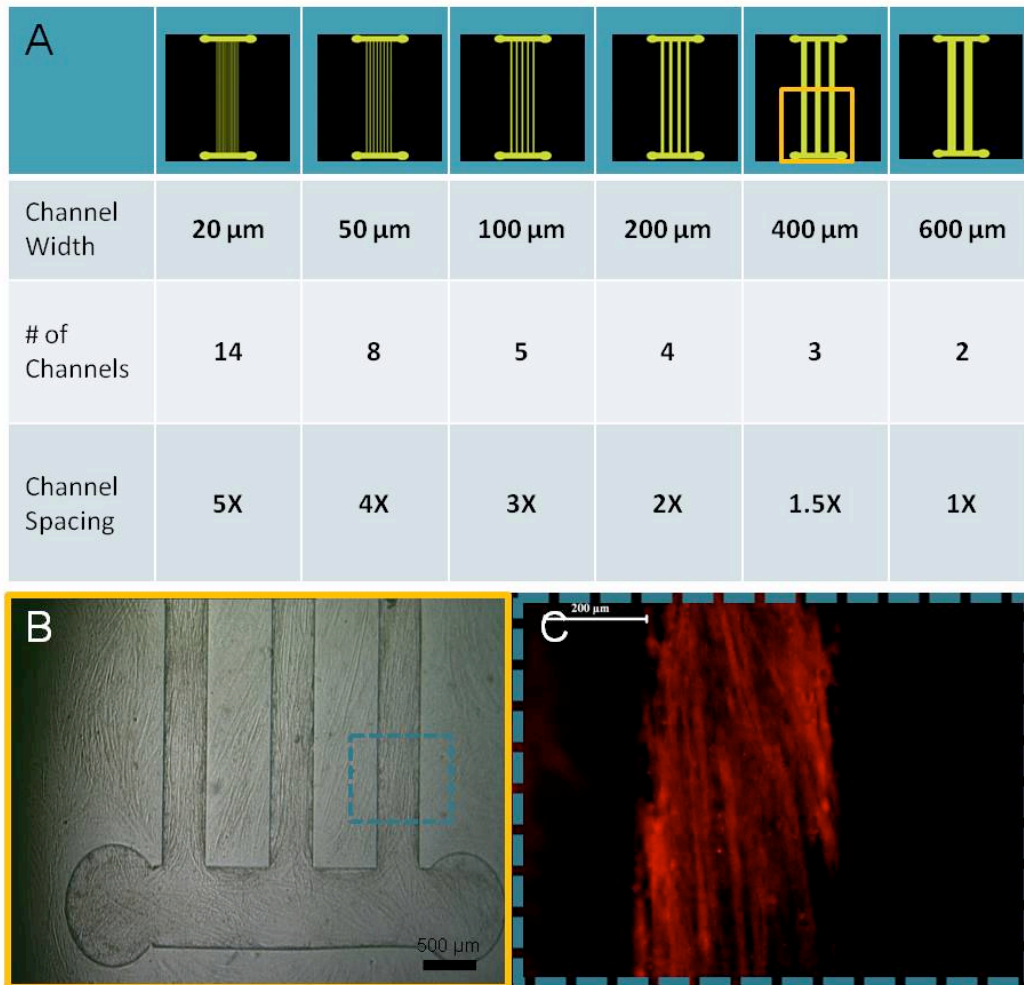


FIGURE 5.11 MICROFABRICATED PDMS CHANNELS FOR MUSCLE CELL GUIDANCE. CHANNEL ARRAYS WERE FABRICATED WITH DIFFERENT WIDTHS AND NUMBER OF CHANNELS (A). C2C12 CELLS ALIGNED AND DIFFERENTIATED WITHIN THE CHANNELS (B). ACTIN STAINING (RED) REVEALS MUSCLE FIBER ALIGNMENT (C).

Some of the issues that we encountered with this approach were that the formed structures were only a monolayer deep and therefore very thin, making them impossible to detach in one piece for transfer to another structure such as a robot body wall. Additionally, as the cells used up the fibronectin and as spontaneous contractions began to occur, regions of the structures would release from the PDMS and flake off, thus destroying the continuity and integrity

of the array. However, it is not entirely surprising, given mammalian muscle is surrounded by multiple layers of collagenous ECM to form bundles of myofibers, that our mouse cells would not form a stable tissue without this support.

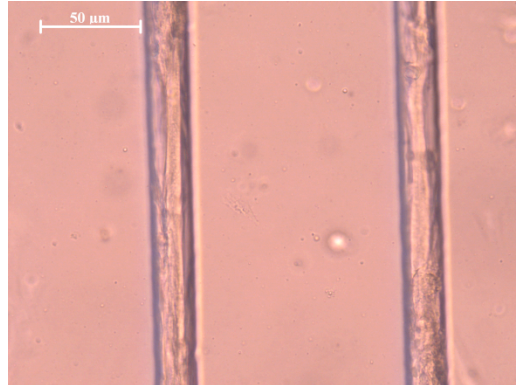


FIGURE 5.12 NARROW PDMS CHANNELS OF 25 μ M WIDTH ALLOW SINGLE MUSCLE FIBERS TO GROW AND ALIGN. SCALE BAR IS 50 μ M.

Therefore, we decided to continue to pursue this technique for insect cells, since we did not expect to have the same issue of cell flaking due to insect muscle's lack of a requirement for surrounding ECM. However, we found that uncoated, silanized PDMS is not an appropriate culture surface for insect cells. We therefore needed a coating for this surface that would initially encourage cells to attach, proliferate and differentiate. Ideally, the cells would eventually detach from the PDMS when the coating was used up, resulting in free-standing, patterned muscle structures.

5.3.3 ECM extraction and coating

As discussed previously, our focus was providing the cells with a physiologically-relevant environment to promote controlled muscle formation specific for the insect system. Although laminin and thrombospondin should potentially provide a suitable surface for cell attachment, we chose to isolate the

extracellular matrix of *M. sexta* larval body walls, and generate a protein solution from the material as an additional option for surface coatings. Decellularization of biological tissue, including muscle, can be performed without damaging the components of the ECM (Gillies *et. al.*, 2010). In fact, an entire organ may be decellularized effectively by perfusing the sample with a 1% solution of sodium dodecyl sulfate (SDS), followed by water, then a 1% Triton-X-100 solution (Ott *et. al.*, 2008). For our system, which has a more simplistic structure since the larva is essentially a tube, decellularization could be achieved simply by perfusion with 1% SDS (Figure 5.13).

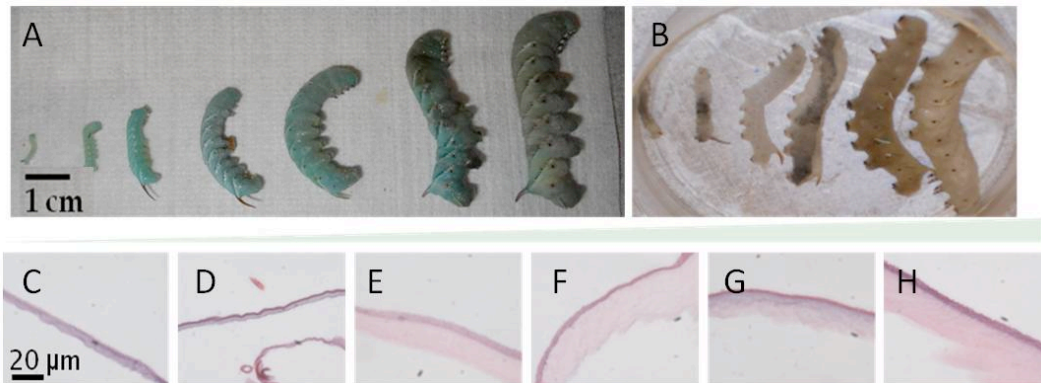


FIGURE 5.13 DECELLULARIZATION OF *M. SEXTA* LARVAE. LARVAE AT DIFFERENT STAGE OF DEVELOPMENT (A). THE SAME LARVAE AFTER PERFUSION WITH SDS FOR 12 HOURS (B). THE SMALLEST LARVA FROM PANEL A WAS NOT ABLE TO BE DECELLULARIZED DUE TO ITS SMALL SIZE. HISTOLOGICAL SECTIONS WITH H&E STAINING OF ECM LEFT BEHIND AFTER DECELLULARIZATION (C – H). SECTIONS ARE ORDERED FROM SMALLEST (C) TO LARGEST (H).

Larvae of varying sizes were humanely sacrificed by freezing (Figure 5.13A). The individuals were then defrosted and punctured at either end with 26-gauge needles. 1% SDS solution was perfused through the larvae for 12 hours, resulting in nearly clear samples that retained their morphological features (Figure 5.13B). The darkened regions on some of the samples were due to

oxidation of the hemolymph, which occurs when it is exposed to air and could not be washed away.

Decellularized larvae were histologically processed and stained with hemotoxylin and eosin (Figure 5.13C – H). The darker stained outer layer was most likely chitin and was observed for all body sizes. The lighter stained inner layer was likely extracellular cuticular proteins secreted by epidermal cells and assembled into lamellae by a hormone-induced process that varies from instar to instar (Wolfgang & Riddiford, 1986). The relative thickness of the protein lamellae was highest in the larger, 5th instar larvae; for the purpose of extracting maximal protein per individual, we chose to extract proteins from 5th instar larvae only.

ECM proteins were solubilized in a solution of pepsin in 0.1M HCl, sterile filtered, and neutralized. In addition to choosing the stage at which to isolate ECM proteins, we also had to decide whether or not to include ECM derived from the gut, as the lining for this organ remains after the decellularization process as well. We prepared protein solutions both containing this membrane (“Not Scraped”) and with the gut ECM removed (“Scraped”). We quantified the protein content of both solutions and found the “Scraped” solution to be approximately 6mg/mL and “Not Scraped” was approximately 8mg/mL, as determined by a Bradford Assay (Figure 5.14).

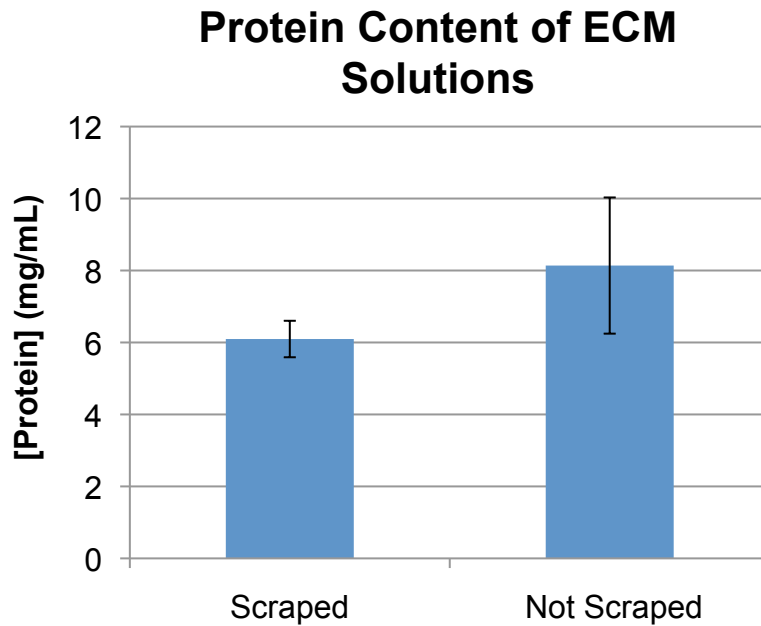


FIGURE 5.14 PROTEIN CONCENTRATIONS OF ECM SOLUTIONS DERIVED FROM *M. SEXTA* BODY WALLS.

We coated PDMS substrates with a variety of proteins that are either physiologically relevant for mammalian muscle (fibronectin, laminin), insect muscle (laminin, thrombospondin, ECM solution), or that are often used to promote cell adhesion in general (poly-d-lysine, Cell-Tak). Phase contrast imaging was performed as the cells developed to evaluate cell coverage and cell growth (Figure 5.15C – G). For some studies, cell extension and cell numbers were quantified (Figure 5.15A and B).

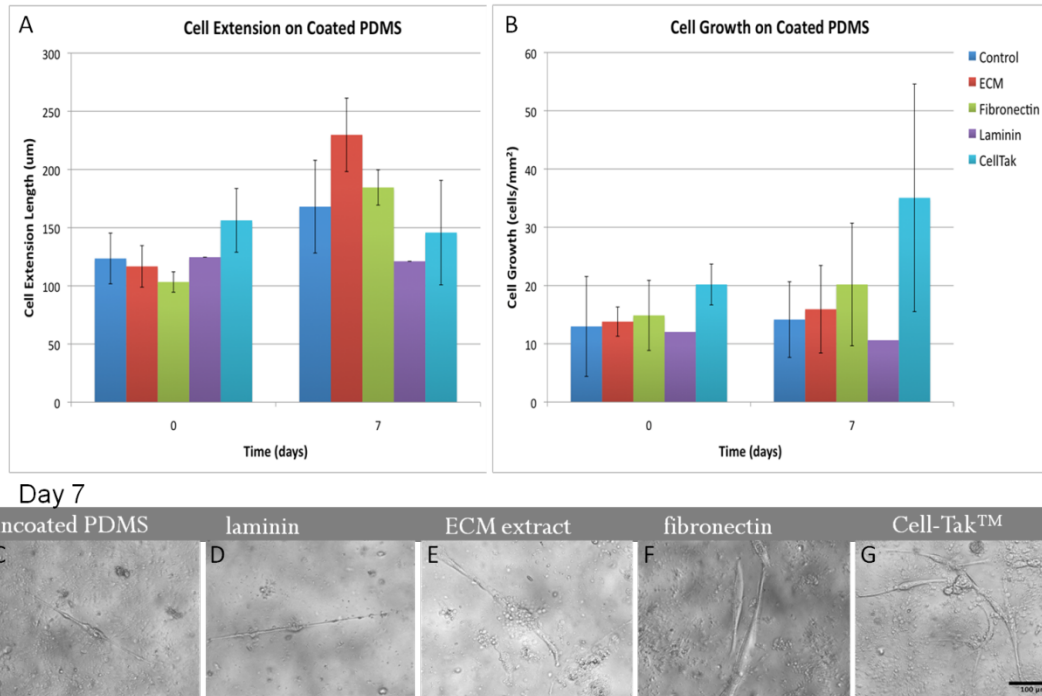


FIGURE 5.15 COATING STUDY OUTCOMES. CELL EXTENSION (A) AND CELL NUMBERS (B) WERE MEASURED ON PDMS COATED WITH EITHER ECM EXTRACT, FIBRONECTIN, LAMININ, CELL-TAK, OR UNCOATED. PHASE CONTRAST IMAGING SHOWS CELL MORPHOLOGY AND COVERAGE ON EACH OF THE COATINGS AT DAY 7 (C – G).

Although we did see favorable results with ECM extract-coated and Cell-Tak-coated PDMS dishes, the cells did not form highly contractile networks as they reliably do on plastic. We could potentially overcome these limitations but optimizing coating solution concentrations and coating protocols, using a mixture of ECM extract and Cell-Tak, or inducing gelation in the ECM solution.

These studies are ongoing and in future work, we hope to be able to use the results of these studies to grow insect muscle on a variety of substrates and in specific regions using microcontact printing methods (described in more detail in Chapter 1). However, in order to achieve optimal outcomes in the short-term, we chose to use the substrate the cells developed most robustly on, namely, tissue culture-treated plastic.

5.3.4 Scaffold-free constructs constrained by PDMS chambers

As a result of the difficulty of cultivating the cells on substrates besides plastic, we chose in the short-term to move forward with approaches that allow the cells to grow on tissue culture-treated plastic, while simultaneously developing coating regimes to use in future work. For generating constructs on plastic, we discovered that a high-density cell suspension seeded in a Petri dish resulted in the formation, eventual detachment, and contraction of scaffold-free muscle constructs (Figure 5.16A, B). The contractions were found to be coordinated over large regions of the constructs; for example, an entire branch of the structure would bend in unison. We performed confocal imaging of these structures after one month in culture and found that the majority of the tissue remained viable, with the exception of the most interior regions (Figure 5.16C).

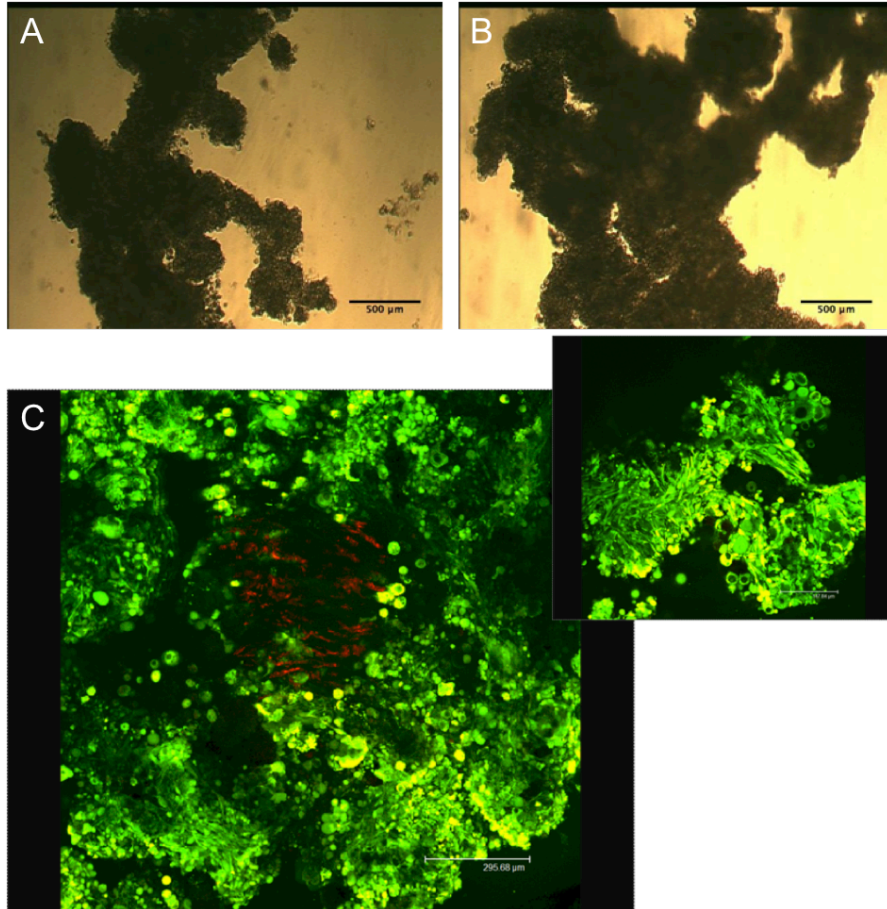


FIGURE 5.16 STRUCTURE AND VIABILITY OF SELF-ASSEMBLED, MM-SCALE MUSCLE CONSTRUCTS. HIGH CELL DENSITY SEEDINGS RELIABLY RESULTED IN THE FORMATION OF 3D SCAFFOLD-FREE MUSCLE TISSUES, WHICH DETACHED FROM THE CULTURE PLASTIC AND CONTINUED TO CONTRACT FOR PERIODS OF >1 MONTH (A, B). LIVE/DEAD STAINING AND CONFOCAL IMAGING OF A 1-MONTH OLD CONSTRUCT REVEALED EXTENSIVE CELL VIABILITY, WITH NECROSIS OCCURRING ONLY IN THE INTERIOR-MOST REGIONS (C). MUSCLE FIBERS IN THE BRANCHES OF THE STRUCTURES WERE FOUND TO BE WELL-ALIGNED (INSET).

The successful formation of viable, functional scaffold-free 3D constructs encouraged us, however, we desired to control the geometry and dimensions of our constructs for eventual design and control of directional force output. Thus, we attempted high-density cell molding using stencils cut from 1 – 2mm-thick sheets of PDMS elastomer (Figure 5.17). Chambers were cut by hand using computer-generated templates and a scalpel under a dissecting microscope.

Cells were seeded in dry chambers that had been previously sterilized in ethanol. A seeding density of 1.5 embryos/mm² was found to be appropriate for reliably forming viable, contractile constructs.

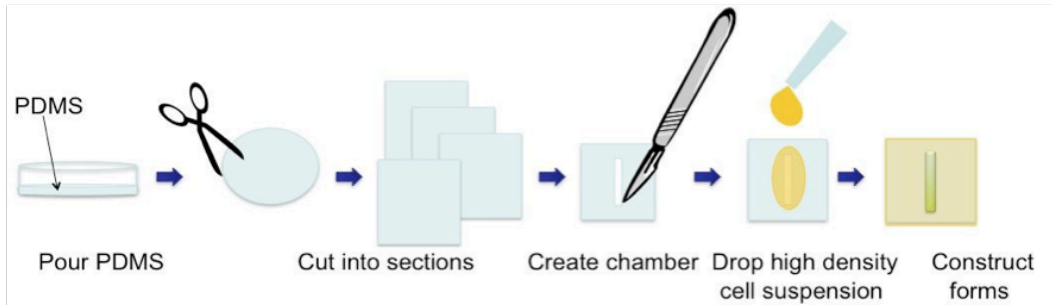


FIGURE 5.17 SCHEMATIC REPRESENTATION OF PROCESS FOR FORMING SCAFFOLD-FREE INSECT MUSCLE CONSTRUCTS.

Within two weeks of culture, cells within the chamber reached confluence, fused with one another, and began contracting. Constructs continued maturing, with 2 – 3 month-old constructs observed to continue to sustain coordinated, continuous contractions. Constructs were visible with the naked eye and could easily be detached from the dishes with the gentle aid of forceps (Figure 5.18).

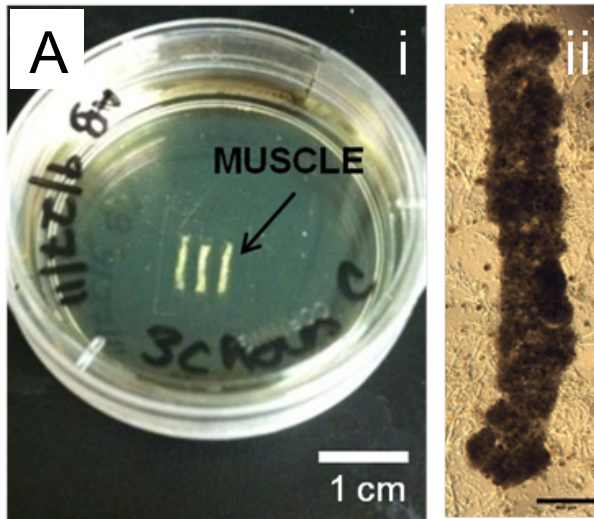


FIGURE 5.18 INSECT MUSCLE CONSTRUCTS FORMED WITH PDMS TEMPLATES. PHOTOGRAPH (AI) AND MICROGRAPH (AII) OF MUSCLE CONSTRUCTS AFTER AT LEAST 2 WEEKS OF CULTURE.

Additionally, we found that this straight-forward method of generating muscle constructs allowed for a wide range of geometries and formats to be created. We have successfully generated rings, oblong structures, eyelet shapes, and have incorporated silk sutures and stainless steel pins as end-point materials, with which the cells grow around and integrate.

5.4 Insect construct characterization

As discussed in Chapter 3, our cell populations are comprised of a heterogeneous mixture of cell types. When we form 3D scaffolds with these cells, we observe very dense packing, and contractions persist over the entire dimensions of the structure, though not always unidirectionally. We wanted to identify muscle fibers within the constructs, so we stained them for myosin heavy chain and troponin-T (Figure 5.19). We found that many of the cells comprising the constructs were not myogenic. This was surprising, considering that our 2D

cultures are enriched in myogenic cells. It is possible that the close cell-cell contact induced by the construct molding process stimulates other cells types such as fibroblasts and epithelial cells to proliferate. However, we did observed cross-striated muscle fibers running through the constructs (Figure 5.19B, D). Though these appear to be sufficient for inducing tissue-wide contraction, in future studies we seek to increase the purity of muscle cells to enhance force output.

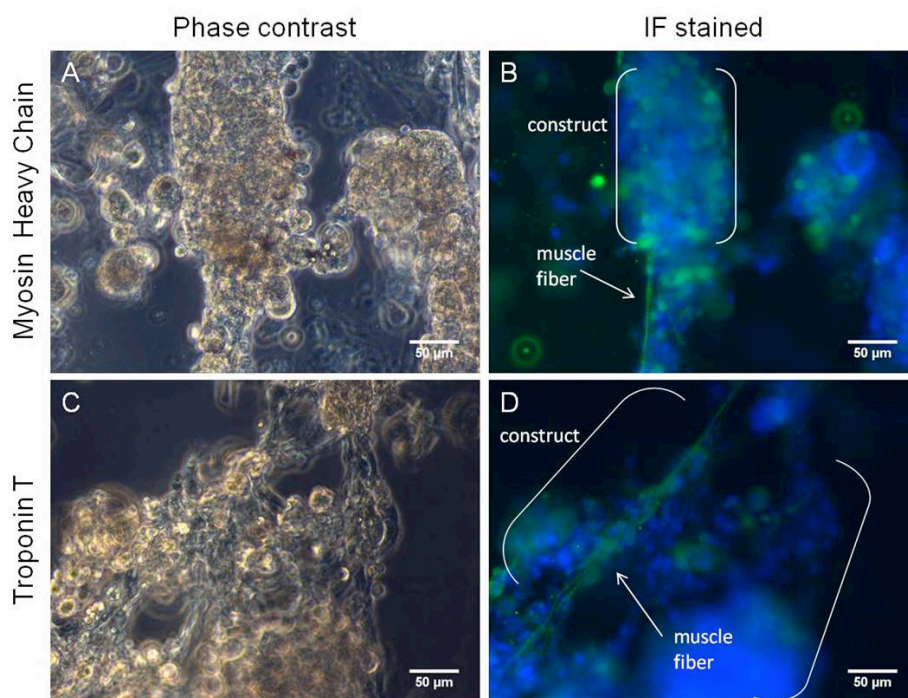


FIGURE 5.19. IMMUNOFLUORESCENCE STAINING OF 3D MUSCLE CONSTRUCTS. PHASE CONTRAST IMAGES SHOW OVERALL CONSTRUCT MORPHOLOGY (A, C), WHILE STAINED IMAGES SHOW EITHER MYOSIN HEAVY CHAIN (B) OR TROPONIN-T (D) IN GREEN, NUCLEI IN BLUE. MUSCLE FIBERS AND CONSTRUCT BOUNDARIES ARE SHOWN AS INDICATED.

As mentioned above, our scaffold-free constructs contract spontaneously. Unlike with C2C12 electrospun silk-gel constructs (Section 5.2.2), where contraction was limited to small, isolated regions, insect constructs contracted

over the entire dimensions of the structure. We wanted to again look at the time scales over which these contractions occur, so we used IOM analysis again to track movement in the structure from videos of contractions. An example of the resulting activity tracking is shown in Figure 5.20.

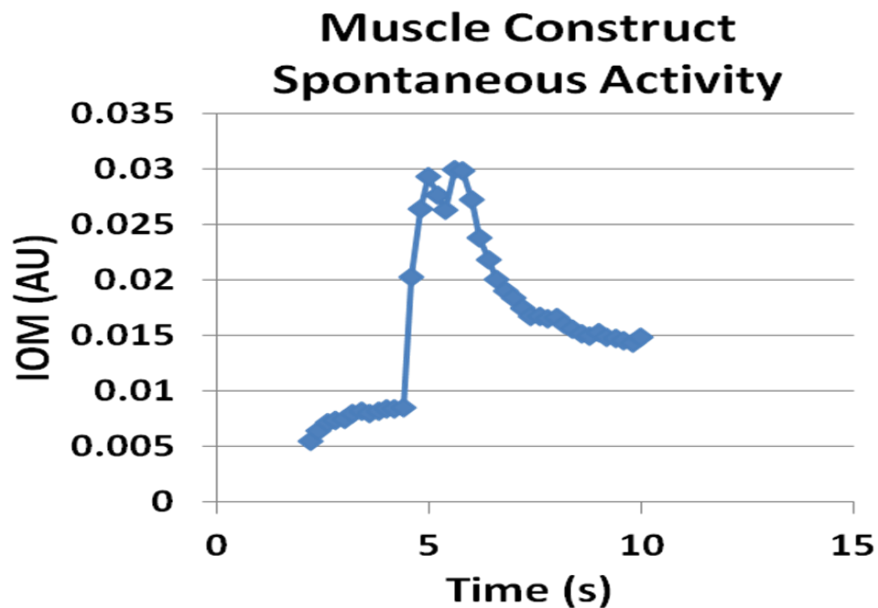


FIGURE 5.20 SPONTANEOUS CONSTRUCT CONTRACTILE ACTIVITY. AVERAGE PIXEL INTENSITY FOR EACH FRAME OF A 10 SECOND VIDEO WAS PLOTTED TO REVEAL CONSTRUCT CONTRACTION DYNAMICS.

When a 10s video of construct contraction was analyzed, we see a distinct peak where the entire construct underwent spontaneous movement. At the peak of the contraction, there was a slight relaxation, followed by an additional contraction, which can be seen in the plot by the double peak. Upon relaxation, the construct does not return fully back to baseline. The overall time course of the contraction is around 2.4s. Given the force produced by such a contraction, we could use this information to design robotic devices with optimal step length based on these inherent dynamic characteristics of the muscle.

5.5 Alignment improvement

Although we observed spontaneous contractions, we wanted to examine the degree of alignment in our constructs, because they will produce maximal force when the muscle fibers comprising them are well-aligned. We stained our 1mm-wide structures for actin, and visualized them under confocal microscopy (Figure 5.21). We found that contact guidance, and perhaps tissue contraction, had guided the cells on the exterior edges of the construct to align. For each construct analyzed, the well-aligned region was found to be about 150 μm wide at either edge. Therefore, we decided to test constructs of varying widths for their degree of alignment to see if we could improve the overall organization of the muscle constructs.

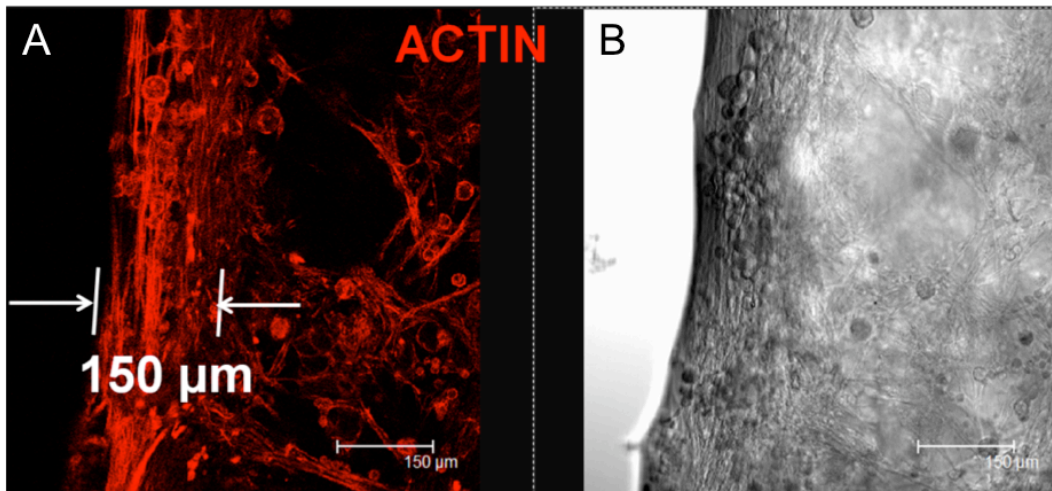


FIGURE 5.21 ALIGNMENT OF MUSCLE FIBERS WITHIN INSECT MUSCLE CONSTRUCTS. ACTIN STAINING (RED) REVEALS THAT FIBERS ALIGN TO 150UM AWAY FROM THE OUTER EDGE OF THE CONSTRUCT (A). PHASE CONTRAST (B). SCALE BARS ARE 150 UM.

Construct chambers were designed with 1mm, 500 μm , and 250 μm channel thicknesses. We seeded proportionally fewer cells in the narrower channels, to eliminate possible effects of seeding density. In 250 μm channels,

cell aligned well into a single bundle, with all of the cells following the same axis of alignment as the channel walls (Figure 5.22A). When these constructs contracted, they did so in unison and unidirectionally. In 500 μ m-wide channels, the majority of the structure is well-aligned, though there are some dense regions where uniform cell directionality may be lost (Figure 5.22B). 1mm-wide constructs are much more dense than in the other conditions, and overall muscle fiber alignment is limited to the outer edges (Figure 5.22C).

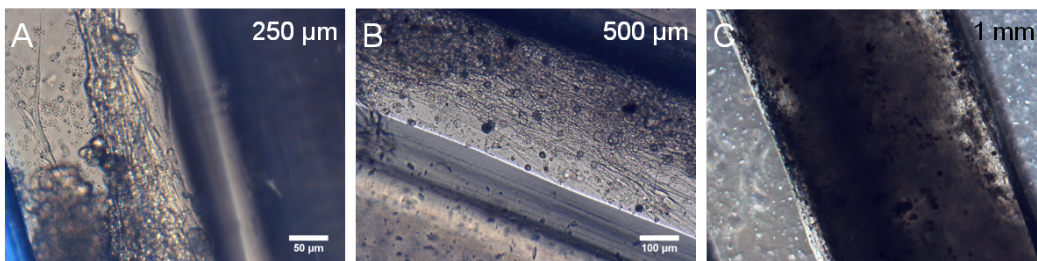


FIGURE 5.22. MUSCLE CELL ALIGNMENT IN CHANNELS OF VARYING WIDTHS. PHASE CONTRAST IMAGES SHOWING CELLULAR ALIGNMENT IN 250UM-WIDE CHANNELS (A) AND 500UM-WIDE CHANNELS (B). DENSE CONSTRUCT FORMATION IS SEEN IN 1MM-WIDE CHANNELS (C).

Our results indicated that channels 250 μ m - 500 μ m wide are suitable for guiding overall cellular alignment in our muscle constructs. However, phase contrast imaging doesn't allow us to see cellular alignment in denser scaffolds or to quantify differences in cellular alignment. Therefore, in follow-up experiments, we will study and quantify alignment in varying-width chambers using staining, confocal imaging, and imaging analysis.

5.6 Multifiber version

We were very interested in moving toward multifiber versions of our muscle constructs. Our initial PDMS molding method was not directly translatable to generating multifiber arrays; cutting out such shapes manually would result in

very small, free standing structures that would have to be placed by hand. We have explored several alternative methods for achieving multifiber constructs; one of which is to utilize the cells' naturally occurring process during muscle development, whereby muscle fibers reach out toward tendon progenitor cells, in order to reach their insertion points in the developing cuticle. Our approach to mimicking this process *in vitro* was to generate construct chambers with narrow micro-gaps between the individual fibers and the two end channels, perpendicularly-oriented at either side (Figure 5.23A).

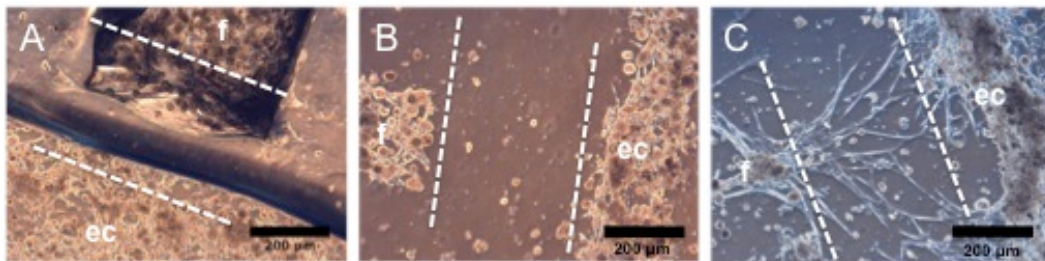


FIGURE 5.23 MICROGAP CONSTRUCTS FOR FORMING MULTIFIBER ARRAYS. CONSTRUCT CHAMBERS ARE CREATED WITH SMALL GAPS BETWEEN THE FIBERS (F) AND THE END CHANNEL (EC, A). AFTER A WEEK OF CULTURE, THE CONSTRUCT CHAMBERS ARE REMOVED, OPENING THE GAP BETWEEN THE FIBERS AND THE END CHANNEL (B). WITHIN 4 DAYS, MUSCLE FIBERS BEGIN TO MIGRATE AND BRIDGE THE GAP BY REACHING TOWARD AND FUSING WITH MUSCLE FIBERS IN THE END CHANNEL (C). DOTTED LINES INDICATED ORIGINAL GAP BOUNDARIES.

The constructs were allowed to form for one week before the PDMS construct chamber was carefully removed, leaving behind only the constructs with a gap of about 300 μ m separating the fibers and end channels (Figure 5.23B). After only 4 days, muscle fibers had already begun to migrate and extend outward into the gap, reaching until they had contacted muscle fibers on the other side (Figure 5.23C).

We stained the resulting structures to visualize filamentous actin and nuclei. We found abundant actin filaments in the gap regions, though they

stained much more faintly than the actin fibers in the constructs (Figure 5.24). This may indicate that although the cells migrated into the gap and connected with end channel cells, they may have needed more time to develop mature actin filaments as seen in active muscle fibers.

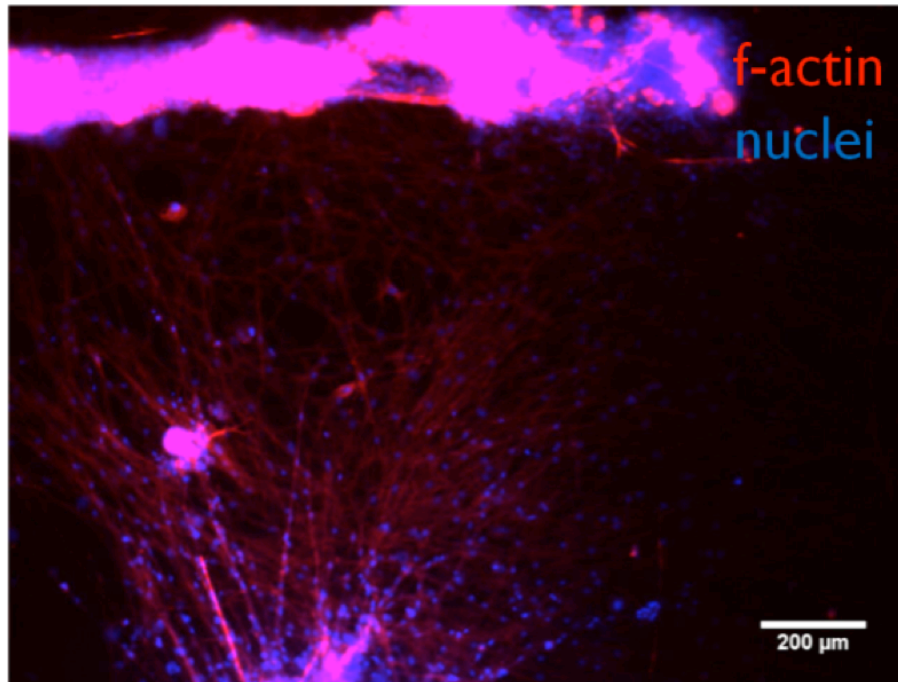


FIGURE 5.24. ACTIN STAINING OF GAP BETWEEN FIBERS AND END CHANNEL CONSTRUCTS AFTER ONE WEEK OF GAP-CROSSING. FILAMENTOUS ACTIN IS SEEN IN RED, NUCLEI ARE BLUE.

Although the resulting structures were not entirely continuous, we were able to see some good contact and bridging of the gaps with time (Figure 5.25). We hope that this proof-of-concept study may be further improved by shortening the overall dimensions of the structure. Furthermore, the isolation and strategic placement of tendon-like epithelial cells in the end channels would foster an even stronger migrational response from the muscle.

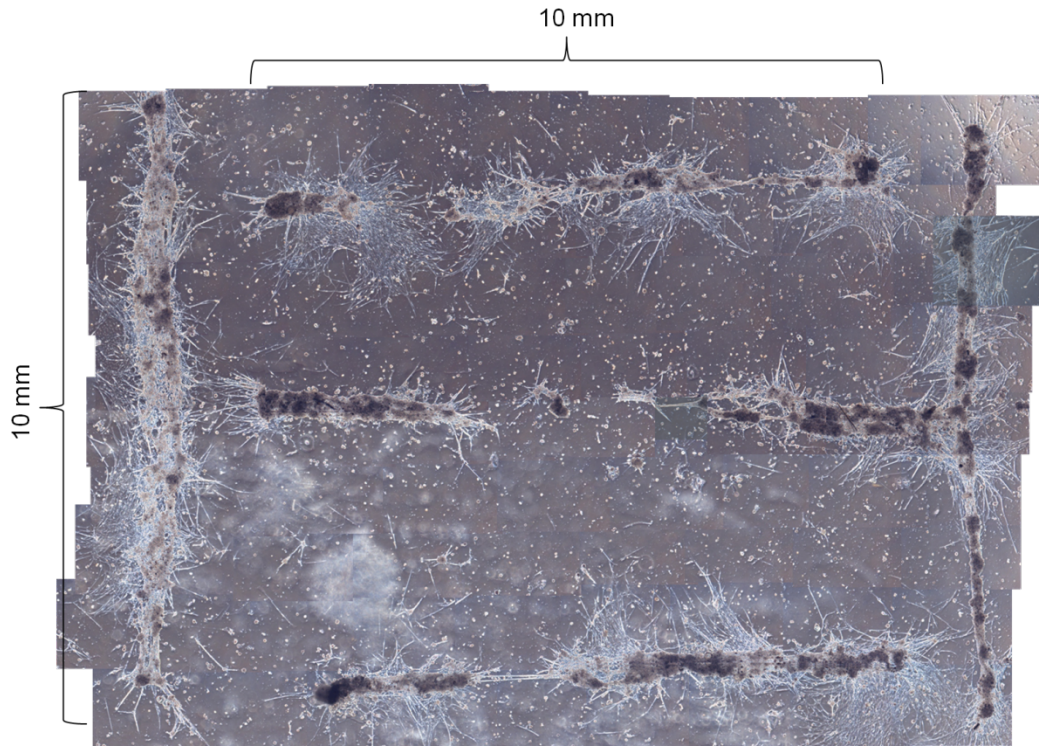


FIGURE 5.25 PHASE CONTRAST IMAGES STITCHED TOGETHER TO SHOW OVERALL MULTIFIBER CONSTRUCT SHAPE AND CONNECTIVITY, ALTHOUGH THE STRUCTURE IS NOT ENTIRELY CONTINUOUS, CLEAR REGIONS OF CELL BRANCHING AND REACHING ARE OBSERVED.

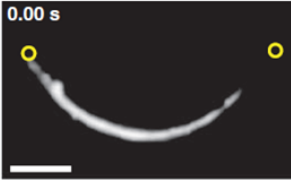

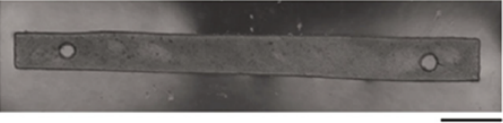
5.7 Performance testing

The measurement of forces and strains from our system is crucial, not only to comparing the present work to previous attempts at bioactuation, but to track our own progress in improving force outcomes, and for designing appropriate robotic platforms to demonstrate locomotion. As a result, we investigated the force and strain output from our constructs.

Table 5.1 highlights some of the recent attempts at generating bioactuator constructs using mammalian cells. These muscle-based structures are either characterized by their displacement, which is determined using video analysis, or by their force productions, which is measured using a force transducer. Typical force production measurements from cardiomyocytes, which contract

spontaneously, and C2C12 cells, which are electrically stimulated, are on the order of 1 μN (Horiguchi *et. al.*, 2009; Fujita *et. al.*, 2010).

TABLE 5.1 EXAMPLES FROM BIOACTUATOR LITERATURE OF CONSTRUCT DESIGNS AND MEASURES OF SUCCESS.

Group	Measures (Displacement or force)	Method
Feinberg, <i>et. al.</i> (2007) 	0.25 mm	Image analysis
Horiguchi, <i>et. al.</i> (2009) 	1.7 μN 15.5 μm	Force transducer Image analysis
Fujita, <i>et. al.</i> (2010) 	6 μN	Force transducer

Force transducer setups are often custom-built, but their components tend to be very similar. The construct to be tested is anchored in a Petri dish or vertical bath at one end; we use a PDMS block to pin our muscles in place (Figure 5.26). The construct is then attached to a force transducer at the other; when the muscle contracts, the force transducer sensor detects the strain as a

result of the Wheatstone bridge component of the sensor. The current generated by the Wheatstone bridge is converted into a digital display on a computer. The sensor may be calibrated using a one-point calibration by attaching a known weight to the sensor and recording its electrical output; thus we have a linear relationship between electrical output from the sensor device in mV to a mass, which can then be converted to force.

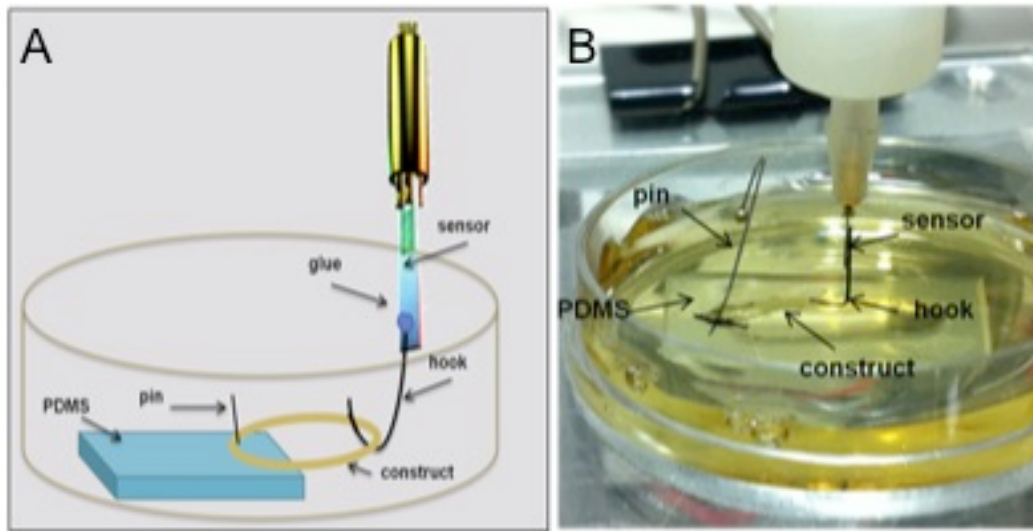


FIGURE 5.26 SCHEMATIC (A) AND EXPERIMENTAL SETUP (B) FOR MEASURING FORCE PRODUCTION FROM CONTRACTILE MUSCLE CONSTRUCTS.

We recorded measurements from a spontaneously contracting ring, and found that its force production was in the range of the sensor device. We acquired a baseline range, which we correlated with 0 mg produced (Figure 5.27A), and measured the maximum voltage change at the peaks of spontaneous contractions, which were negative due to the experimental setup (Figure 5.27B). Based on these measurements, we found an average force output of $20.4 \pm 9.4 \mu\text{N}$. We have previously determined the thicknesses of our constructs to be around $22 \mu\text{m}$. We can approximate our constructs to a

rectangle, rather than a cylinder, as they mimic the flat, ribbon-like geometry characteristic of insect muscle. The ring that was tested had channel widths of $400\mu\text{m}$, so we can estimate our cross-sectional area as $8800\mu\text{m}^2$. Thus our specific force production was, on average, $2.32\text{mN}/\text{mm}^2$.

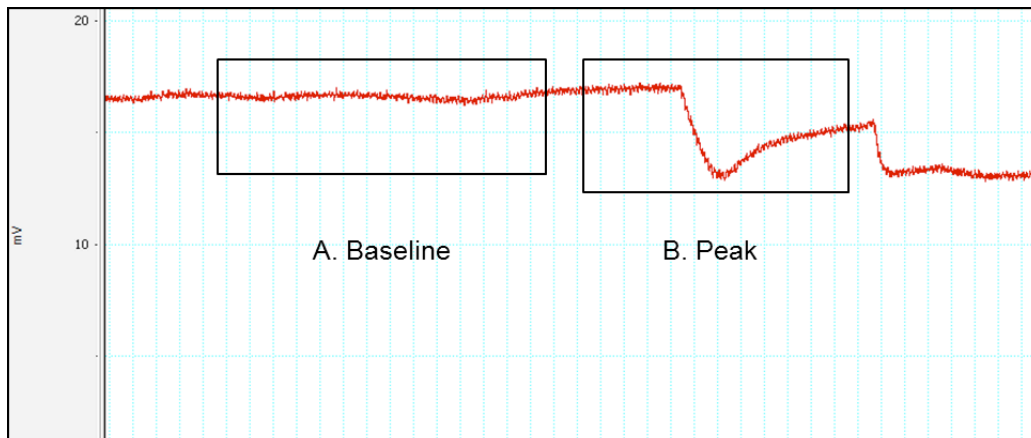


FIGURE 5.27 EXAMPLE TRACE FROM FORCE MEASUREMENT DATA, SHOWING BASELINE REGION (A), AND A SPONTANEOUS CONTRACTION (B).

In future work, we plan to test all of our construct formats and geometries to determine baseline force values for each. We will then improve our construct force output using mechanical and electrical stimulation, chemical additives, and physical reinforcement. We can also use the force data generated from these experiments to design appropriate robotic structures for generating locomotion from the activity of the cells.

5.8 Summary

We explored several approaches to generating tissue engineered skeletal muscle using the widely-applied mouse C2C12 myoblast line, including silk-

glycerol films, silk sponges, and electrospun silk-collagen structures. While we identified one configuration that allowed for spontaneous contraction of the cells within the matrix, this approach was not directly translatable to insect cells, likely due to the physiological differences between insect and vertebrate muscle.

We thus took a more physiologically-relevant approach to generating insect muscle constructs, including micropatterned channel arrays, and PDMS templates. We found we could generate mature, contractile muscle structures most readily using PDMS templates, which could easily be designed to generate ring, eyelet, and linear muscle actuators.

We characterized these structures using immunofluorescence staining and contractile analysis, optimized the channel width for improved alignment, and are now developing multifiber arrays to increase force output. When we measured the forces generated spontaneously by ring structures, we found they generated forces an order of magnitude higher than previous attempts using mammalian cardiomyocytes or C2C12 cells.

5.9 References

- Dennis RG & Kosnik PE. (2000) Excitability and isometric contractile properties of mammalian skeletal muscle constructs engineered *in vitro*. *In Vitro Cell. Dev. Biol. - Animal* 36:327 – 3.
- Feinberg AW, Feigel A, Shevkopyas SS, Sheehy S, Whitesides GM, et al. (2007) Muscular thin films for building actuators and powering devices. *Science* 317:1366 - 1370.
- Fujita H, Nedachi T, Kanzaki M. (2007) Accelerated *de novo* sarcomere assembly by electric pulse stimulation in C2C12 myotubes. *Exp. Cell Res.* 313:1853 - 1865.
- Fujita H Shimizu K, Nagamori E. (2010) Novel method for measuring active tension generation by C2C12 myotube using UV-crosslinked collagen film. *Biotechnol. Bioeng.* 106(3):482 – 489.
- Gil ES, Park S-H, Tien LW, Trimmer B, Hudson SM, Kaplan DL. (2010) Mechanically robust, rapidly actuating, and biologically functionalized macroporous poly(*N*-isopropylacrylamide)/silk hybrid hydrogels. *Langmuir* 26(19):15614 – 15624.
- Gillies AR, Smith LR, Lieber RL, Varghese S. (2010) Method for decellularizing skeletal muscle without detergents or proteolytic enzymes. *Tissue Eng. C* 17(4):383 – 389.
- Hayakawa T, Kunihiro T, Dowaki S, Uno H, Matsui E, Uchida M, Kobayashi S, Yasuda A, Shimizu T, Okano T. (2011) Noninvasive evaluation of contractile behavior of cardiomyocyte monolayers based on motion vector analysis. *Tissue Eng. C* 18(1):21 – 32.
- Herron TJ, Lee P, Jalife J. (2012) Optical imaging of voltage and calcium in cardiac cells and tissues. *Circ. Res.* 110:609 – 623.
- Horiguchi H, Imagawa K, Hoshino T, Akiyama Y, Morishima K. (2009) Fabrication and evaluation of reconstructed cardiac tissue and its application to bio-actuated microdevices. *IEEE Trans. Nanobiosci.* 8(4):349 - 355.
- Lawrence BD, Marchant JK, Pindrus MA, Omenetto FG, Kaplan DL. (2009) Silk film biomaterials for cornea tissue engineering. *Biomaterials* 30(7):1299 – 1308.

- Legant WR, Pathak A, Yang MT, Deshpande VS, McMeeking RM, Chen CS. (2009) Microfabricated tissue gauges to measure and manipulate forces from 3D microtissues. *Proc. Natl. Acad. Sci. USA* 106(25):10097 – 10102.
- Lovett ML, Rockwood D, Baryshyan A, Kaplan DL. (2010) Simple modular bioreactors for tissue engineering: A system for characterization of oxygen gradients, human mesenchymal stem cell differentiation, and prevascularization. *Tissue Eng. C* 16(6):1565 – 1573.
- Lu S, Wang X, Lu Q, Zhang X, Kluge JA, Uppal N, Omenetto F, Kaplan DL. (2010) Insoluble and flexible silk films containing glycerol. *Biomacromol.* 11(1):143 – 150.
- Mandal BB, Gil ES, Panilaitis B, Kaplan DL. (2012) Laminar silk scaffolds for aligned tissue fabrication. *Macromol. Biosci.* DOI:10.1002/mabi.201200230.
- Ott HC, Matthiesen TS, Goh S-K, Black LD, Kren SM, Netoff TI, Taylor DA. (2008) Perfusion-decellularized matrix: using nature's platform to engineer a bioartificial heart. *Nat. Med.* 14(2):213 – 221.
- Shimizu K, Fujita H, Nagamori E. (2012) Evaluation systems of generated forces of skeletal muscle cell-based bio-actuators. *J. Biosci. Bioeng.*
- Wolfgang WJ & Riddiford LM. (1986) Larval cuticular morphogenesis in the tobacco hornworm, *Manduca sexta*, and its hormonal regulation. *Dev. Biol.* 113:305 – 316.
- Wray LS, Rnjak-Kovacina J, Mandal BB, Schmidt DF, Gil ES, Kaplan DL. (2012) A silk-based scaffold platform with tunable architecture for engineering critically-sized tissue constructs. *Biomaterials* 33:9214 – 9224.
- Xia Y & Whitesides GM. (1998) Soft lithography. *Annu. Rev. Mater. Sci.* 28:153 – 184.

Chapter 6. Future directions and conclusions

We have demonstrated a system for developing functional, cell-powered devices. In the future, we can use the present work as a foundation for further refinements, which will result in broad capabilities and applications for our system. For example, the separation of individual cell types into a “cell toolbox” will readily allow for improvements to be made by varying the ratios of different cell types. Immortalization and cryopreservation of the cells will aid in acquiring consistent results and scale-up. Successful pairing of muscle actuators with a biological fuel source will extend their lifetime and functional capabilities. Additionally, the incorporation of modeling will accelerate the development of successful device designs. These and other improvements described in this chapter will lead to the incorporation of insect bioactuators into devices spanning application fields from medicine to defense.

6.1 Further cell system refinement

6.1.1 Cell type separation and purification

One of the areas we have yet to develop fully is the separation of the various types present in insect cell cultures. While we have found favorable results from developing 3-dimensional constructs using mixed cell populations

enriched in myogenic cells, we can further study each cell type individually if we were able to generate pure populations of each. The methods we could potentially use to accomplish cell separation include density gradients, differential adhesion, and cell sorting, or a combination thereof.

Density gradient separation involves the use of solutions of silica particles, commercially known as Percoll. Higher concentrations of Percoll have higher densities than lower concentrations. Separation can be achieved by layering Percoll solutions of varying concentrations, from highest to lowest, and centrifuging cells through this gradient. Based on the size and density of each cell population, cells migrate and stop at different Percoll layer interfaces and can readily be extracted. This approach has been used to collect muscle and neuron-like cells from *M. trossulus* larvae and to enrich the purity of satellite cells isolated from porcine muscle (Odintsova *et. al.*, 2010; Mau *et. al.*, 2008).

Differential adhesion, or preplating, is a strategy often employed to separate muscle cells from other cell types, such as fibroblasts, but could be applied to the cell types in our cultures, as we have not evaluated the adhesion rates of different insect cell types. In vertebrate systems, several studies have shown that fast adhering cells have less myogenic potential than slower adhering cells (Chirieleison *et. al.*, 2012; Gharaibeh *et. al.*, 2008). As a result, one can separate fibroblast-like cell types from myoblast-like cells by collecting media and cells several hours (or days) after initial plating, and transferring them to a new vessel.

Fluorescence-activated cell sorting (FACS) and magnetic-activated cell sorting (MACS) are methods for cell isolation by which cell types are separated out on the basis of expression of specific cell surface markers (van Beijnum *et. al.*, 2008). Using FACS, cells are labeled with antibodies for the cell type of

choice, and the antibodies are fluorescently labeled. The cells are then sorted on the based on the presence or absence of fluorescent signal from each individual cell. Cell preparation for MACS sorting also involves cell identification using antibodies, but instead of attaching a fluorophore, a magnet is used to retain antibody-binding cells, while eluting all others. The purified cell population may then be collected. An example of the potential for cell sorting towards our goals would be to extract tendon-like progenitor cells from the rest of the cell populations, using the cell-surface marker CD-8 (Alves-Silva *et. al.*, 2008). After FACS sorting, the identity of the resulting cell population may be verified with more specific markers that do not have to be extracellularly localized, such as *Stripe*, which is a tendon cell-specific transcription factor that marks early differentiation, or *Delilah*, which is also tendon-cell specific but marks a later differentiation event that requires the presence of muscle cells (Soustelle *et. al.*, 2004).

In addition to separating out cell types from embryonic populations, it is possible to isolate specific cell types separately, and at different life stages, for later recombination and coculture. In preliminary experiments, for example, we have cocultured embryonic muscle cells with pupal fat, as this is a readily available source of predifferentiated and relatively pure adipocytes. In future work, it may also be desirable to isolate neuronal populations and cultivate them separately from muscle before recombining the two. As discussed in Chapter 3, it has been widely demonstrated that the presence of neurons improves differentiation and contractile outcomes in cultured insect muscle. Furthermore, neurons may serve as a “translator” to the muscle of electrical signals delivered via micropatterned electrodes by transmitting these signals to the muscle via glutamate release.

Several strategies for generating pure or nearly pure populations of neuroblasts (neuronal stem cells) and motor neurons have been developed. One of the most widely-used approaches in *Drosophila* is to use a glass capillary to remove cells from embryos at varying stages of development (Küppers-Munther *et. al.*, 2004; Lürer & Technau, 2009). This technique allows for precise control over cell harvesting, even allowing for individual cells to be extracted, but for tissue engineering purposes, a method with higher cell yields is necessary. A more recent approach derives multiple neuronal cell types from larval *Drosophila* brains (Egger *et. al.*, 2013). Once in culture, it may be possible to identify and clone colonies of cells expressing markers for motor neurons. A higher number of cells may be harvested using the methods of Luedeman & Levine (1996). Thoracic ganglia from early *M. sexta* pupae were dissociated and plated at high densities. This approach is most attractive for our purposes, but compatibility between these adult neuronal populations and our embryonic-derived muscles would need to be verified.

6.1.2 Genetic manipulation

One of the advantages to working with an insect cell system is that their genetics are well understood and can be manipulated, not only to understand underlying mechanisms, but also to enhance cellular development and outcomes *in vitro*. In future work, we may be able to leverage these abilities to generate larger, more mature myofibers using genetic manipulation.

Insect muscle development differs from mammalian muscle development in that there are two main types of muscle stem cells that give rise to mature muscle fibers; founder cells (FCs) and fusion-competent myoblasts (FCMs). FCs and FCMs arise from the mesoderm, and are specified in regions of high *Twist*

expression (Baylies *et. al.*, 1998). FCs are very important to muscle development and specification, as they contain the necessary genetic information that will determine the final muscle's position, size, orientation and even innervation (Chen & Olson, 2004). FCMs surround the FCs and fuse with them to form bi and trinucleated cells. Further rounds of fusion result in multinucleated myotubes, which will further mature into functional myofibers. If we could isolate populations of FCs and FCMs, we could potentially determine the optimal ratio with which to combine them to achieve maximal cell fusion and larger myofibers.

Twist is a transcription factor that is expressed throughout the mesoderm during the time that FCs and FCMs are being specified (Thisse *et. al.*, 1988). However, its mesodermal expression alternates between high and low levels in alternating regions. The cells in regions of high *Twist* expression are destined to undergo myogenesis. Researchers can use strains of *Drosophila* that ectopically transcribe *Twist* to generate embryos where nearly all the cells are mesodermally-fated (Artero *et. al.*, 2003). Through the constitutive expression of Toll, dorsoventral polarity is disrupted and only ventral genes are expressed, including *Twist*.

Genetic manipulation has been performed in these *Twist*-expressing embryos to generate relatively pure populations of FCs or FCMs for further genetic study (Artero *et. al.*, 2003). The overexpression of *Ras* induces FC fate in the mesodermal cells, while the overexpression of *Notch* drives cells to become FCMs. FCs may be identified by expression of *vestigial*, as this is a marker of the FC cell type. FCM generation can be verified by *sticks and stones* expression.

Our cell populations at early stages of culture express high levels of *Twist*; therefore, we could simplify the methods used by Artero *et. al.* to direct cell populations to become FCs or FCMs using standard cell transfection techniques,

rather than genetic crosses of whole organisms. If we can transfect our cells to overexpress *Notch* or *Ras*, this procedure could lead to the generation of nearly pure FCM and FC populations, which we could then be used as components of a cell “tool box” (See Section 6.1.5) and be combined at varying ratios to generate larger muscles *in vitro*. Furthermore, since *Drosophila* as a model organism is well-understood genetically and insects in general have greater genetic simplicity than mammals, this strategy could be expanded to drive the enrichment of our cell populations with other useful cell types such as tendon-like cells.

6.1.3 Immortalization and cryopreservation

In future studies, we will pursue the immortalization and cryopreservation of our cells, as this will allow for a more stable and reliable cell population, and more readily enable collaborative research with our cell system.

Immortalized cells have the ability to continually divide indefinitely. Genetic modifications can be used to accomplish this, but in insect cells, spontaneous immortalization is possible through repeated passaging and cultivation. There are several advantages to immortalizing the cells we have obtained to generate a continuous cell line. Often times, variability in the amount of yolk and quality of tissue formed from isolation to isolation are observed; for example, when the colony is not at its normal level of health, the eggs that are harvested may not be fertilized, and therefore yolk cells alone, without embryonic cells, are collected. Additionally, we would like to be able to compare the results of separate experiments, which would be more consistent if similar cells were used for all experiments.

The procedure for obtaining spontaneously immortalized cells is outlined in Figure 6.1. Cells are isolated and cultured in the absence of 20HE to prevent

differentiation, and are passaged and expanded when confluent. Typically with insect cells, the first cultivation may take weeks or months, but subsequent cultures eventually have steady growth rates and can be passaged regularly. We can test cells from each subcultivation by culturing them in the presence of 20HE to confirm that they still have the ability to differentiate into muscle.

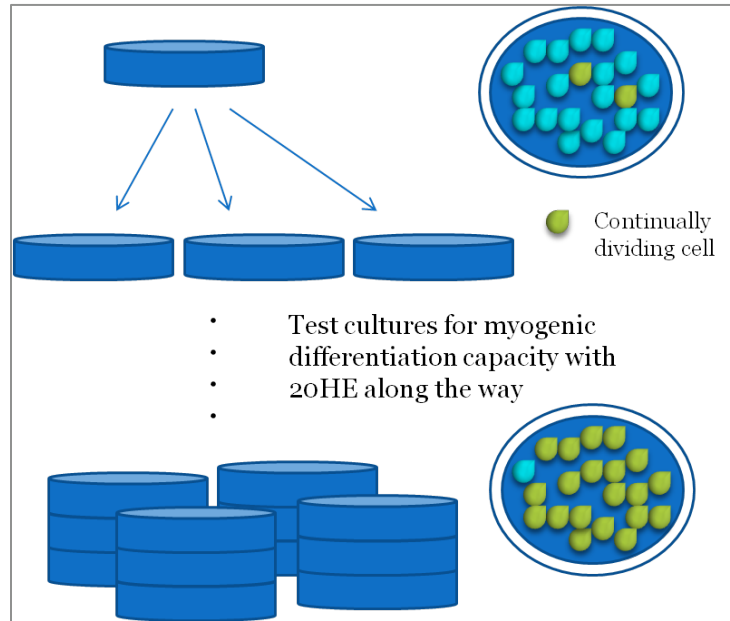


FIGURE 6.1 SCHEMATIC OF EXPERIMENTAL APPROACH TO MYOGENIC CELL IMMORTALIZATION

We carried out a preliminary trial of this approach to see if we could obtain populations of myoblasts. After several weeks of culture, the initial cultivation produced colonies of myoblast-like cells that appeared to be undergoing proliferation, but not differentiation (Figure 6.2). In future work, we will repeat this experiment, but carry it out through multiple passages and confirm proliferation with BrDU staining, and myogenic capacity with 20HE introduction.

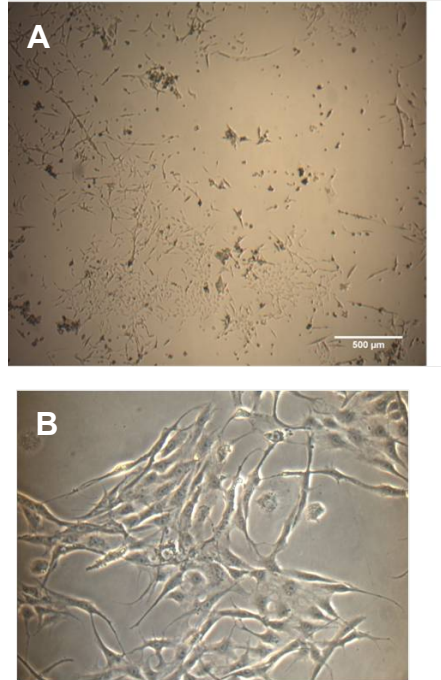


FIGURE 6.2 RESULTS FROM PRELIMINARY IMMORTALIZATION TRIAL. GROUPS OF MONONUCLEATED, BIPOLAR CELLS EMERGE (A). HIGHER MAGNIFICATION IMAGE SHOWS MYOBLAST-LIKE MORPHOLOGY (B).

Once we have a stable population of continuously dividing myogenically-committed cells, we will cryopreserve them for use in future experiments and dissemination to collaborators. A readily-available supply of insect myoblast cells would allow for a consistent cell population, and would enable experiments independent of an *M. sexta* colony. By isolating cells from eggs for each experiment, a degree of variation among individuals is possible, and cell numbers are limited to the number of eggs laid on the previous night. However, cryopreserved cells would allow for a sufficient population of staged cells to be readily available.

In order to maintain a consistent cell population with a readily available supply of cells, the cryopreservation of the *M. sexta* cells was addressed in

preliminary experiments. Glycerol and DMSO were tested as cryoprotectants, and storage times of at least two weeks were used.

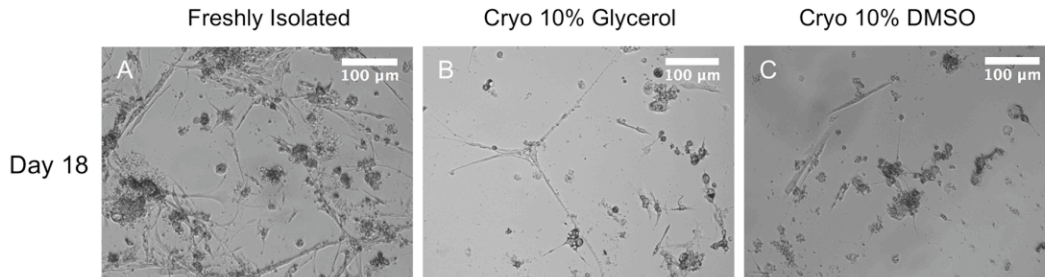


FIGURE 6.3 CRYOPRESERVATION AND RESUSCITATION OF *M. SEXTA* EMBRYONIC CELLS. PHASE CONTRAST IMAGES OF FRESHLY ISOLATED (A) AND RESUSCITATED CELLS. AFTER TWO WEEKS

Upon resuscitation, centrifugation to remove cryoprotectants from the media resulted in cell lysis, since no cells were observed after plating (data not shown). Therefore, the protocol was adjusted so that frozen cells were diluted 1:2 in normal media and plated directly. After an hour of incubation to allow for cell attachment, the cryoprotectant-containing medium was replaced with fresh media. Freshly isolated cells grew, differentiated and contracted spontaneously as expected (Figure 6.3A). We found cells survive cryopreservation in 10% glycerol media and 10% DMSO. Cells obtained from both conditions differentiated into contractile myotubes (Figure 6.3B – C). We tried increasing the concentration of cryoprotectant and found that while cells were able to survive and differentiate when frozen in 15% DMSO, similarly to freshly isolated cells, cells frozen in 15% glycerol did not persist as expected when resuscitated (Figure 6.4). Although many dead cells were observed 4 days after resuscitation, the cells seemed to recover by day 14, where the observed viability neared that of freshly isolated cells.

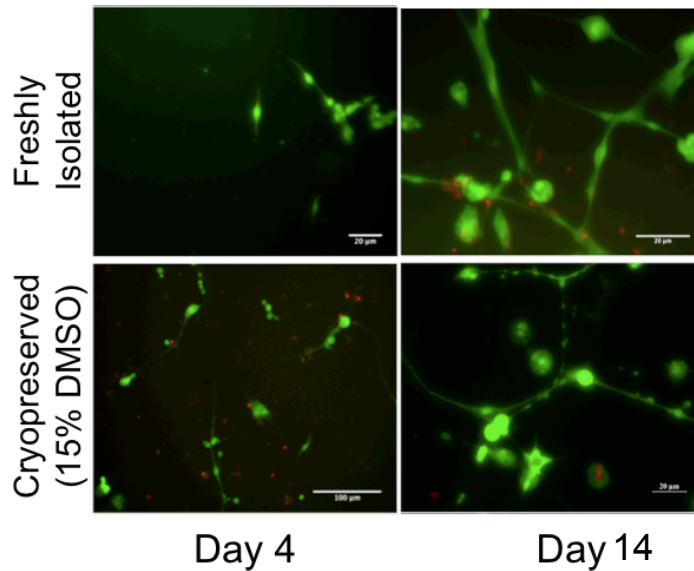


FIGURE 6.4 VIABILITY COMPARISON OF FRESHLY ISOLATED CELLS (A, B) WITH CRYOPRESERVED CELLS (C,D) OVER TIME. GREEN CELLS INDICATE LIVING CELLS, RED INDICATES DEAD CELLS.

In future studies, we will continue these experiments to optimize cryopreservation conditions, and more carefully compare outcomes to freshly isolated cells until we do not observe a loss in cell differentiation and survival upon cryopreserving.

6.1.4 ECM analysis and materials development

We have shown that larval *M. sexta* body walls may be decellularized and solubilized for use as a cell adhesion promoter in Chapter 5. In preliminary experiments, we have also shown that ECM is produced our cells *in vitro*, and we can collect this material by lysing and removing cells. The compositions and differences between these two materials may be further studied to develop an effective coating, and perhaps biomaterial, for improved bioactuator development. Furthermore, a comparison of these two materials will help us

evaluate the ability of cultured cells to carry out normal developmental processes *in vitro*.

Although the identities of the individual cuticular proteins are unknown, we can compare the protein composition of larval-derived ECM solution and *in vitro*-derived ECM on the basis of protein size and proportional amount using gel electrophoresis (Wolfgang & Riddiford, 1986). The presence of laminin and thrombospondin should also be evaluated, as these two proteins contribute to normal muscle development and attachment. Thrombospondin is found at the interface between muscle cells and anchoring tendon-like cells, while laminin is found ensheathing individual muscle cells during myotube extension (Schweitzer *et. al.*, 2010; Yarnitzky & Volk, 1995). Additionally, cell attachment on these two materials should be compared. If the *in vitro*-generated ECM proves to be more effective, it may be possible to isolate only the cells responsible for its synthesis to more effectively produce material for study.

Once an ECM source has been selected, the solution should be concentrated to higher levels than those used in previous experiments. Furthermore, since gels are often used in muscle tissue engineering to promote cell-cell contact and to form a variety of muscle structures, it may be useful to attempt to gel this material and use it as a physiologically-relevant biomaterial for cell encapsulation, allowing us to bypass the limitations of insect cell adhesion on PDMS (Bian *et. al.*, 2009; Hoshino *et. al.*, 2012). The concentrated material can also be patterned on films and devices to promote cell adhesion in specific locations (Cimetta *et. al.*, 2009; Xia & Whitesides, 1998).

6.1.5 Cell type “tool box” and medical device applications

We have shown in Chapter 3 that several cell types exist within our cultures. Some of the cell types, such as yolk cells, are likely beneficial to the cultures, but some cell types, such as certain epithelial populations, can interfere with the development of organized contractile muscle constructs. Still others, such as tendon-like cells, we would like to be able to separate so that we can specify their location within the construct (i.e. at the ends only). Once we have developed methods for generating pure populations of each cell type as described above, we may be able to generate bioactuator constructs with even finer control of organization, dimensions, and output.

With neuronal, tendon, founder, and fusion-competent cell populations in our “toolbox”, we could develop next-generation bioactuated devices where each cell type performs its native function in an optimal manner. For example, a biodegradable silk film with micropatterned electrodes could first be seeded with insect embryonic neurons. These would serve to transmit electrical signals from the electrodes to the muscles in a physiological manner. Next, tendon cells could be added to either end of the film to serve as anchorage points for the muscle. Founder cells and fusion-competent myoblasts are then placed between the tendon cell end points, on top of the neurons. In this way, the conditions found during insect muscle development are recapitulated, where tendon cells signal to muscle cells as the two cell types develop, causing the muscle to migrate and reach toward the tendon cells (Callahan *et. al.*, 1996; Volk & VijayRaghavan, 1994; Becker *et. al.*, 1997). Additionally, ectodermally-derived neurons also signal to the muscle, fostering the muscle cells’ maturation while beginning to form functional neuromuscular junctions between the two cell types. Finally, the

fuel source, which may be yolk cells or fat cells, can be added around the muscle to provide a constant source of energy to power contraction.

The properties of the silk film may be tailored so that it is stiff, and undergoes bending deflection upon muscle contraction, or thin and flexible, such that the film undergoes wrinkling and shortening upon stimulation. In a bending scenario, the silk film may be used as a membrane driving a pneumatic pump; the pressure generated within the pump chamber upon concave to convex shape change in the silk film could drive the release of fluid, drugs or other functions.

6.2 Metabolism

6.2.1 Muscle – yolk cell interactions and metabolic mechanism

Our results from yolk cell separation experiments indicated that yolk cells are important to muscle cell survival long-term in the absence of media changes, however, we have not yet determined which fuel source (carbohydrate, lipid or proline), or which combination thereof, are supplied to the muscle and when.

We can determine the mechanism by which yolk cells support muscle cell survival by repeating our initial cell separation studies, and by extending our analyses to include longer timepoints, intracellular metabolic analysis, and by enriching the yolk cell only cultures with additional yolk cells from 8h embryos. We will confirm any results we find by inhibiting cellular machinery, such as preventing lipolysis through a triglyceride lipase inhibitor (Arrese & Soulages, 2009). The overall goal of this work will be to determine which fuel substrates, and when, are mobilized by yolk cells to muscle cells for extended muscle cell survival and function.

6.2.2 Muscle – fat interactions

In addition to separating muscle cells from yolk cells, we have begun preliminary experiments to investigate the interactions between muscle cells and another potential fuel source, fat cells. We would like to examine the effects of a tissue engineered fat supply on our muscle cultures, both indirectly and directly. In initial evaluations, we have found that the exposure of cultured embryonic fat to immature muscle cells, both indirectly and directly, results in the development of muscle with intracellular fat depots. Therefore, a next step would be to coculture mature fat with differentiated muscle, to determine if the two cell types are compatible at these stages. If we find this is not the case, then we may resort to the cells we suspect interact with our muscle cells in culture, yolk cells.

6.3 Construct output improvement

6.3.1 Reinforced structures

In future work, in addition to spatially organizing cell types as described in Section 6.1, we will seek to improve the overall organization of our constructs and take a more rational approach to the design of their dimensions. Additionally, we will begin to work with the muscles as a material; for example, we have demonstrated that we can reinforce the structure of the constructs by twisting them into a helical structure, as shown in Figure 6.5. Twist actuators of this design have greater resilience since they are in tension without being stretched to their full extension. Additionally, an actuator of this type can convert tensile force produced upon shortening into torsion, which could result in rotational movement (Murata *et. al.*, 2008).

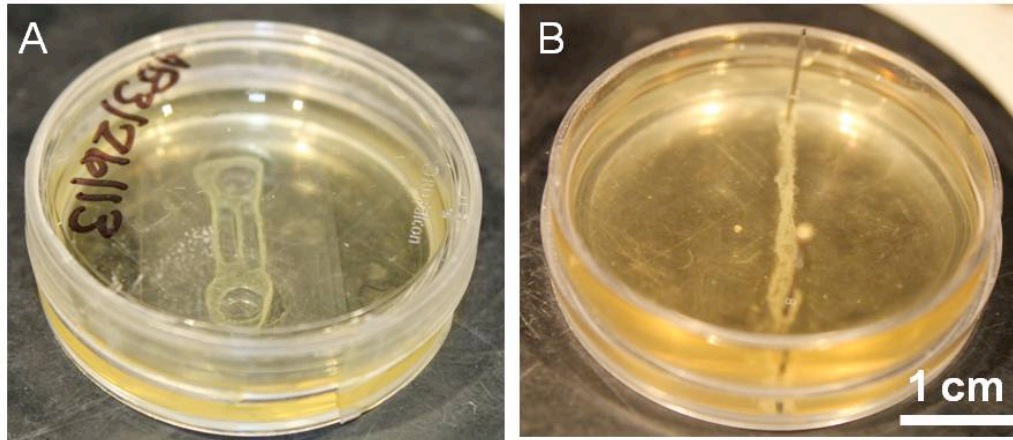


FIGURE 6.5 MULTIFIBER CONSTRUCT REINFORCEMENT. A MULTIFIBER CONSTRUCT WITH THREE PARALLEL FIBERS (A) WAS MECHANICALLY REINFORCED BY DETACHING IT FROM ITS SUBSTRATE, TRANSFERRING IT TO A PDMS-COATED DISH, AND WINDING IT 3 TIMES AROUND. THE STRUCTURE WAS THEN PINNED DOWN AS A PROOF-OF-CONCEPT FOR FUTURE CONSTRUCT REINFORCEMENT STUDIES (B).

6.3.2 Mechanical stimulation

Mechanical stimulation will be applied to our cultures to additionally enhance the elasticity and mechanical properties of the muscle, for more robust outcomes. Mechanical conditioning may improve our bioactuator outcomes by enhancing the organization and alignment of our cells, and by increasing their resilience and strength (Riehl *et. al.*, 2012). Furthermore, preconditioning with cyclic mechanical stimulation has resulted in improved force production both *in vitro* and after *in vivo* implantation (Moon *et. al.*, 2008). Enhanced myofiber diameter and percent area of myofibers have also been observed to increase significantly in tissue engineered muscle constructs subjected to 8 days of mechanical stimulation (Powell *et. al.*, 2002).

In our lab, we have several options for applying static or cyclic strain to our insect bioactuators. The commercially-available FlexCell system allows for ease of regimen specification, and up to 24 samples can be run at one time, but

it is intended for 2D cultures, so 3D conditioning would not necessarily apply the user-specified strains. Furthermore, multiple stimulation regimes cannot be run at once. However, this system could be useful for initial studies to examine in the responses of our cells to mechanical strain in 2D. The lab has developed a bioreactor to perform mechanical stimulation in previous work (Kluge *et. al.*, 2011). This device could be useful for our studies, although it was designed for constructs much larger than our tissues. Another device that may provide a simple and effective method for subjecting our cells to dynamic mechanical environments is a stretch apparatus developed by the Eschenhagen lab, which allows for ring structures to be looped over metal bars that cyclically change their spacing (Zimmermann *et. al.*, 2001).

6.4 Controlling contraction

6.4.1 Electrical stimulation

Electrical stimulation parameters have been developed for tissue engineered vertebrate muscle, mainly for the purposes of measuring force production using a force transducer. Effective parameters for murine cell-derived skeletal muscle constructs typically range from 0.29 – 13V/mm, with pulse durations of 1.2 - 10ms, and frequencies of 0.5 – 40 Hz, depending on whether twitch or tetanic contractions are desired (Dennis & Kosnik, 2000; Yamasaki *et. al.*, 2009; Fujita *et. al.*, 2010). Insect dorsal vessels were successfully stimulated *in vitro* using 20ms square pulses at 1Hz, with voltage amplitudes ranging from 0.14 – 1.43V/mm (Akiyama *et. al.*, 2010). Our lab has access to a custom-designed stimulator and bath electrical stimulation chambers that utilize carbon rod electrodes with platinum wire leads (Tandon *et. al.*, 2009).

Although bath stimulation is widely used in electrical stimulation studies of tissue engineered muscle, we would eventually like to be able to stimulate the bioactuator through biomaterials patterned with electrodes. This design would require that the muscles be in direct contact with the electrodes, and that the material would be flexible enough to deform with the muscle when it contracts. Our lab has already developed such flexible electrodes, which are incorporated into thin silk films (Hwang *et. al.*, 2012).

6.4.2 Chemical stimulation

Contraction may also be induced chemically using compounds such as caffeine. Caffeine stimulation results in over five times the tension production of an electrically stimulated tetanus contraction (Schwartz & Ruff, 2002). However, one of the limitations of this technique is the dependence on diffusion for the compound to arrive at and subsequently be removed from the vicinity of the cell, which may prevent successive contractions to be induced rapidly. Furthermore, in preliminary experiments, we have observed that contractions last for several seconds; the muscle takes many times longer to relax than it does when spontaneously contracting. Although these observations suggest that chemical stimulation may not be the best approach for locomotion, it may be useful for stimulating infrequent contractions, as for a pump or other biomedical device.

6.5 Device design and modeling to achieve locomotion

6.5.1. Moving PDMS structures

We have begun to design and build structures that will lead towards the generation of locomoting devices powered by our insect bioactuators. Initially, we plan to determine the appropriate geometry of silicone posts, such that they are

sufficiently small and flexible enough for muscle actuators to deflect them. Then, we will apply these dimensions to the posts of silicone devices, shown in Figure 6.6. Eventually, when muscle construct force production has been optimized, we will fabricate less flexible crawlers, which will undergo a greater amount of displacement upon contraction.

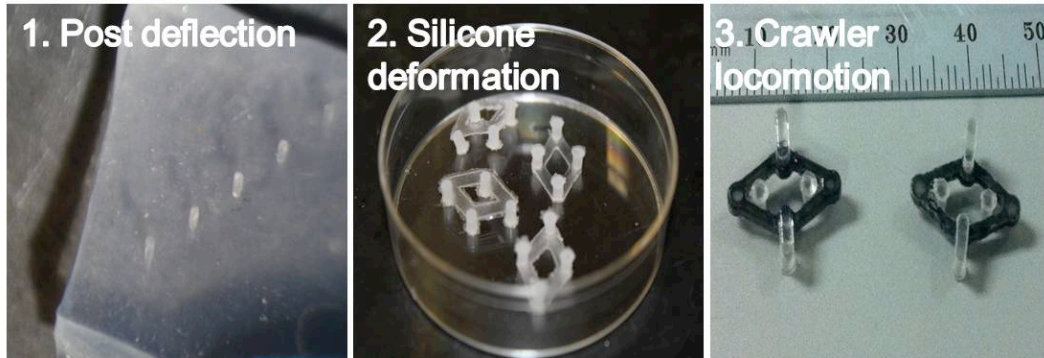


FIGURE 6.6 FABRICATED STRUCTURES FOR DEVELOPING LOCOMOTIVE MUSCLE-POWERED DEVICES. 1. WE WILL USE ELASTOMER POST ARRAYS TO DETERMINE OPTIMAL SIZE AND SPACING OF POSTS. 2. NEXT, SILICONE STRUCTURES WILL BE DEFORMED WITH MUSCLE ACTUATORS. 3. FINALLY, A DEVICE WILL BE POWERED BY MUSCLE ACTUATORS.

We have already begun testing silicone elastomeric micropillars for deflection by muscle constructs (Figure 6.7). Ring-type muscle constructs are looped around the posts of a micropillar array (posts are 200 - 300 μ m in diameter). We are presently using video analysis to determine the degree of deflection the posts undergo upon muscle contraction with different post diameters, aspect ratios and spacing.

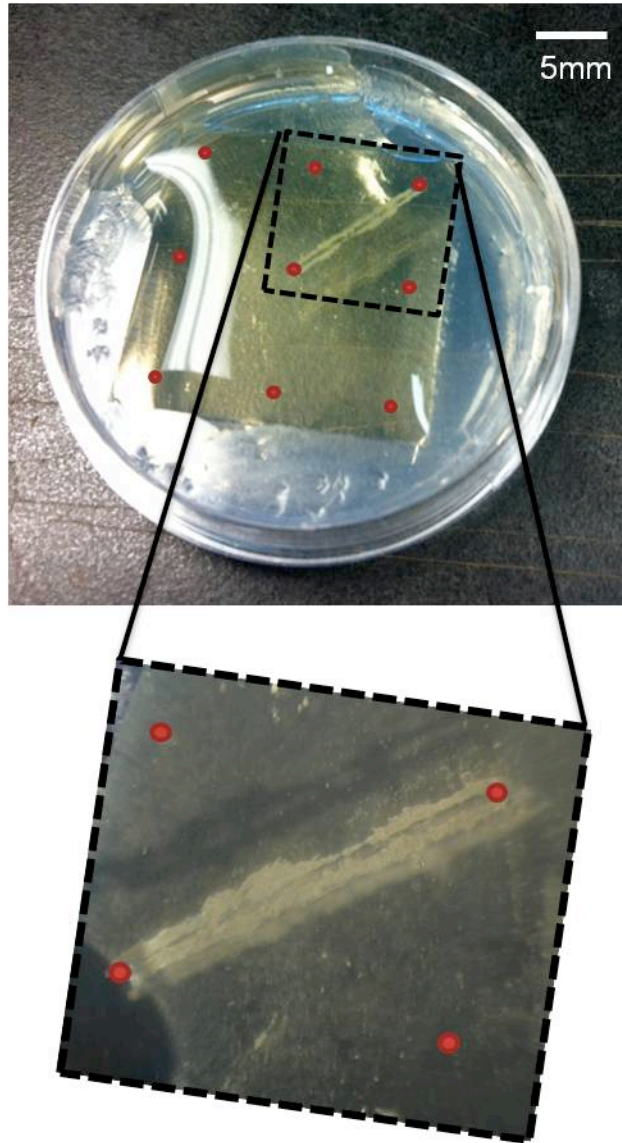


FIGURE 6.7 RING-TYPE MUSCLE ACTUATOR LOOPED OVER SILICONE POSTS FOR DEFLECTION ANALYSIS. RED DOTS INDICATE SILICONE POST PLACEMENT.

Additionally, we are working with small silicone devices to determine the feasibility of integrating muscle constructs. We took eyelet-shaped constructs and looped them around the posts of the elastomeric device, which had been pinned down such that the posts were oriented with minimal distance between one another (Figure 6.8A, B). We then released the device, which returned to its

original conformation, and the muscle construct remained intact and taut, which will be desirable for future locomotion of the structures (Figure 6.4C). Thus we can conclude that the muscle constructs may be integrated with such devices, and we will continue designing and testing such devices as we improve our muscle force output.

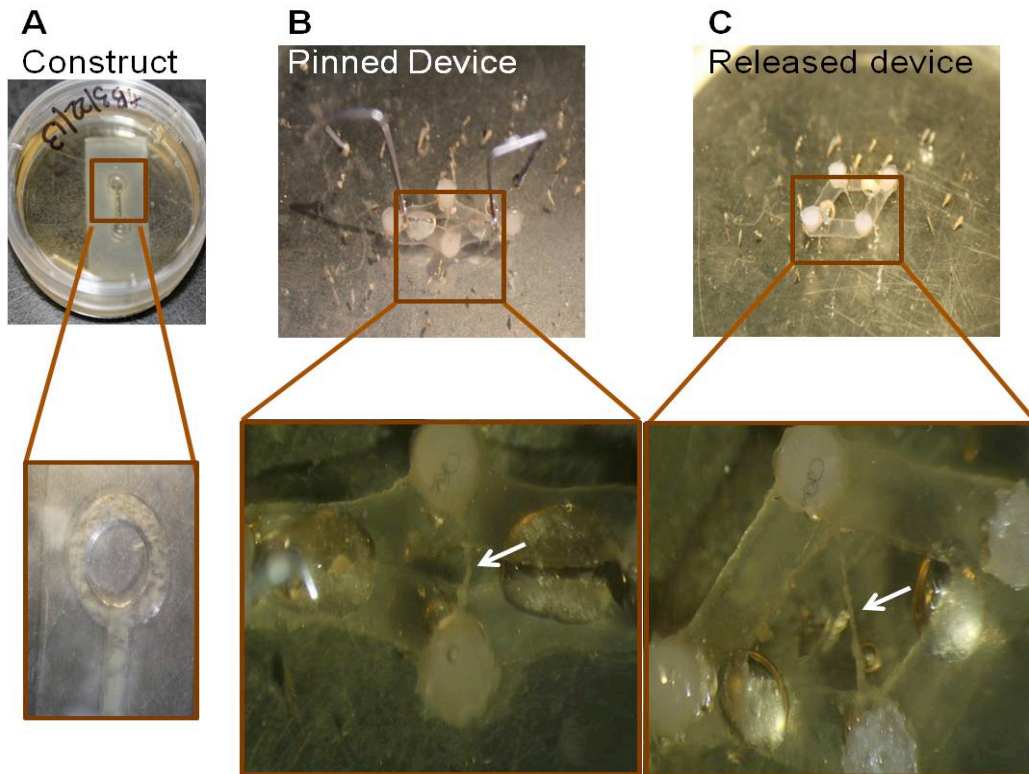


FIGURE 6.8 CONSTRUCT INTEGRATION WITH ELASTOMERIC DEVICES. EYELET CONSTRUCTS WERE USED, WHICH HAVE A RING STRUCTURE AT EITHER END (A). THE DEVICE WAS PINNED IN PLACE SUCH THAT THERE WAS MINIMAL DISTANCE BETWEEN THE TWO POSTS, AND THE MUSCLE STRUCTURE WAS LOOPED OVER THE POSTS (B). WHEN THE DEVICE WAS RELEASED, THE MUSCLE MAINTAINED ITS INTEGRITY AND WAS PULLED TAUT (C). WHITE ARROWS IN INSETS INDICATE MUSCLE CONSTRUCT.

6.5.2 Modeling bioactuated devices

Now that we have explored and verified the ease with which we can integrate our muscle actuators with synthetic silicone structures, we can begin to model deformation and deflection outcomes of the silicone structures based for

varying geometries and dimensions of devices. Furthermore, since we have acquired preliminary data regarding the force output of the muscle constructs, we can design and model a silicone device that theoretically should deflect or move, based on our muscle data (Paetsch & Dorfmann, 2013). This approach will rationalize our device designs and accelerate the process of defining device sizes and geometries that are appropriate for our bioactuator system.

6.6 Silk-based biodegradable robots

The lamellar silk scaffolds used for C2C12 muscle constructs in Section 5.2.2 were applied to insect cells (Figure 6.5A). Briefly, lamellar aligned silk scaffolds were prepared at 1mm thickness, cut to dimensions of 5mm x 15mm, and autoclaved in water. The scaffolds were then coated in Scraped ECM solution for one hour at room temperature (Section 5.3.3). A small volume of high-density insect cell suspension was then seeded on the scaffolds in non-tissue culture treated plates, and flooded the next day (Figure 6.5B). This process is outlined in Figure 6.5C.

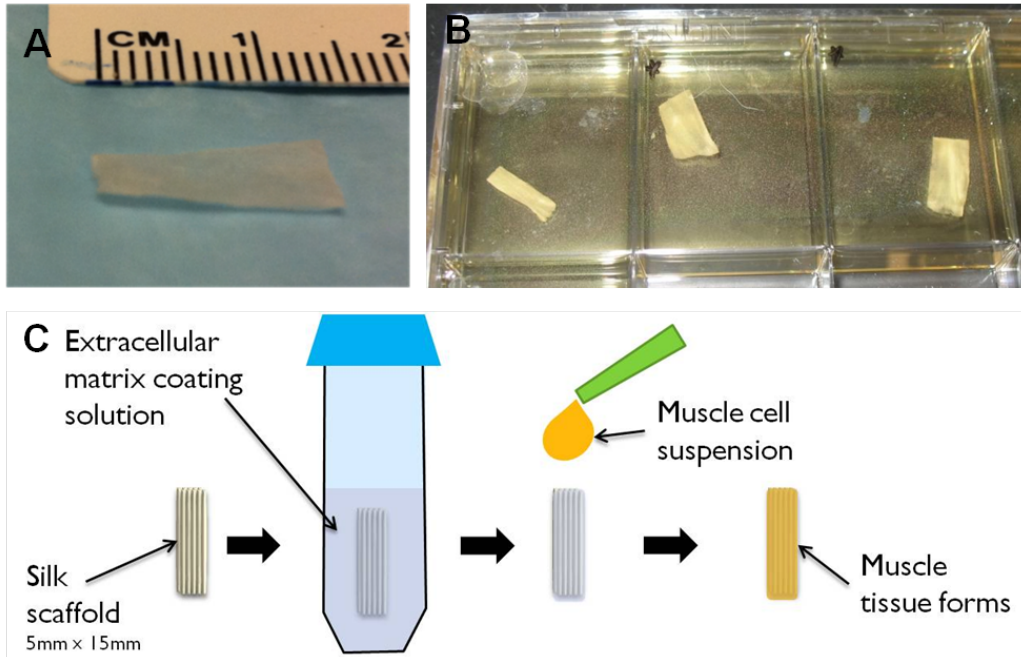


FIGURE 6.5 INSECT CELLS SEEDED ON SILK LAMELLAR SCAFFOLDS. SILK SCAFFOLDS USED FOR STUDY (A). SILK SCAFFOLDS SEEDED WITH INSECT CELLS (B). PROCESS FOR SILK SCAFFOLD PREPARATION AND SEEDING (C).

After culturing for 14 days, scaffolds were stained with a LIVE/DEAD kit and imaged using confocal microscopy. We found that in scaffolds with large pores, there was good cell integration, but the structure of the scaffold was not organized enough to guide muscle cell alignment (Figure 6.6A). Scaffolds with smaller pores had fewer cells on the interior, but achieved good cellular alignment (Figure 6.6B). Scaffolds comprised of a 50:50 blend of 3% silk and 3% tropoelastin were found to have optimal results, allowing for both high cellularity and muscle alignment (Figure 6.6C).

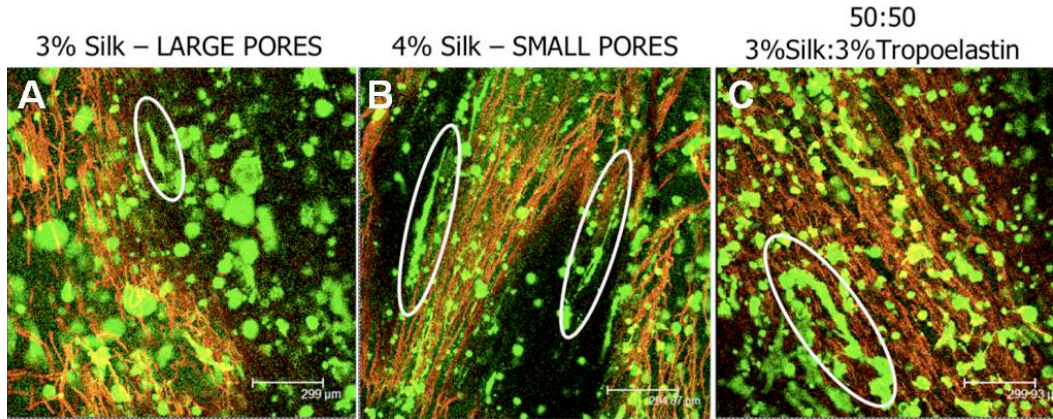


FIGURE 6.6 LIVE/DEAD IMAGING OF INSECT CELLS ON LAMELLAR SILK SCAFFOLDS. OVERALL CELLULARITY WITHIN 3% SILK SCAFFOLDS WAS GOOD, BUT NOT VERY MANY ALIGNED CELLS WERE OBSERVED (A). CELLULAR ALIGNMENT WAS INDUCED BY 4% SILK SCAFFOLDS, BUT CELLULARITY WAS REDUCED (B). CELLULARITY AND CELL ALIGNMENT WERE IMPROVED WITH 50:50 SILK:TROPOELASTIN BLEND SCAFFOLDS (C). GREEN INDICATES LIVE CELLS. RED INDICATES SILK SCAFFOLD. WHITE OVALS INDICATE ALIGNED CELLS. SCALE BARS ARE 300 UM.

In future studies, we will reduce the thickness of these structures from 1mm to about 250 μm, increase the cell density, and determine whether such structures are suitable to simultaneously act as an actuator and body wall structure.

6.7 Conclusions

In this thesis, we have demonstrated the isolation and culture of a unique and useful cell system from *M. sexta* embryos. The cells are mainly myogenic in nature, but also contain neurons, yolk cells, and other cell types as well. These cell populations contract spontaneously and are viable for long periods of time without maintenance (Baryshyan *et. al.*, 2012). We investigated their metabolism to probe the mechanism for extended cell survival, which is a novel and fascinating property of our system. While further studies need to be performed, we found the insect cellular metabolism to be quite different from mouse muscle,

and the yolk cell populations within our cultures may be contributing to the differences we see in energy substrate production and usage. Finally, we generated 3D contractile muscle constructs from our cells, using a simple approach, which results in scaffold-free constructs. This is another unique property to our cell system, and mammalian muscle cell types often require and ECM component such as a gel or scaffold to hold the tissue together.

Our focus now and in future work will be to study the fundamental biology and metabolism of our cell population, while simultaneously improving on our functional muscle structures to enhance force output and control contraction. As we learn more about our system, we will be able to design robotic devices, or apply our structures to existing designs, to achieve function that may be useful in microtechnology, robotics, and medicine.

6.6 References

- Akiyama Y, Iwabuchi K, Furukawa Y, Morishima K. (2010) Electrical stimulation of cultured lepidopteran dorsal vessel tissue: an experiment for development of bioactuators. *In Vitro Cell. Dev. Biol. – Animal* 46:411 – 415.
- Alves-Silva J, Hahn I, Huber O, Mende M, Reissaus A, Prokop A. (2008) Prominent actin fiber arrays in *Drosophila* tendon cells represent architectural elements different from stress fibers. *Mol. Biol. Cell* 19:4287 – 4297.
- Arrese EL & Soulages JL. (2010) Insect fat body: Energy, metabolism and regulation. *Annu. Rev. Entomol.* 55:207 – 225.
- Artero R, Furlong EE, Beckett K, Scott MP, Baylies M. (2003) Notch and Ras signaling pathway effector genes expressed in fusion competent and founder cells during *Drosophila* myogenesis. *Development* 130(25):6257 – 6272.
- Baryshyan AL, Woods W, Trimmer BA, Kaplan DL. (2012) Isolation and maintenance-free culture of contractile myotubes from *Manduca sexta* embryos. *PLoS ONE* 7(2):e31598.
- Baylies MK, Bate M, Gomez MR. (1998) Myogenesis: A view from *Drosophila*. *Cell* 93:921 – 927.
- Becker S, Pasca G, Strumpf D, Min L, Volk T. (1997) Reciprocal signaling between *Drosophila* epidermal muscle attachment cells and their corresponding muscles. *Development* 124:2615 – 2622.
- Bian W, Liao B, Badie N, Bursac N. (2009) Mesoscopic hydrogel molding to control the 3D geometry of bioartificial muscle tissues. *Nat. Protoc.* 4(10):1522 – 1534.
- Callahan CA, Bonkovsky JL, Scully AL, Thomas JB. (1996) *derailed* is required for muscle attachment site selection in *Drosophila*. *Development* 122:2761 – 2767.
- Chen EH & Olson EN. (2004) Towards a molecular pathway for myoblast fusion in *Drosophila*. *TRENDS Cell Biol.* 14(8):452 – 460.
- Chirieleison SM, Feduska JM, Schugar RC, Askew Y, Deasy BM. (2012) Human muscle-derived cell populations isolated by differential adhesion rates: Phenotype and contribution to skeletal muscle regeneration in Mdx/SCID mice. *Tissue Eng. A* 18(3 – 4):232 – 241.
- Cimetta E, Pizzato S, Bollini S, Serena E, De Coppi P, Elvassore N. (2009) Production of arrays of cardiac and skeletal muscle myofibers by micropatterning techniques on a soft substrate. *Biomed Microdevices* 11(2):389 – 400.

- Dennis RG & Kosnik PE. (2000) Excitability and isometric contractile properties of mammalian skeletal muscle constructs engineered in vitro. *In Vitro Cell. Dev. Biol. – Animal* 36:327 – 335.
- Egger B, van Giesen L, Moraru M, Sprecher SG. (2013) *In vitro* imaging of primary neural cell culture from *Drosophila*. *Nat. Protoc.* 8(5):958 – 965.
- Fujita H, Shimizu K, Nagamori E. (2010) Novel method for measuring active tension generation by C2C12 myotube using UV-crosslinked collagen film. *Biotechnol. Bioeng.* 106(3):482 – 489.
- Gharaibeh B, Lu A, Tebbets J, Zheng B, Feduska J, Crisan M, Peault B, Cummins J, Huard J. (2008) Isolation of a slowly adhering cell fraction containing stem cells from murine skeletal muscle by the preplate technique. *Nat. Protoc.* 3(9):1501 – 1509.
- Hoshino T, Imagawa K, Akiyama Y, Morishima K. (2012) Cardiomyocyte-driven gel network for bio mechano-informatic wet robotics. *Biomed. Microdevices* 14:969 – 977.
- Hwang S-W, Tao H, Kim D-H, Cheng H, Song J-K, Rill E, Brenkle MA, Panilaitis B, Won SM, Kim Y-S, Song YM, Yu KJ, Ameen A, Li R, Su Y, Yang M, Kaplan DL, Zakin MR, Slepian MJ, Huang Y, Omenetto FG, Rogers JA. (2012) A physically transient form of silicon electronics. *Science* 337(6102):1640 – 1644.
- Kluge JA, Leisk GG, Cardwell RD, Fernandes AP, House M, Dorfmann AL, Kaplan DL. (2011) Bioreactor system using noninvasive imaging and mechanical stretch for biomaterial screening. *Ann. Biomed. Eng.* 39(5):1390 – 1402.
- Kuppers-Munther B, Letzkus JJ, Luer K, Technau G, Schmidt H, Prokop A. (2004) A new culturing strategy optimizes *Drosophila* primary cell cultures for structural and functional analyses. *Ve. Biol.* 269:459 – 478.
- Luedeman R & Levine RB. (1996) Neurons and ecdysteroids promote the proliferation of myogenic cells cultured from the developing adult legs of *Manduca sexta*. *Dev. Biol.* 173:51 – 68.
- Luer K & Technau GM. (2009) Single cell cultures of *Drosophila* neuroectodermal and mesectodermal central nervous system progenitors reveal different degrees of developmental autonomy. *Neural Dev.* 4:30 – 46.
- Mau M, Oksbjerg N, Rehfeldt C. (2008) Establishment and conditions for growth and differentiation of a myoblast cell line derived from the *semimembranosus* muscle of newborn piglets. *In Vitro Cell. Dev. Biol. – Animal* 44:1 – 5.
- Moon DG, Christ G, Stitzel JD, Atala A, Yoo JJ. (2008) Cyclic mechanical preconditioning improves engineered muscle contraction. *Tissue Eng. A* 14(4):473 – 482.
- Murata I, Yamashita M, Yokoi H. (2008) US Patent #20080066574 A1

- Odintsova NA, Dyachuk VA, Nezhlin LP. (2010) Muscle and neuronal differentiation in primary cell culture of larval *Mytilus trossulus* (Mollusca: Bivalvia). *Cell Tissue Res.* 339:625 – 637.
- Paetsch C & Dorfmann A. (2013) Non-linear modeling of active biohybrid materials. *Int. J. Non-Linear Mech.* 56:105 – 114.
- Powell CA, Smiley BL, Mills J, Vandeburgh HH. (2002) Mechanical stimulation improves tissue-engineered human skeletal muscle. *Am. J. Physiol. Cell Physiol.* 283:1557 – 1565.
- Riehl BD, Park J-H, Kwon IK, Lim JY. (2012) Mechanical stretching for tissue engineering: Two-dimensional and three-dimensional constructs. *Tissue Eng. B* 18(4):288 – 300.
- Schwartz LM & Ruff RL. (2002) Changes in contractile properties of skeletal muscle during developmentally programmed atrophy and death. *Am. J. Physiol. Cell Physiol.* 282:C1270 – C1277.
- Schweitzer R, Zelzer E, Volk T. (2010) Connecting muscles to tendons: tendons and musculoskeletal development in flies and vertebrates. *Development* 137:2807 – 2817.
- Soustelle L, Jacques C, Altenhein B, Technau GM, Volk T, Giangrande A. (2004) Terminal tendon cell differentiation requires the glide/gcm complex. *Development* 131(18):4521 – 4532.
- Tandon N, Cannizzaro C, Chao P-HG, Maidhof R, Marsano A, Au HTH, Radisic M, Vunjak-Novakovic G. (2009) Electrical stimulation systems for cardiac tissue engineering. *Nat. Protoc.* 4:155 – 173.
- Thisse B, Stoetzel C, Gorostiza-Thisse C, Perrin-Schmitt F. (1988) Sequence of the *twist* gene and nuclear localization of its protein in endomesodermal cells of early *Drosophila* embryos. *EMBO* 7(7):2175 – 2183.
- Van Beijnum JR, Rousch M, Castermans K, van der Linden E, Griffioen AW. (2008) Isolation of endothelial cells from fresh tissues. *Nat. Protoc.* 3(6):1085 – 1091.
- Volk T & VijayRaghavan K. (1994) A central role for epidermal segment border cells in the induction of muscle patterning in the *Drosophila* embryo. *Development* 120:59 – 70.
- Wolfgang WJ & Riddiford LM. (1986) Larval cuticular morphogenesis in the tobacco hornworm, *Manduca sexta*, and its hormonal regulation. *Dev. Biol.* 113:305 – 316.
- Xia Y & Whitesides GM. (1998) Soft Lithography. *Annu. Rev. Mater. Sci.* 28:153 – 184.
- Yamasaki K, Hayashi H, Nishiyama K, Kobayashi H, Uto S, Kondo H, Hashimoto S, Fujisato T. (2009) Control of myotube contraction using electrical pulse stimulation for bio-actuator. *J. Artif. Organs* 12:131 – 137.

Yarnitzky T & Volk T. (1995) Laminin is required for heart, somatic muscles, and gut development in the *Drosophila* embryo. *Dev. Biol.* 169:609 – 618.

Zimmermann W-H, Schneiderbanger K, Schubert P, Didie M, Munzel F, Heubach JF, Kostin S, Neuhuber WL, Eschenhagen T. (2002) Tissue engineering of a differentiated cardiac muscle construct. *Circ. Res.* 90:223 – 230.

Chapter 7. Experimental

7.1 Procedures for cell isolation

7.1.1 *M. sexta* embryo staging

Eggs were collected from a foam substrate moistened with a tobacco infusion and hung in a flight cage populated by *M. sexta* adults. At the end of each 3 hour collection period, eggs were manually detached from the substrate and maintained at 26°C for an additional 19 hours.

7.1.2 Isolation and culture of *M. sexta* myoblasts

Culture medium preparation

Culture medium was prepared according to Luedeman and Levine (1996), with minor modifications. All reagents were purchased from Invitrogen (Carlsbad, CA) or Sigma-Aldrich (St. Louis, MO), unless otherwise indicated. Medium was prepared with 70% Leibovitz's L15 medium, 18% Grace's Insect Medium, 12% fetal bovine serum (FBS), 3.4 mg/mL yeast extract, 3.4 mg/mL lactalbumin hydrolysate (MP Biomedicals, Solon, OH), 0.37 mg/mL α -ketoglutaric acid, 1.21 mg/mL D (+)-glucose monohydrate, 0.67 mg/mL malic acid, 60 μ g/mL succinic acid, 60 μ g/mL imidazole, 1% Anti-Anti, 0.5% 1X RPMI 1640 vitamin mix, and 0.5% 1X RPMI 1640 amino acid mix. Medium was prepared with 1.14 mg/mL ethylene glycol-bis(2-aminoethyl)-N,N,N',N'-tetraacetic acid (EGTA) for initial plating and without EGTA for general maintenance and differentiation

(Bernstein *et. al.*, 1978). Unless otherwise stated, a concentration of 20 ng/mL 20-hydroxyecdysone (20-HE) was used to induce myogenic differentiation. Medium was sterile filtered before use and the pH was adjusted to 6.5 with sterile 1M NaOH.

Cell isolation

After 19 hours of incubation, embryos were counted, washed twice with dH₂O and sterilized in 25% bleach for 2 minutes. Embryos were then washed twice with water and transferred to a 60-mm Petri dish. EGTA-containing medium was used to wash the embryos once before they were transferred in 5 mL media to a 7 mL Dounce homogenizer (Wheaton, Millville, NJ). Cells were released by lysing the embryos with 6 gentle strokes using plunger B. The homogenate was transferred to a 50 mL conical tube and centrifuged twice, each for 3 minutes at 85 ×g to remove excessive yolk material and pellet the cells. The pellet was then resuspended in medium and plated at a density of 5 embryos/cm². Plates were incubated at 26°C for 1 – 2 hours to allow for cell adhesion. Culture dishes were then placed on a rotational shaker for 10 minutes at 100 rpm, 26°C. The cells were gently aspirated and refreshed with an appropriate volume of EGTA-free medium. All plates were sealed with Parafilm and placed in a humidified incubator at 26°C.

7.1.3 Applying mammalian culture conditions

Lactate analysis

Extracellular lactate was evaluated using the EnzyChrom L-Lactate Assay Kit (BioAssay Systems, Hayward, CA) and was performed using 4X or 8X diluted

samples in 96-well plates following to the manufacturer's protocol. Cell counts were determined from phase contrast images using ImageJ (NIH) software.

7.1.4 Differentiation with 20-hydroxyecdysone

Culture preparation

Media was prepared as described in Section 9.1.2, except that varying doses of 20-HE were added. Cells were harvested as in Section 9.1.2, in EGTA-containing media with the appropriate experimental levels of 20-HE present.

Myotube width analysis

At least 5 images were acquired for each condition. ImageJ software was used to measure the widths of each myotube in the image. For 20ng/mL 20HE, 24 cells were measured. For 80ng/mL 20HE, 43 cells were measured. The widths of each cell for each condition were binned in 2 μm ranges and plotted as a histogram to visualize the spread of cell sizes within a condition.

7.1.5 Proliferation with juvenile hormone

Culture preparation

Media was prepared as described in Section 9.1.1, except that varying doses of methoprene, a juvenile hormone mimic, were added. Cells were harvested as in Section 9.1.2, in EGTA-containing media with the appropriate experimental levels of methoprene present.

BrDU incorporation and staining

At each time point, a 0.3 mg/mL BrDU stock was added to each sample for a final media concentration of 3 $\mu\text{g}/\text{mL}$ (N=3). The cells were replaced in the

incubator for an additional 3h, after which the cells were fixed in 10% neutral buffered formalin for 45 min. Cells were permeabilized in 0.1% Triton-X-100 and rinsed with phosphate buffered saline (PBS). DNA was denatured for 30 min in 2 N HCl at 37°C. 0.1 M borate buffer (38 mg/mL sodium borate in water, pH 8.5) was used to neutralize the samples. The cells were then washed in PBS and blocked with 10% goat serum. Anti-BrDU mouse monoclonal antibody (Abcam, Cambridge, MA) was diluted 1:500 in 10% goat serum. Samples were incubated overnight at 4°C. On the next day, samples were washed with PBS prior to incubation in AlexaFluor488 goat anti-mouse secondary antibody (1:200) and DAPI (1:1000), diluted with 2% goat serum. After incubation for 1 hour, samples were washed with PBS before imaging with a Leica fluorescence microscope. 7 fields of view were acquired per well, with an average of 55 cells counted per field.

7.1.6 Statistical analysis

All assays were performed with a minimum sample size of n=3. Experimental groups were compared using a two-sided Student's t-test in Microsoft Excel. Statistically significant values are defined as indicated.

7.2 Procedures for cell characterization

7.2.1 Cell type identification

Immunofluorescence staining

Samples for immunostaining were prepared according to Das *et. al.*, with minor modifications (2007). Briefly, samples were fixed in cold methanol for 5 – 7 minutes. Wells were washed with PBS and permeabilized in a solution of 1 wt%

bovine albumin serum (BSA) and 0.05 wt% saponin in PBS for 5 minutes. The permeabilization solution was removed before the samples were blocked for 30 minutes in 1 wt% BSA with 10% goat serum. Samples were then incubated overnight at 4°C in primary antibody against waterbug flight muscle myosin (Babraham Institute, Cambridge, UK), diluted 1:5 in permeabilization solution. The following day, samples were washed twice with PBS and incubated in a solution of AlexaFluor488 F(ab')₂ fragment of goat anti-mouse IgG (1:200 dilution) and DAPI (1:1000 dilution) for 2 hours. Samples were washed with PBS before visualizing using a Leica fluorescence microscope.

Histological processing and staining of developing embryos

Embryos were incubated at 26°C for 19 hours as described in Section 9.1.1. The eggs were then pierced with a needle to allow for permeation of the fixative through the egg's outer layer or chorion. The eggs were incubated in 4% neutral buffered formalin for 45 minutes, processed through an ethanol dehydration series into xylene, and embedded in paraffin. Following sectioning, mounting, and deparaffinization, 10µm sections were stained with hematoxylin and eosin. Images were acquired using a Leica inverted microscope equipped with a CCD camera.

Oil Red O staining

Oil Red O stain was used to view lipid droplets within yolk and/or fat cell types. A 3.5 mg/mL solution of Oil Red O powder in isopropanol was used as the stock solution. Cells were fixed in 4% neutral buffered formalin for 45 minutes. A 60% working solution of Oil Red O stock in PBS was filtered through a 0.22µm filter. Working solution was then added to each well and incubated on a shaker

for 45 minutes. The samples were washed thoroughly in PBS and imaged using a Leica inverted microscope equipped with a CCD camera.

7.2.2 Prolonged survival

Cultures were initiated using the methods described in Section 8.1.1 and 8.1.2. At designated timepoints, cultures were stained using a LIVE/DEAD kit, as outlined in Section 8.1.6.

7.2.3 Spontaneous contractile activity

Cultures were initiated using the methods described in Section 8.1.1 and 8.1.2.

Index of movement analysis

Index of movement analysis was performed according to Fujita *et. al.* [18], with minor modifications. Briefly, videos of contracting cells (1600 x 1200 pixels) were acquired on a Leica microscope with a 20X objective lens using Leica LAS MultiTime imaging software. Five images recorded at 700 ms intervals were analyzed from each video. For a single index of movement value, the first image was subtracted from the remaining four to generate four absolute value images. These were then added together to create a single differential image. The average pixel intensity for the differential image was normalized to a scale of 0 to 1, with 1 as the value representing the greatest displacement in pixel intensity; this value was considered the index of movement. The index of movement reflects the degree of cellular contraction occurring in the field during the 2.8s interval of data collection. Plots of change in IOM over time were generated by evaluation the index of movement for at least three videos in three fields of each

condition. Average pixel intensity was measured for each frame of a single video and plotted to reveal contraction dynamics. For visualizing the IOM for a single video, the differential image was pseudocolored on a scale ranging from 0 to 255.

Actin staining

Filamentous actin was visualized by staining fixed and permeabilized cells with rhodamine-conjugated phalloidin, following the manufacturer's protocol. Briefly, cells were fixed in 4% formalin for 15 minutes at room temperature and washed with PBS before permeabilizing in 0.1% Triton-X-100. The samples were washed with PBS again before blocking in 1% BSA for 30 minutes at room temperature. Rhodamine-phalloidin working solution was prepared at 1:40 ratio of rhodamine-phalloidin stock solution to PBS. Cells were incubated in the working solution to 20 minutes at room temperature, washed with PBS, and visualized using a Leica fluorescence microscope.

7.3 Procedures for metabolic analyses

7.3.1 Metabolic comparison with mouse muscle

Culture preparation

Insect cells were plated as described in Section 2.2. After 2 days, the media was aspirated and replaced with fresh control medium (1.23 g/L) or low-glucose medium, which contained 0.27g/L added glucose monohydrate. At each time point, 35 μ L of medium was collected from each well and phase contrast imaging was performed. Medium samples were stored at 4°C until the time of assay.

Culture of cells from established mouse cell line C2C12

P3 C2C12 (CRL-1772 ATCC, Manassas, VA) cells were expanded in T-flasks in growth medium consisting of high glucose Dulbecco's Modified Eagle's medium (4.5 g/L glucose), supplemented with 10% FBS, 1% MEM non-essential amino acids, and 1% Anti-Anti. Cells were detached using a 0.25% trypsin-EDTA solution, centrifuged at 313 $\times g$ for 10 minutes, resuspended and counted. Cells were plated at a seeding density of 5×10^3 cells/cm². Cultures incubated at 37°C, 20% O₂, 5% CO₂. Seven hours following plating, the medium was switched to differentiation medium, which consisted of DMEM supplemented with 10% horse serum, 1% non-essential amino acids, and 1% anti-anti. The cells were then cultured for an additional 2 days before the start of the experiment. At t=0, the medium was aspirated and replaced with either control differentiation media, or low-glucose media which contained 1g/L glucose. At each time point, 35 μ L of medium was collected from each well and phase contrast imaging was performed. Medium samples were stored at 4°C until the time of assay.

Metabolic assays

Glucose media concentrations were determined using the Glucose (GO) Assay Kit. Samples were diluted 40X or 80X and the assay was carried out in 96-well plates according to the manufacturer's protocol. Glucose concentrations were calculated and corrected for losses due to sampling following Equation (1) from Gawlitta *et al.* (2007):

$$c'_0 = c_0$$
$$c'_p = \left(0.035 \sum_{q=0}^{p-1} c_q \right) + \frac{(1 - 0.035p)c_p}{1}$$

(1)

where c_0 = Initial concentration

c'_0 = Corrected initial concentration

c_p = Concentration of sample p

c'_p = Corrected concentration of sample p

Lactate assays were performed and analyzed as described in Section 9.1.3.

High performance liquid chromatography

Proline and alanine concentrations in media samples were determined using high performance liquid chromatography in gradient elution mode using a Nova-Pak C18 Cartridge (4 μ m, 3.9 x 150 mm, Waters, Milford, MA). The separation module (Alliance 2690, Waters) was equipped with a multi-

wavelength fluorescence detector (2475, Waters). An AccQFluor Reagent Kit (Waters) was used for precolumn derivatization of amino acid standards and samples, according to the manufacturer's instructions. Amino acid detection was accomplished at an excitation of 250 nm and emission of 395 nm.

7.3.2 Subtractive media experiments

Medium preparation

Insect culture medium was prepared as described in Section 8.1.2, with the exception that either glucose, or amino acid mix, or yeast extract, or FBS was omitted from the recipe. For cultures omitting FBS, Leibovitz's 15 media was supplied to compensate for the balance volume that was excluded.

Cell culture and imaging

Cells were staged, isolated and cultured as entailed in Sections 8.1.1 and 8.1.2. All isolation procedures were performed with the experimental medium formulation. Cultures were imaged using a phase contrast microscope at specific time points.

Metabolic analyses

Medium samples were collected and analyzed according to Section 8.3.1.

7.3.3 Influence of vitellophages

Oil Red O staining and quantification

Cultures at different time points were fixed and stained with Oil Red O as described in 8.2.1.

Yolk and embryonic cell separation

Percoll gradients were formed for the separation of yolk cells and embryonic cells. Sterile Percoll was diluted 9:1 in 10X PBS to establish a stock isotonic Percoll solution (SIP). From this solution, 15%, 25%, and 60% Percoll solutions were prepared. Discontinuous gradients were formed by gently layering 3 mL 60% Percoll, 6 mL 25% Percoll, and 3mL 15% Percoll in a 15 mL conical. 2.5 mL of cell suspension was added on top; for centrifugation balance, 1 mL media was used. The gradients were spun for 25 minutes at 1800 xg . The cells collected at the layer interfaces were diluted in 12 mL media for each interface and centrifuged for 10 min at 200 xg . Finally, the pelleted cells were resuspended in an appropriate amount of media and plated in well plates. For control (unseparated) Percoll cultures, gradients were formed with 3 mL 60% Percoll and 9 mL 15% Percoll. The remaining procedures were carried out as above. Phase contrast images were acquired from all conditions at regular time points. LIVE/DEAD staining and imaging was performed according to Section 8.1.7.

Embryonic cells and yolk cells were also separated by manual dissection. Staged embryos were washed briefly in 25% bleach and transferred to media. A drop of media was placed in a 60-mm dish under a dissecting microscope. 4 eggs were dissected at a time; the eggs were lysed by squeezing with fine forceps and pulled open. Yolk cells were clearly visible and identified by their large size and round morphology. Larger fragments of the embryo, comprised of embryonic cells, could also easily be discerned under the dissecting microscope. A 1mL syringe fitted with a 26G needle was used to separately collect yolk cells or embryonic cells into separate dishes. For control conditions, both embryonic cells and yolk cells were collected together. Once the required number of

embryos had been dissected, the cell suspensions were transferred to 50mL conical, brought to a final volume of 5 mL, and centrifuged for 5 min at 200 *xg*. The cell pelleted were resuspended in an appropriate amount of medium, and plated into well plates. Cells were imaged at regular intervals, and Oil Red O staining and imaging was performed as described in 8.2.1. Lipid quantification was performed as described above. Metabolic analyses were carried out according to Section 8.3.1.

7.4 Procedures for 3D construct formation

7.4.1 Silk-glycerol films

Silk solution preparation

Silk solutions were prepared as described previously (REFS). Briefly, *B. mori* silkworm cocoons (Tajima Shoji Co., Ltd., Yokohama, Japan) were cut into small fragments and boiled in a 0.02M sodium carbonate solution for 20 minutes to remove sericin proteins, washed with distilled water, and the resulting fibroin material was allowed to air dry overnight. The fibroin was then dissolved in a 9.3M lithium bromide solution for 4 – 6 hours at 60°C. The solution was then dialyzed against distilled water through a cellulose membrane with a 3500 molecular weight cut-off for 48 hours. Remaining debris was removed from the resulting solution, which had a concentration of 6 – 8% w/v.

Silk-glycerol film preparation

Silk solutions were obtained as described in 9.4.1 “Silk solution preparation”. 1%, 3% and 4% w/v silk solutions were generated by diluting 6-8% silk solutions in deionized water. 20% and 40% glycerol-silk solutions were

prepared by blending a 20wt% glycerol stock solution with either a 4%, 3% or 1% w/v silk solution. Silk-glycerol films were cast into sterile 12-well plates and allowed to air dry in a sterile laminar flow hood overnight. Films were then incubated in 70% ethanol for 1 – 2 hours to sterilize the films and induce beta-sheet formation in the silk. The films were then washed with PBS 3 times for 20 minutes each. Finally, films were coated with fibronectin for 1 hour at room temperature, followed by incubation in media at 37°C for at least 20 minutes prior to cell seeding.

Cell culture

C2C12 mouse cells were cultured as described in 9.3.1 “Culture of cells from established mouse cell line C2C12”. After passaging, cells were seeded on sterilized silk-glycerol films at a density of 5000 cells/cm². The cells were incubated in proliferation medium for 4 days, followed by differentiation medium for at least 7 days, with medium changes every 2 – 3 days, as described in Section 7.3.1.

Actin staining

Cells were stained with rhodamine-conjugated phalloidin as described in Section 8.2.3.

7.4.2 Electrospun silk-gel constructs

Silk Electrospinning

Silk solutions were prepared as described in 9.4.1 “Silk solution preparation”. 6% silk solutions were obtained by diluting 7-8% silk solutions in deionized water. 6% Silk solutions were blended with polyethylene oxide (PEO)

in a 4:1 6% silk:PEO v/v ratio with stirring for 15 minutes. Silk-PEO solutions were then loaded into a 5 – 20mL syringe and allowed to degas at ambient conditions before being loaded into a syringe pump.

The electrospinning setup was assembled as described previously (Wittmer *et. al.*, 2011). An aluminum foil collector was prepared by folding a sheet of aluminum foil so that two vertical, parallel walls were formed 10 cm apart. Aligned silk-PEO mats were generated by collecting silk fibers on the specialized aluminum foil collector at a distance of 8” from the capillary, with 10 – 12 kV of applied voltage at a flow rate of 0.02mL/min for 3-5 minutes.

Substrate preparation

PDMS-coated dishes were prepared using a Sylgard 184 silicone elastomer kit (Dow Corning, Midland, MI). Component A and Component B were mixed in a 9:1 wt ratio, with vigorous stirring for 3 minutes. The solution was then degassed in a vacuum chamber and approximately 2mL of the solution was gently poured into a 35-mm Petri dish. The dishes were then either allowed to cure on a level surface, covered at room temperature for forty-eight hours, or in a 60°C oven for four hours.

Sections of aligned silk-PEO fibers were gently cut from the collector and transferred to a PDMS-coated 35-mm dish. Segments of braided size 0 silk suture were cut to 5cm and placed at either end of the electrospun silk-PEO mat. The sutures were pinned in place with Minuet pins, with two pins used for each suture end, for a total of 8 pins per construct. The silk fibers were methanol-annealed by adding 2 mL 100% methanol to each dish, and allowing the dish to sit in the hood, uncovered, until the methanol had evaporated.

Sterilization and coating

Substrates and dishes were sterilized in two steps. First, the dish was incubated in 4mL 70% ethanol for 20 minutes before the ethanol was aspirated, and the dish was washed three times with sterile PBS. The ethanol sterilization process was then repeated. The substrates were then allowed to air dry in the hood.

Silk-PEO fibers and silk sutures were coated with fibronectin by first preparing a sterile 20µg/mL fibronectin working solution in PBS from a 0.1mg/mL fibronectin stock solution. Each substrate was coated with 100µL fibronectin working solution and allowed to dry in the hood. Substrates were then washed with 3mL PBS.

Next, a second sterilization was performed by adding 2 mL growth medium to each dish and exposing the substrates to UV light in the hood for one hour. Finally, dishes were placed in a 37°C, 20% O₂, 5% CO₂ incubator for up to 60 hours before seeding cells.

Cell seeding and maintenance

Cells were cultivated, passaged and collected as described in Section 9.3.1. Type I collagen (R&D Systems, Gaithersberg, MD) was prepared according to the manufacturer's instructions for a final concentration of either 2 mg/mL or 1.5mg/mL. A small volume of media was added to the collagen before it gelled, and the mixture was seeded onto electrospun silk fibers. Cells were maintained in proliferation media for 4 days, and were incubated in differentiation media for 2 weeks.

Immunofluorescence

Cells were stained for immunofluorescence imaging according to Section 7.2.1, except that a 1:40 dilution of rhodamine-phalloidin was included in the secondary antibody solution. Constructs were imaged using a confocal microscope.

7.4.3 PDMS channels

7.4.4 Extracellular matrix extraction and coating

7.4.5 Self-assembly in PDMS chambers

7.4.6 Construct characterization

7.4.7 Force production testing

7.5 References

Bernstein SI, Fyrberg EA, Donady JJ. (1978) Isolation and partial characterization of *Drosophila* myoblasts from primary cultures of embryonic cells. *J. Cell Biol.* 78:856 - 865.

Das M, Wilson K, Molnar P, Hickman JJ. (2007) Differentiation of skeletal muscle and integration of myotubes with silicon microstructures using serum-free medium and a synthetic silane substrate. *Nat. Protocols* 2(7):1795 - 1801.

Gawlitta D, Oomens CWJ, Bader DL, Baaijens FPT, Bouten CVC. (2007) Temporal differences in the influence of ischemic factors and deformation on the metabolism of engineered skeletal muscle. *J. Appl. Physiol.* 103:464 - 473.

Luedeman R & Levine RB. (1996) Neurons and ecdysteroids promote the proliferation of myogenic cells cultured from the developing adult legs of *Manduca sexta*. *Dev. Biol.* 173:51 - 68.

Wittmer CR, Claudepierre T, Reber M, Wiedemann P, Garlick JA, Kaplan D, Egles C. (2011) Multifunctionalized electrospun silk fibers promote axon regeneration in the central nervous system. *Adv. Funct. Mater.* 21:4232 – 4242.